Electrochemical Engineering with Thin Film Polymer Electrolytes

Christopher G. Arges, PhD

April 29th, 2021

GAMRY INSTRUMENTS

LSU
LOUISIANA STATE UNIVERSITY

Presentation overview

High-temperature polymer electrolyte membranes (HT-PEMs) and binders for fuel cells

Studying the electrochemical properties of electrode ionomer binders as thin films

~~Activity coefficients of ions in thin film polymer electrolytes~~

M. Ramos-Garcés, R. Kumar, C.G. Arges, *RSC Adv.* **2021**

Q. Lei, R. Kumar, C.G. Arges., *J. Mater. Chem. A.* **2020**

Louisiana State University in Baton Rouge

LSU has 34,000 students and 1200 endowed oak trees

Louisiana ranks 2nd in the US for chemical manufacturing

About my lab: polymeric materials engineered with precision over <u>6 orders of magnitude</u> in length scale

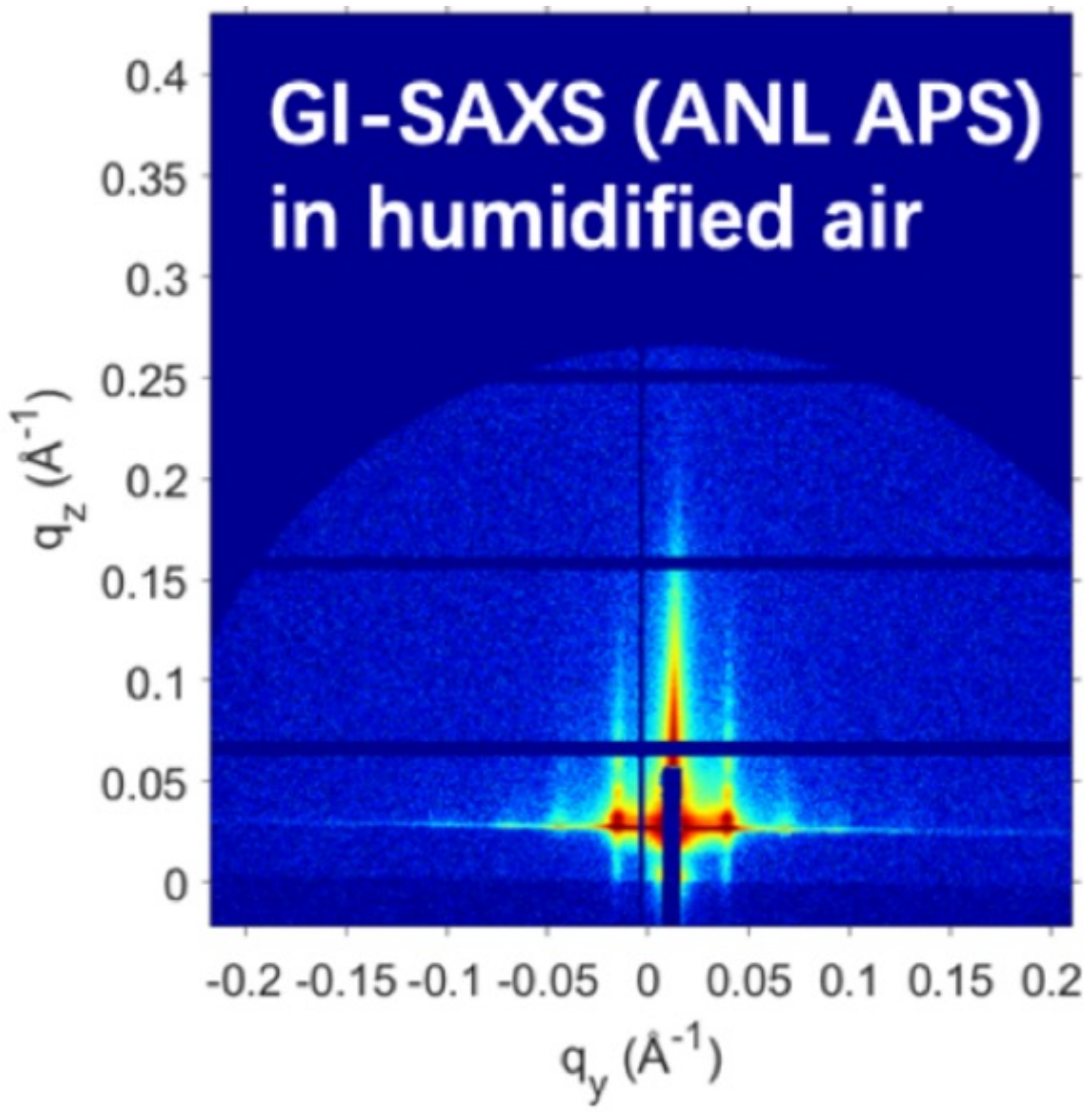

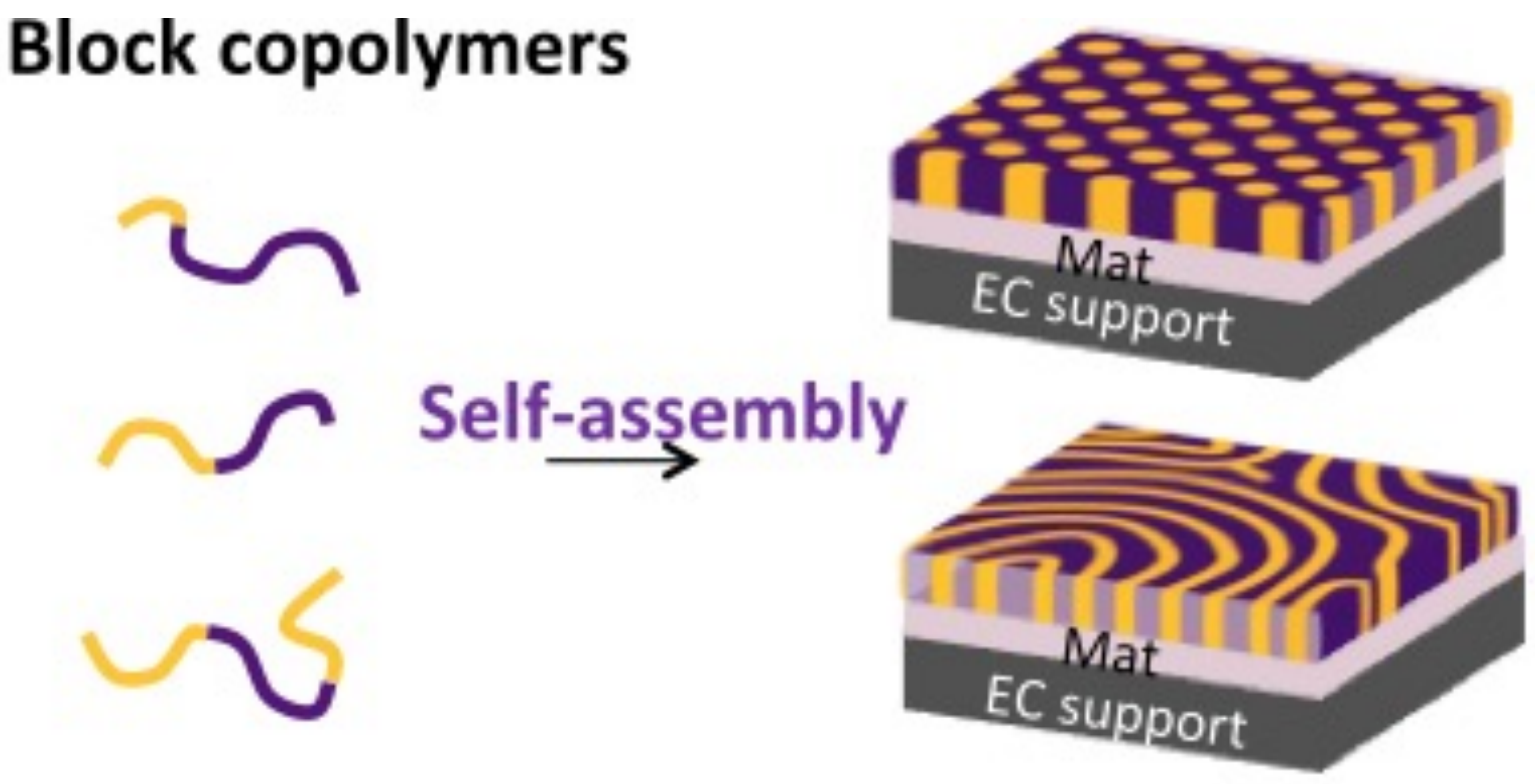

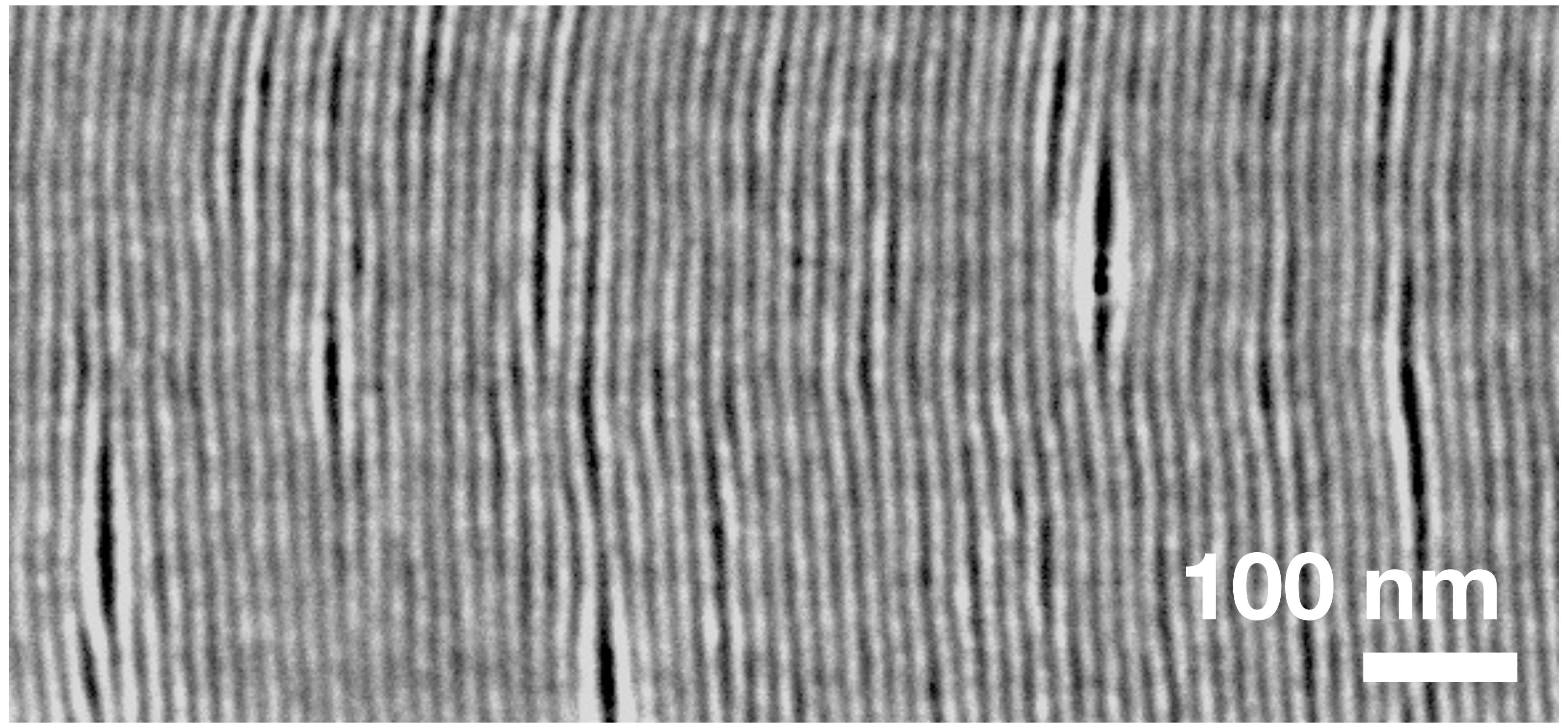

Model systems with long-range order and high fidelity nanostructures

Inform fundamental transport, kinetic, and thermodynamic properties at the molecular level

S.Kole, <u>C.G. Arges</u> *et al.* *J. Mater. Chem. A.* **2021**

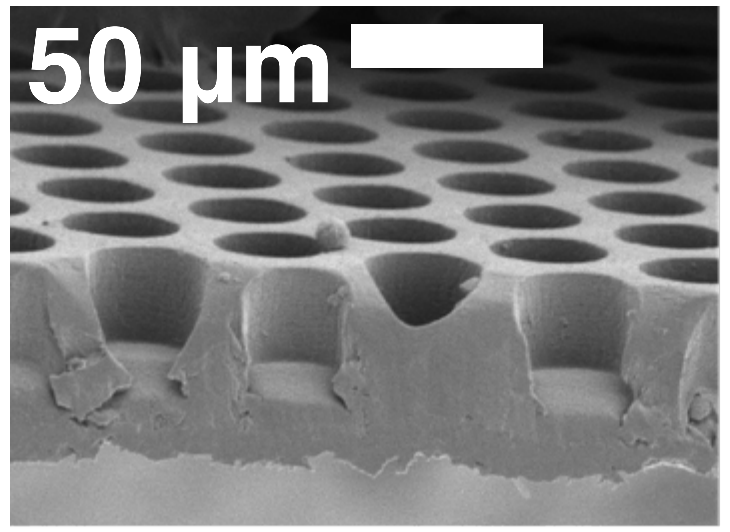

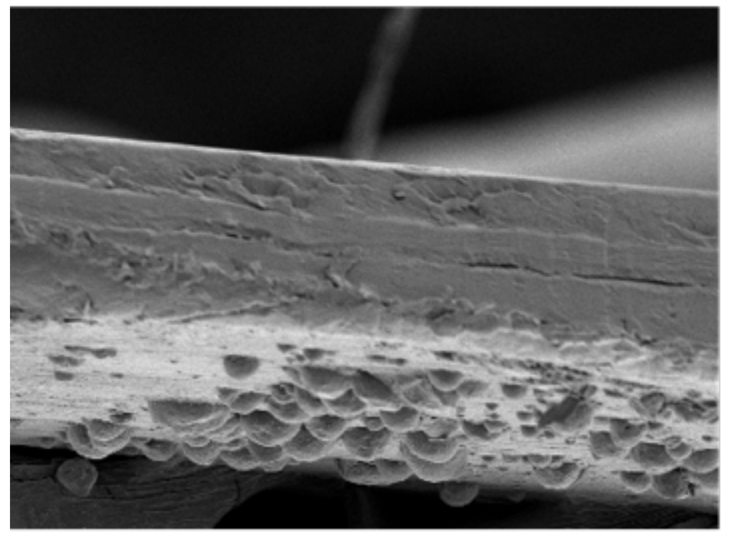

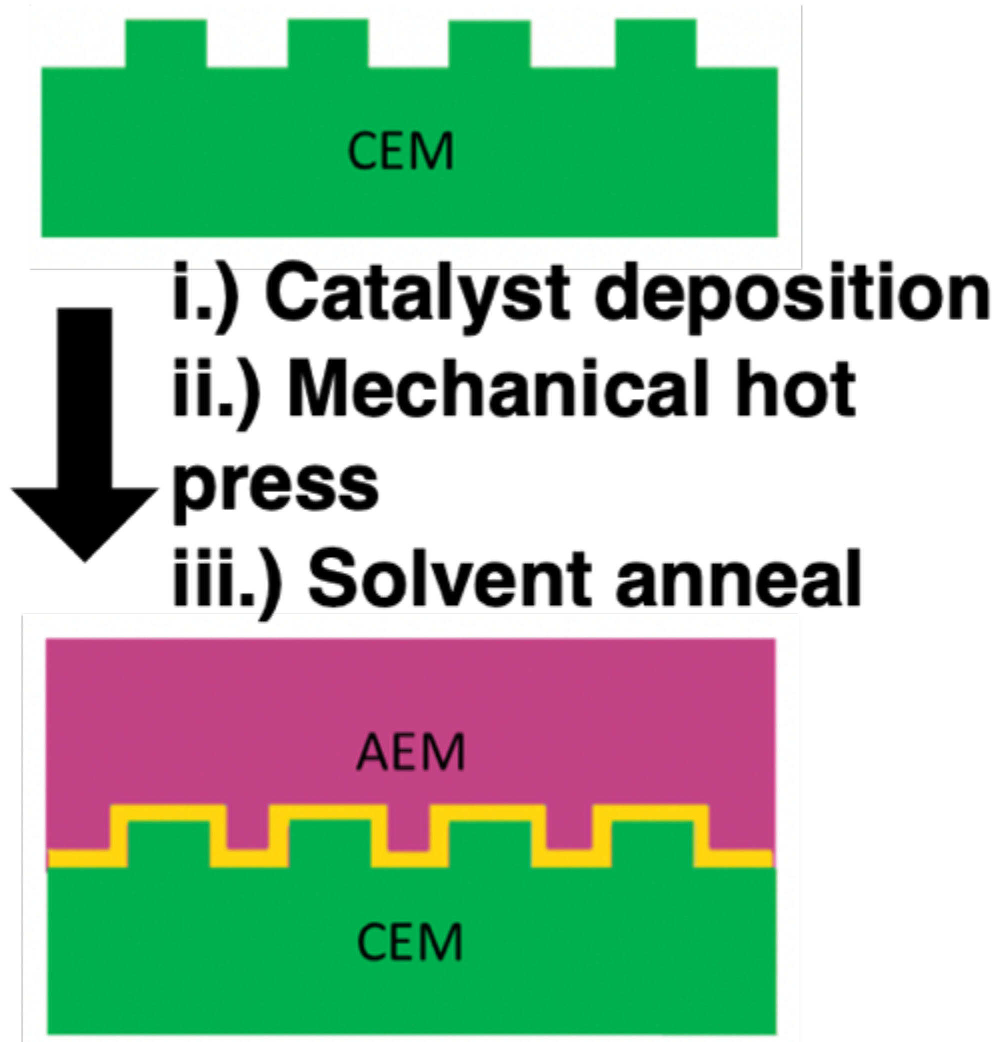

Bipolar membrane

V.M. Palakkal, <u>C.G. Arges</u> *et al. npj Clean Water* **2020**

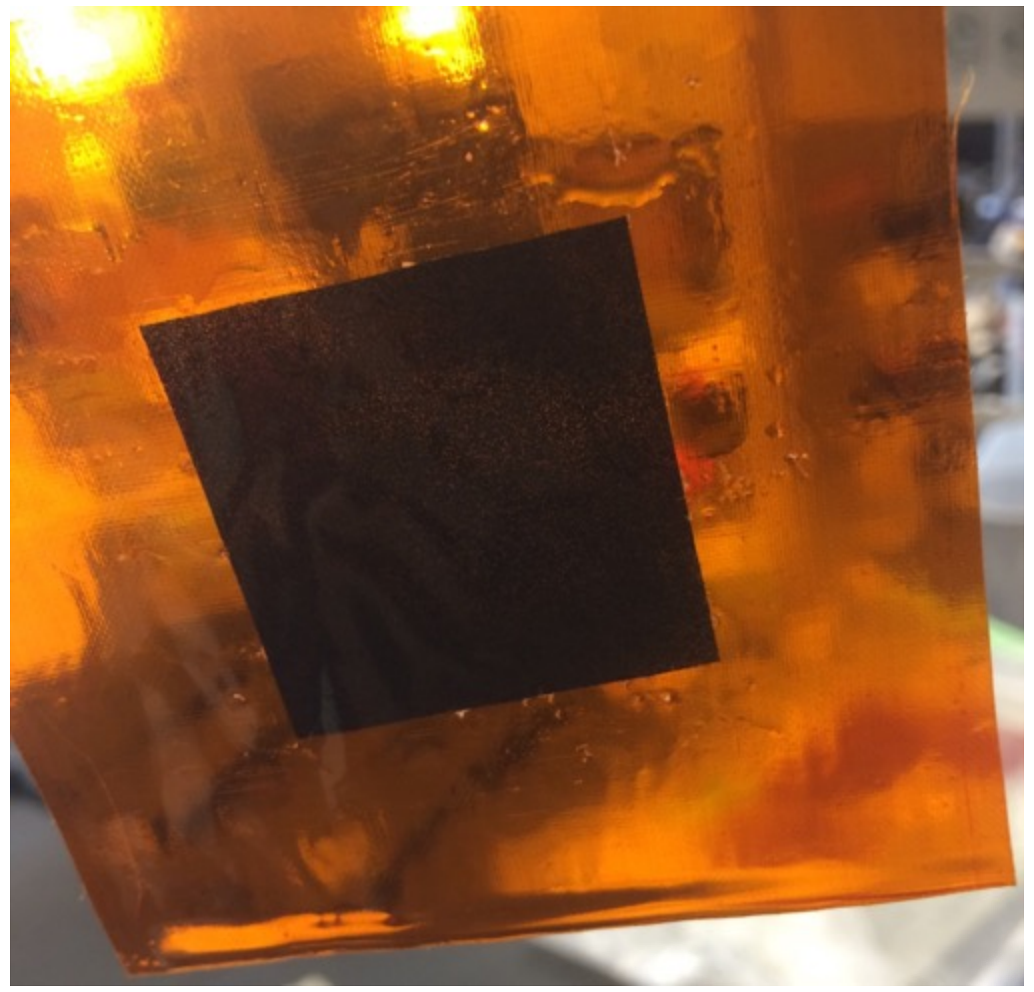

Cell level studies in Arges Lab

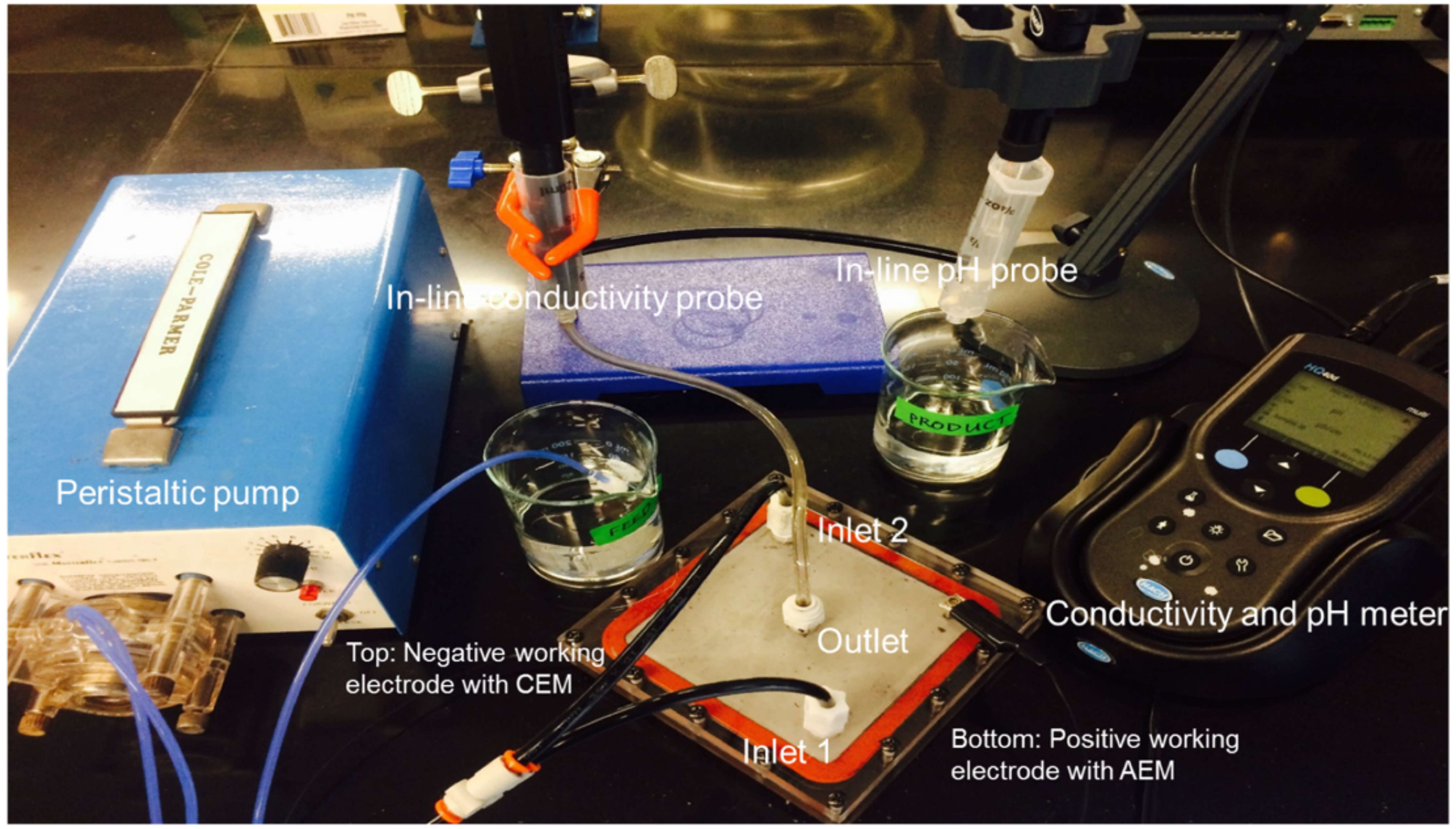

Membrane capacitive deionization unit for electrochemical separations

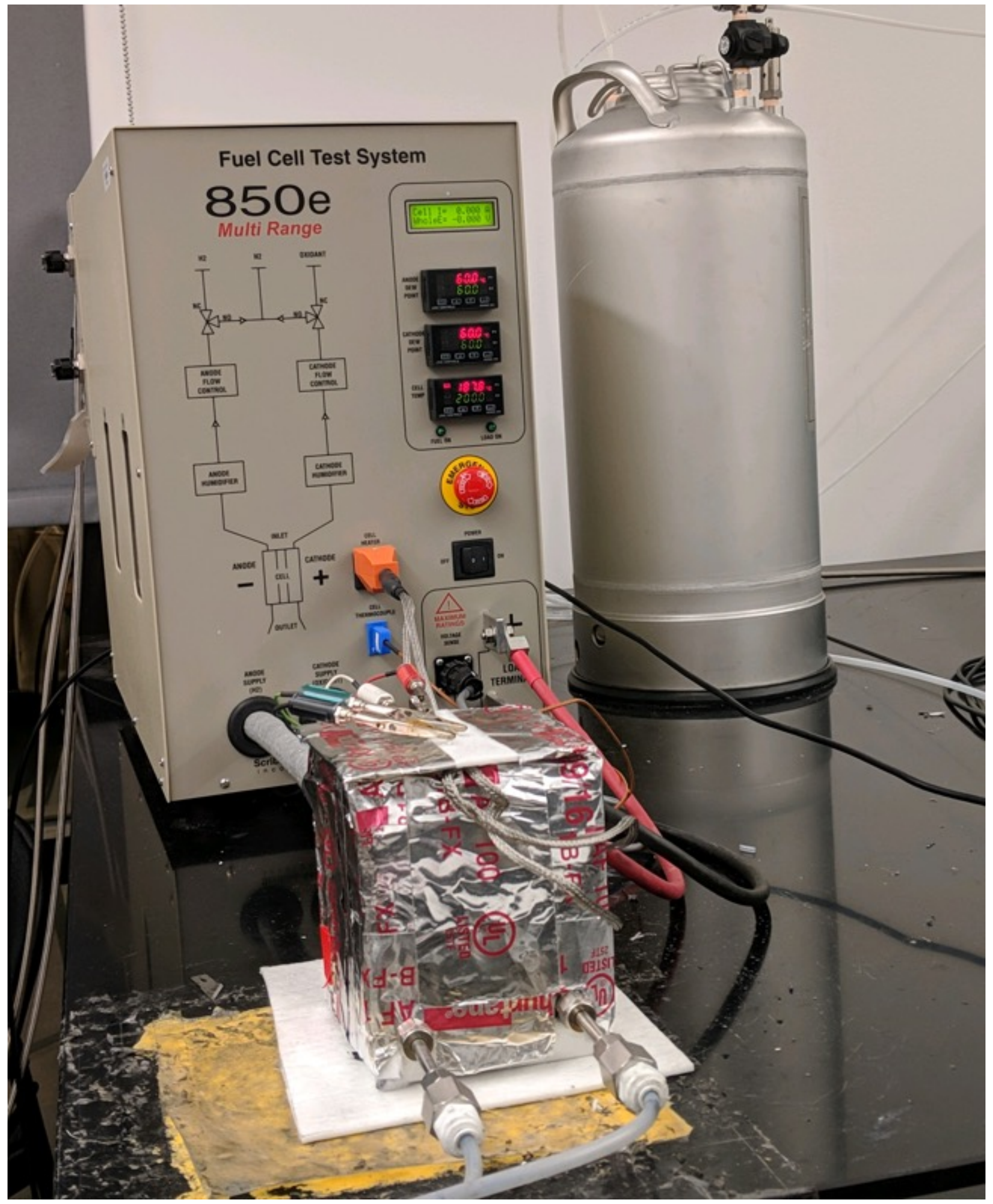

Gas handling test station - fuel cell and electrolysis

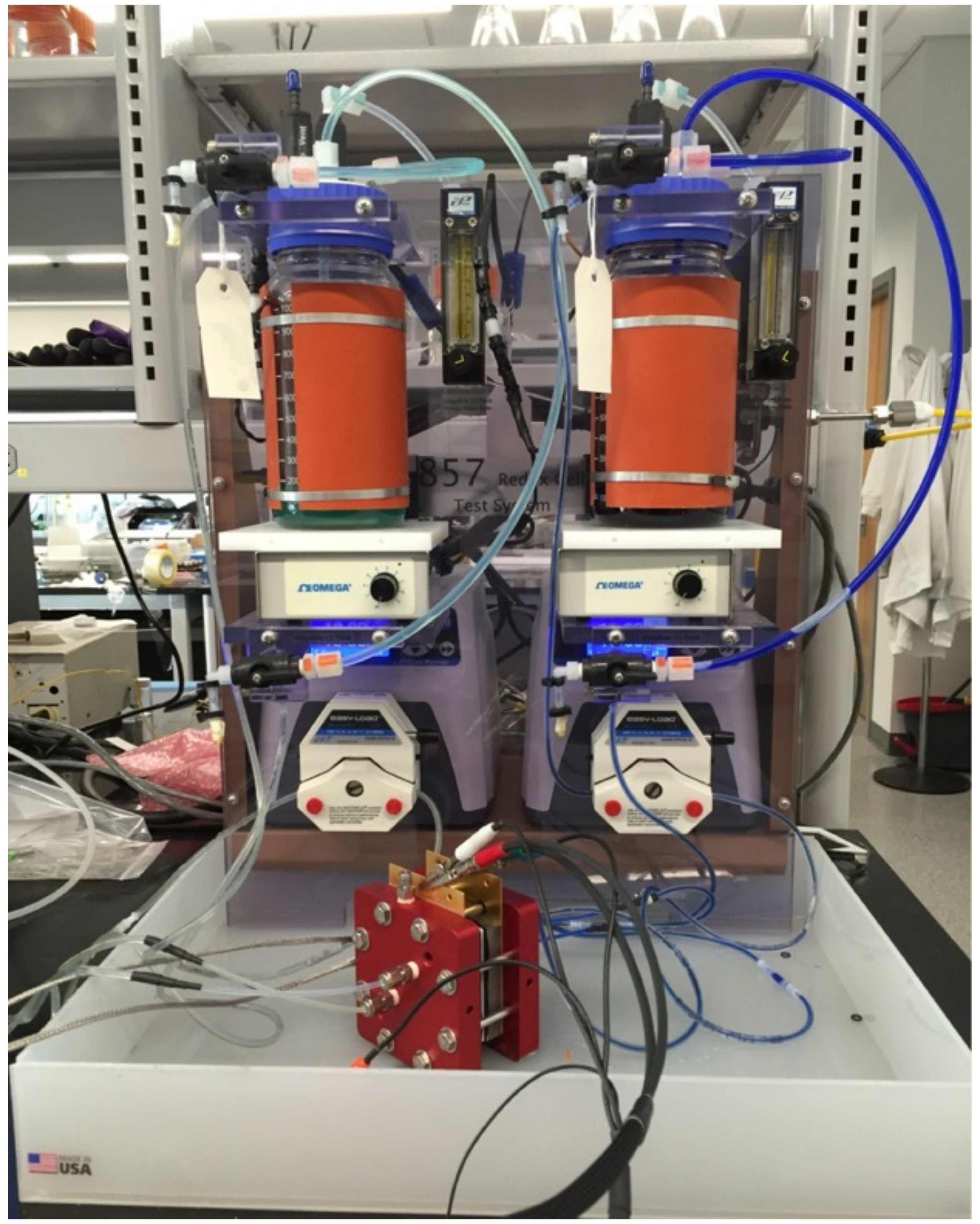

Liquid handling test station - flow battery and electrolysis

Presentation overview

High-temperature polymer electrolyte membranes (HT-PEMs) and binders for fuel cells

Studying the electrochemical properties of electrode ionomer binders as thin films

Future directions and concluding remarks

I see an electric vehicle in your future

All of GM's vehicles will be electric by 2035

Tesla - the most valuable car company

2021 Toyota Mirai Fuel Cell Electric Vehicle
(~ 400 mile range)

Vehicle electrification is critical to the 50% GHG reduction goal by 2030

Fuel cell electric vehicles (FCEVs) v. battery electric vehicles (BEVs)

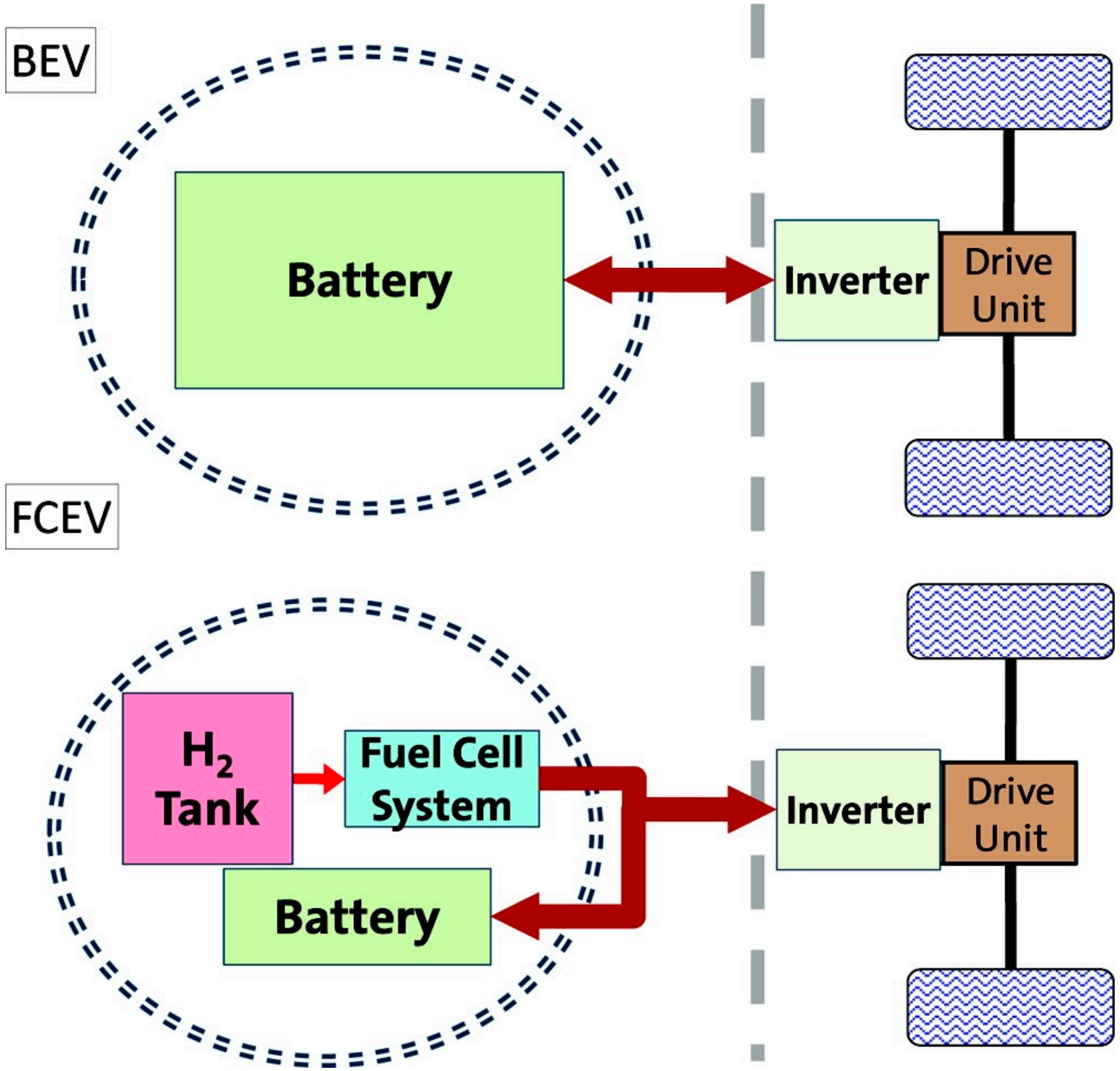

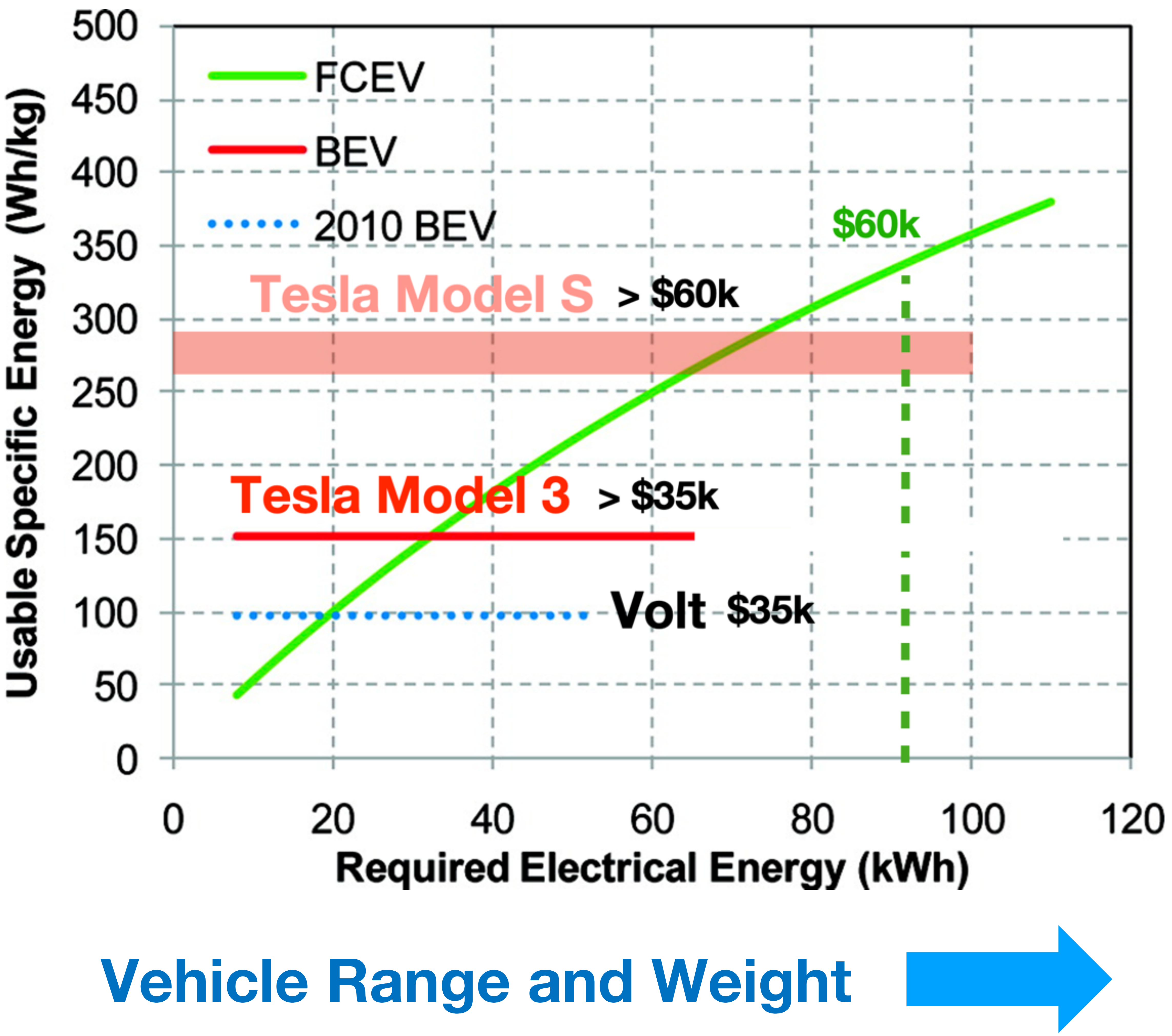

F. Wagner, M. Mathias, *J. Phys. Chem. Lett.*, **2010**

Both battery electric vehicles (BEVs) and fuel cell electric vehicles (FCEVs) warrant continued strong development investment, given the strong societal need for full vehicle electrification ….

One plausible scenario is that both technologies will have a place in the automotive future, with batteries finding theirs in smaller cars for short trips, while *fuel cells find application in larger vehicles used regularly for longer trips*. ~ *General Motors (2010)*

Fuel cell

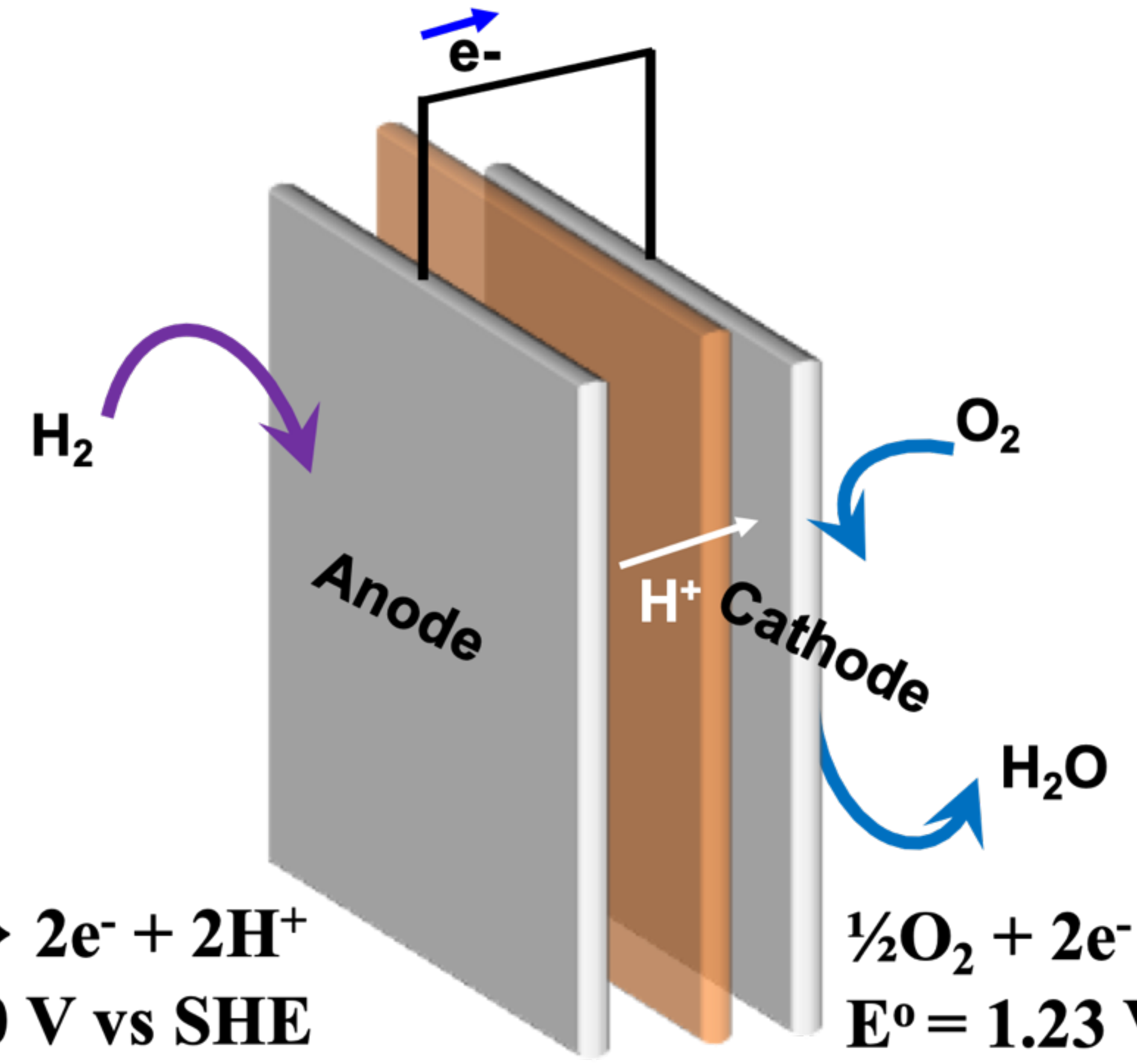

$H_2 \longrightarrow 2e^- + 2H^+$
$E^o = 0$ V vs SHE

$\frac{1}{2}O_2 + 2e^- + 2H^+ \longrightarrow H_2O$
$E^o = 1.23$ V vs SHE

F. Wagner, M. Mathias, *J. Phys. Chem. Lett.*, **2010**

Fuel cell stacks - modular systems

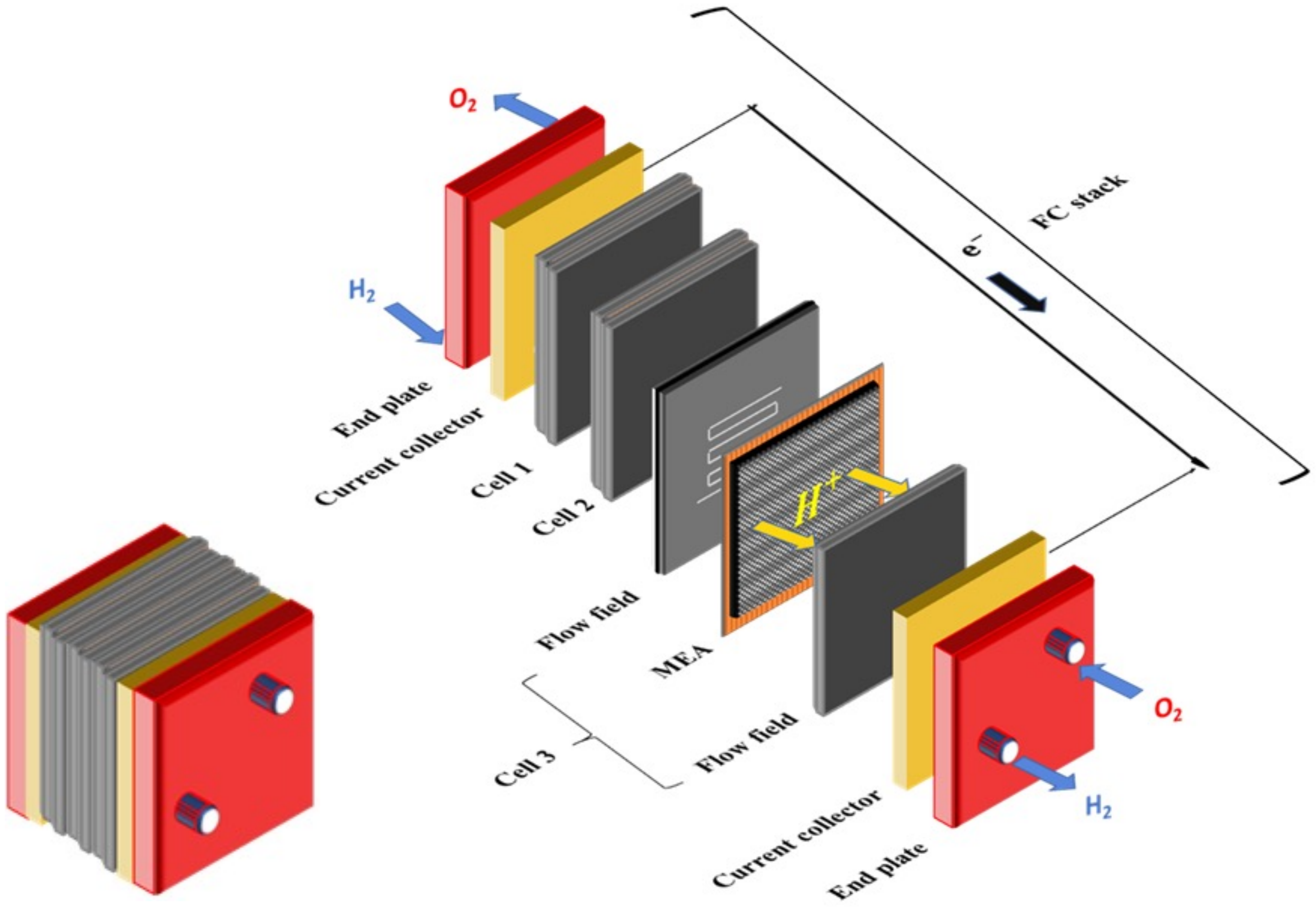

Power = I x V

The stack requires coolant delivered by a radiator because the redox reactions in each cell generates heat

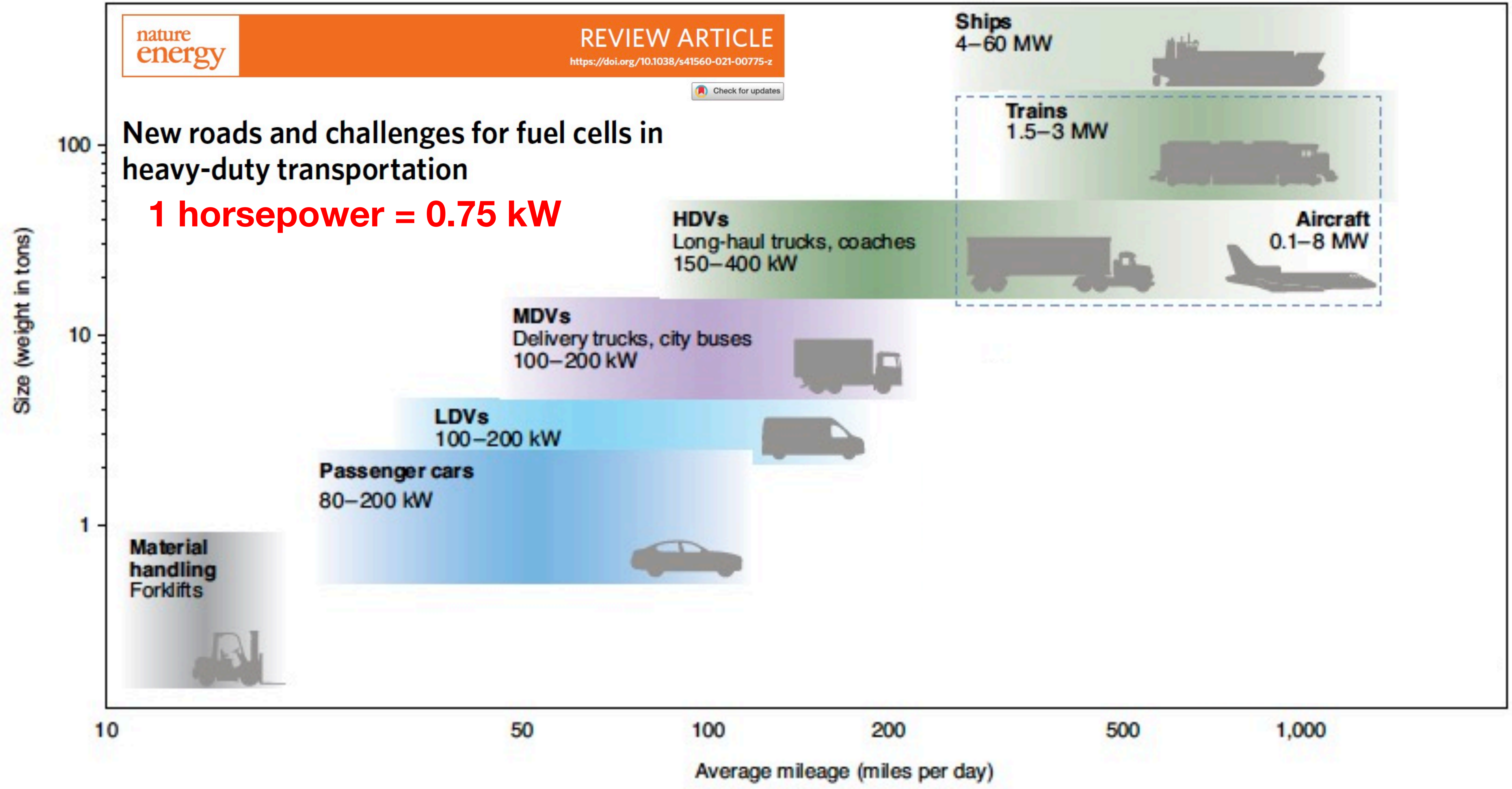

Vehicle Range and Weight

D.A. Cullen, A. Kusoglu, *et al.*, *Nature Energy*, **2021**

HDVs and fuel cell stack heat management

Heavy duty vehicles (HDVs)

<u>**HDV (class 8 tractor trailers) - US DOE**</u>
- **up to 400 kW stacks**
- **25,000 hours of stability**
- **$80 kW^{-1}**
- **68% efficiency**

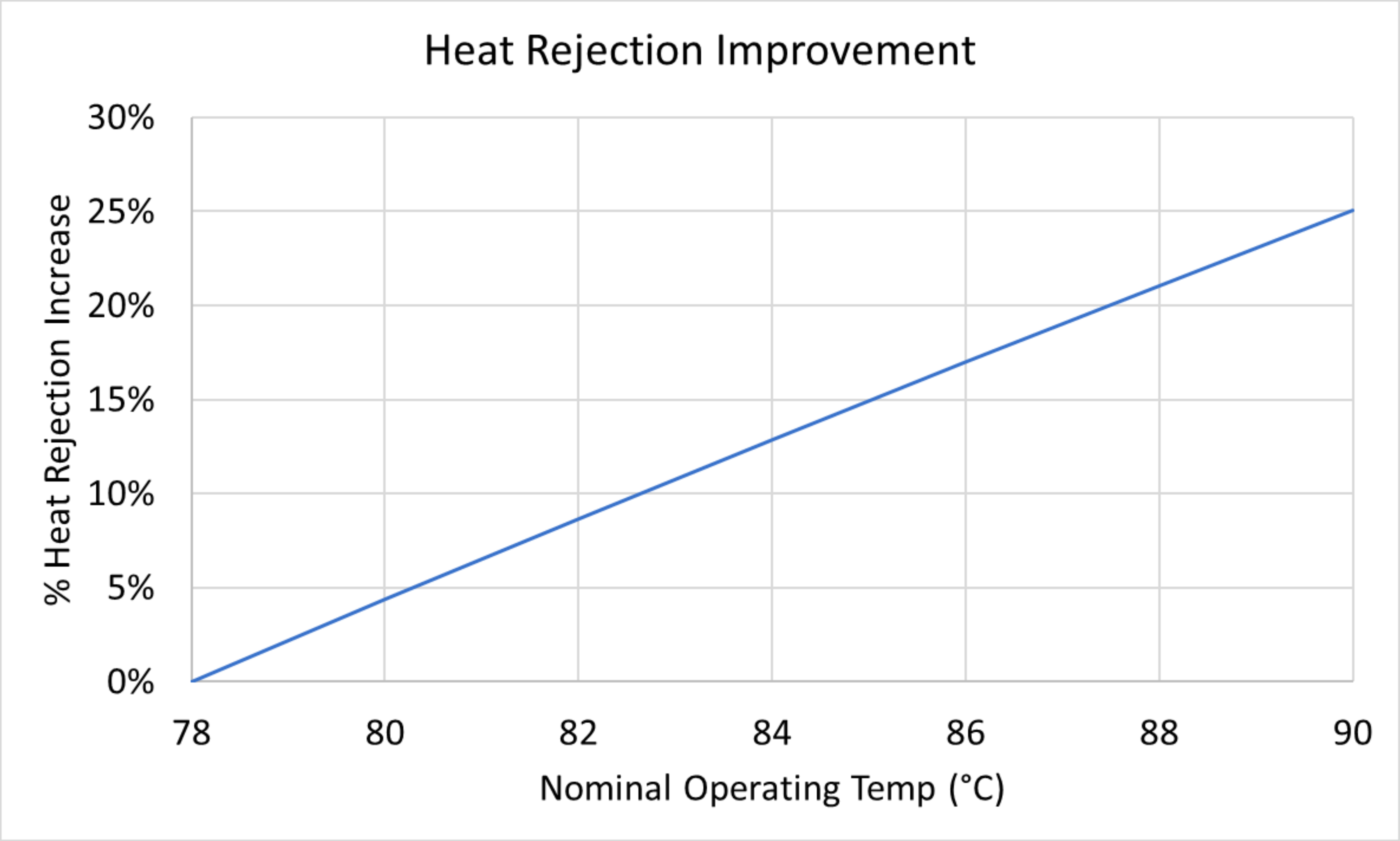

$$Q = UA(T_{stack} - T_{environment})$$

Operating the cell at higher temperatures yields better heat rejection

D. Papageorgopoulos, US DOE, HFTO, **2020**

V. Murthi, US DOE HTPEM Workshop, Nikola Motor **2020**

Limitations of Nafion® at elevated temperatures

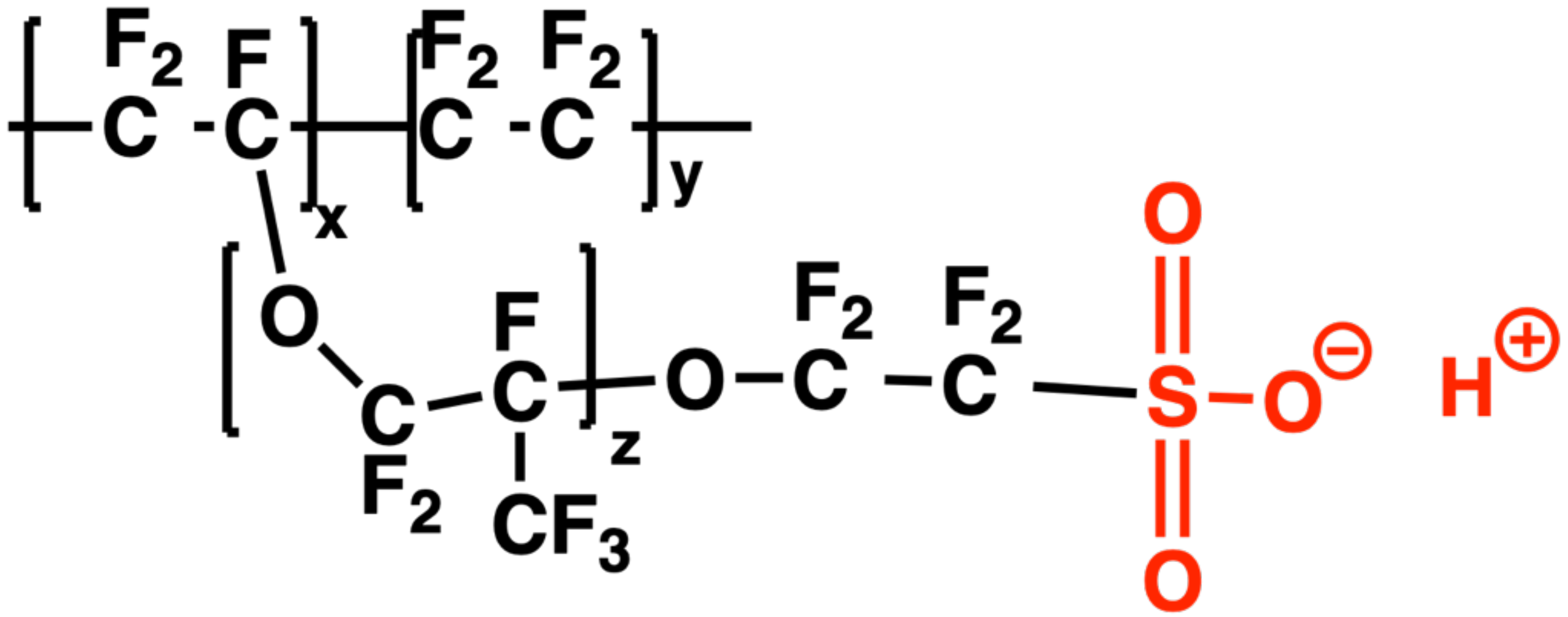

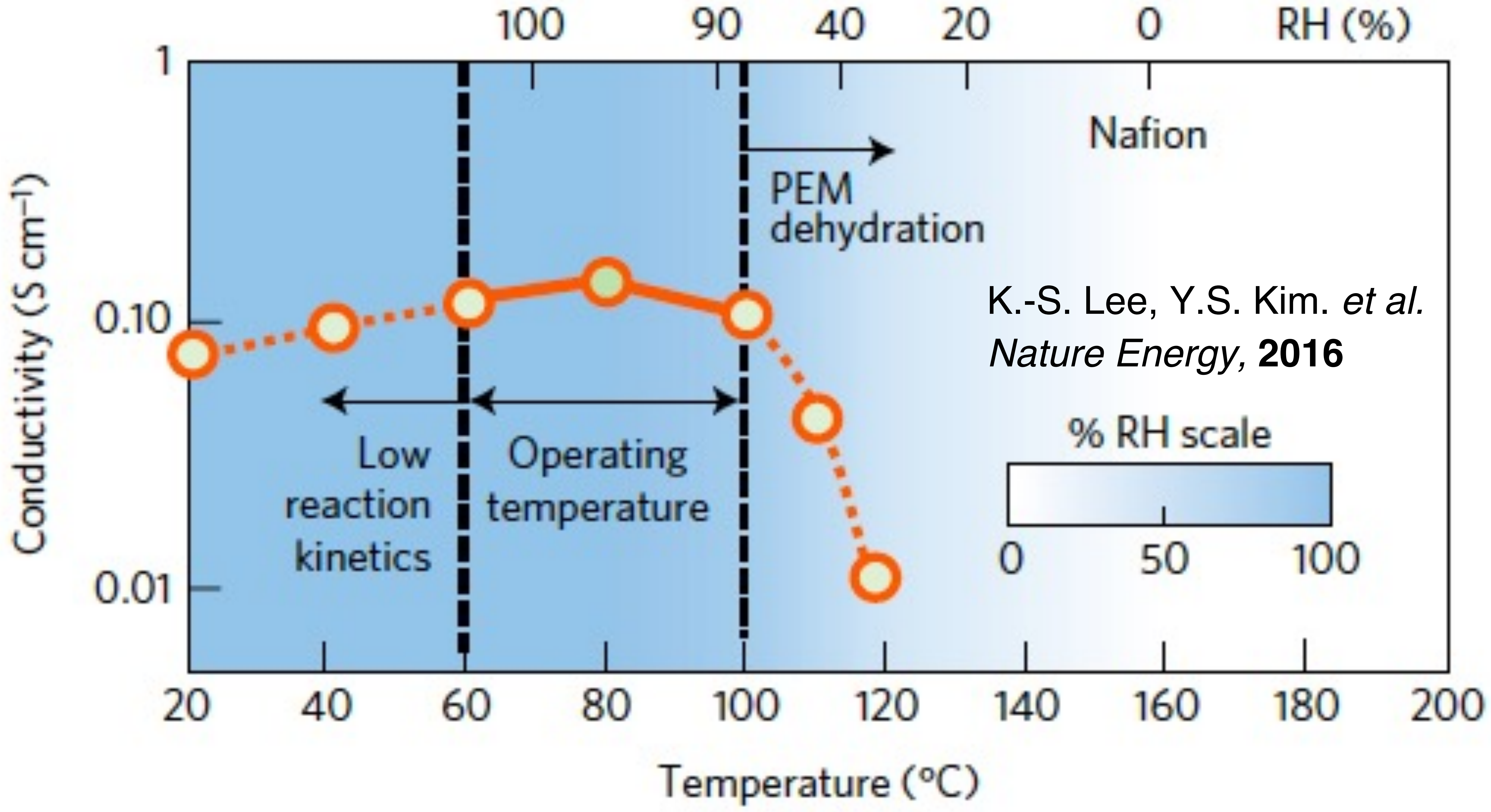

$$\eta_{ohmic} = iR = i\frac{\delta}{\kappa}$$

η_{ohmic} = ohmic overpotential (V)
κ = ionic conductivity
R = area specific resistance (Ω-cm^2)
δ = membrane thickness
i = current density (A cm^{-2})

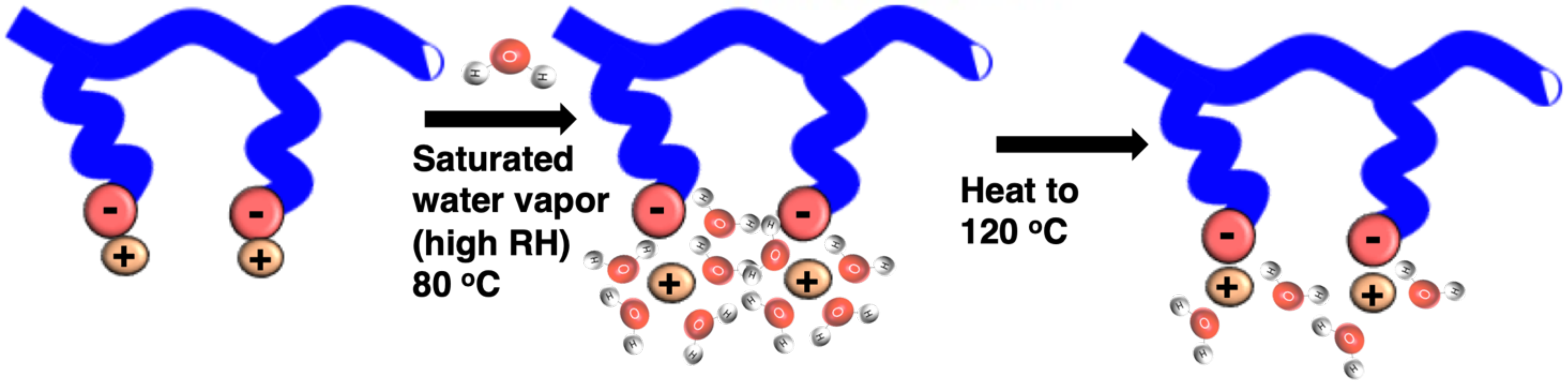

Condensed water within the PFSA dissociates ionic charge pairs & mediates conductivity

New HT-PEM based on phosphate ion-pairs

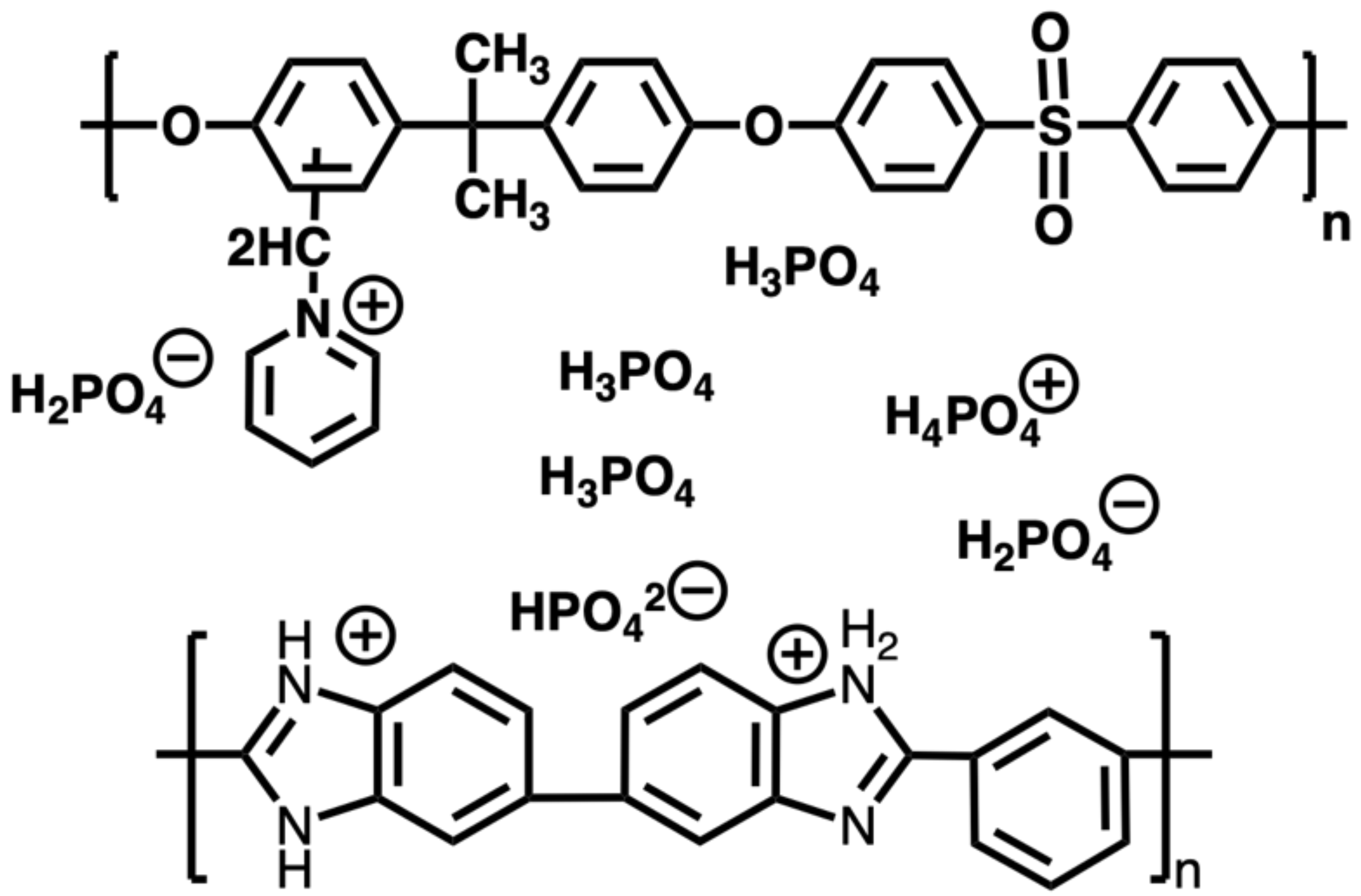

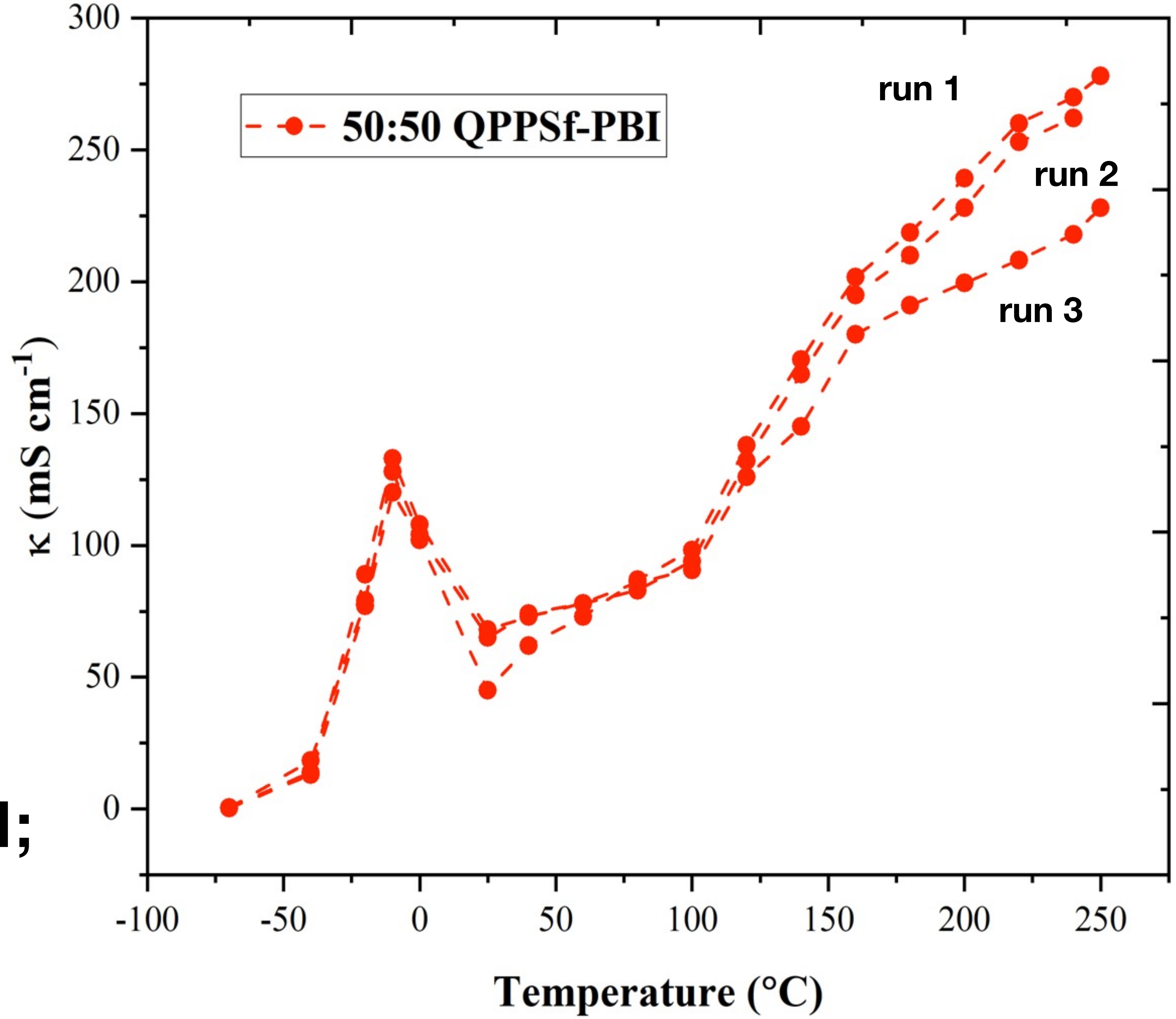

Stable membrane across a wide range of conditions: 220 °C/0% RH and 80 °C/40% RH; >100 hours in fuel cell at 200 °C

A. Chaichi, G. Venugopalan C.G. Arges, M.R. Gartia, *ACS Applied Energy Materials*, **2020**

G. Venugopalan, C.G. Arges *et al., ACS Applied Energy Materials*, **2020**

C.G. Arges, *U.S. Patent Application #62,656,538* **2018**

Preparation of polycation-PBI blends for use as HT-PEMs

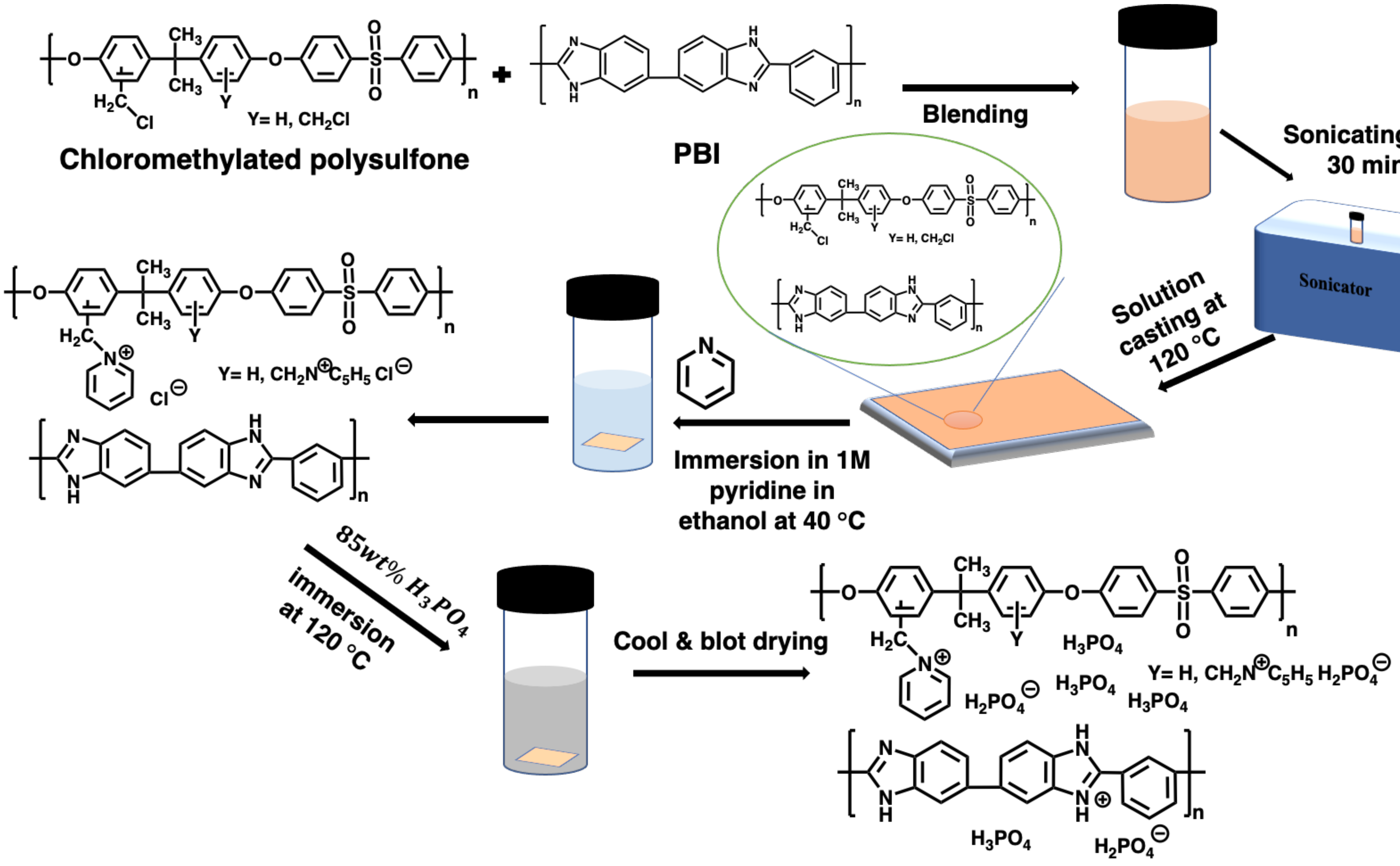

Dr. Gokul Venugopalan
PhD 2021

Fuel cell performance with new HT-PEMs

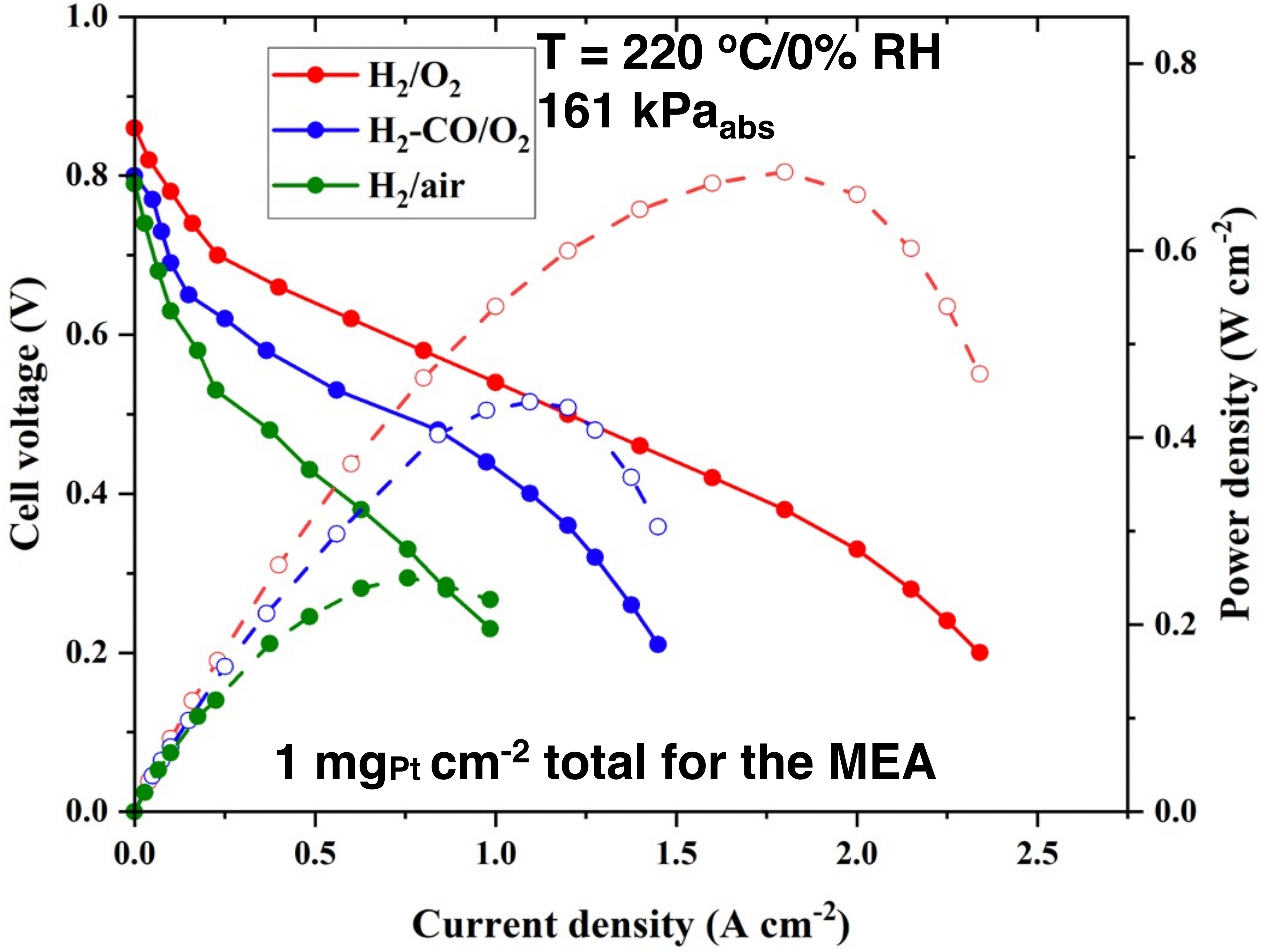

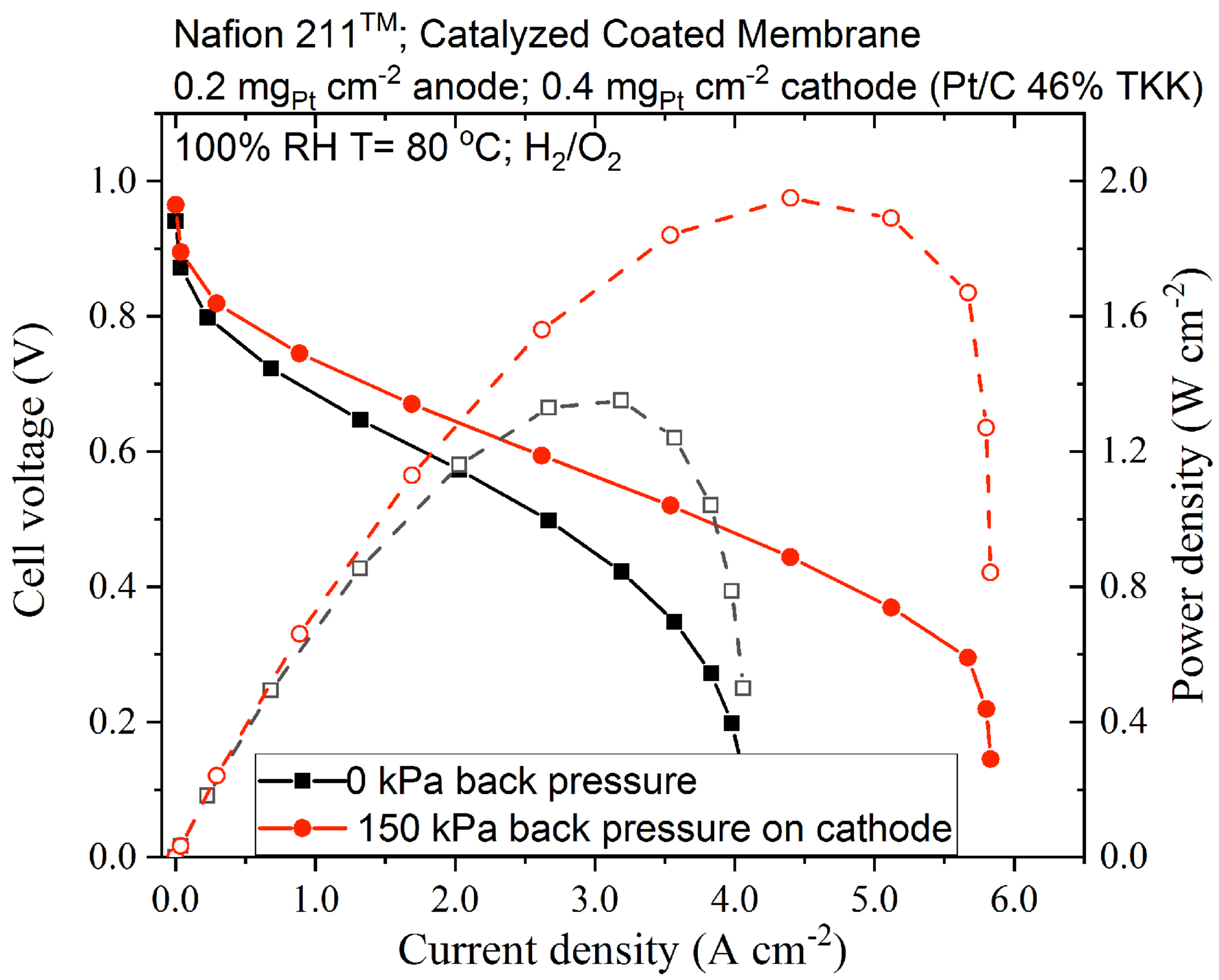

Troy Porter
LSU BS ChE 2018
now at Jacobs Engineering

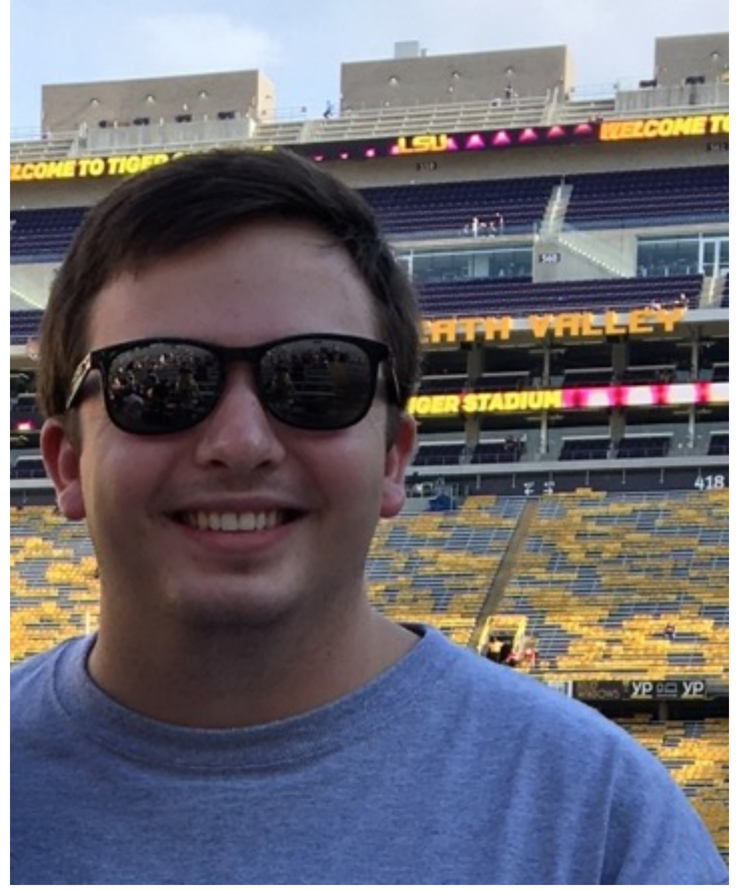

Reasonable power density was attained

Cell could be operated with 25% CO in the fuel stream

G. Venugopalan, C.G. Arges *et al.*, *ACS Applied Energy Materials*, **2020**

Electrode ionomer has a profound impact on performance

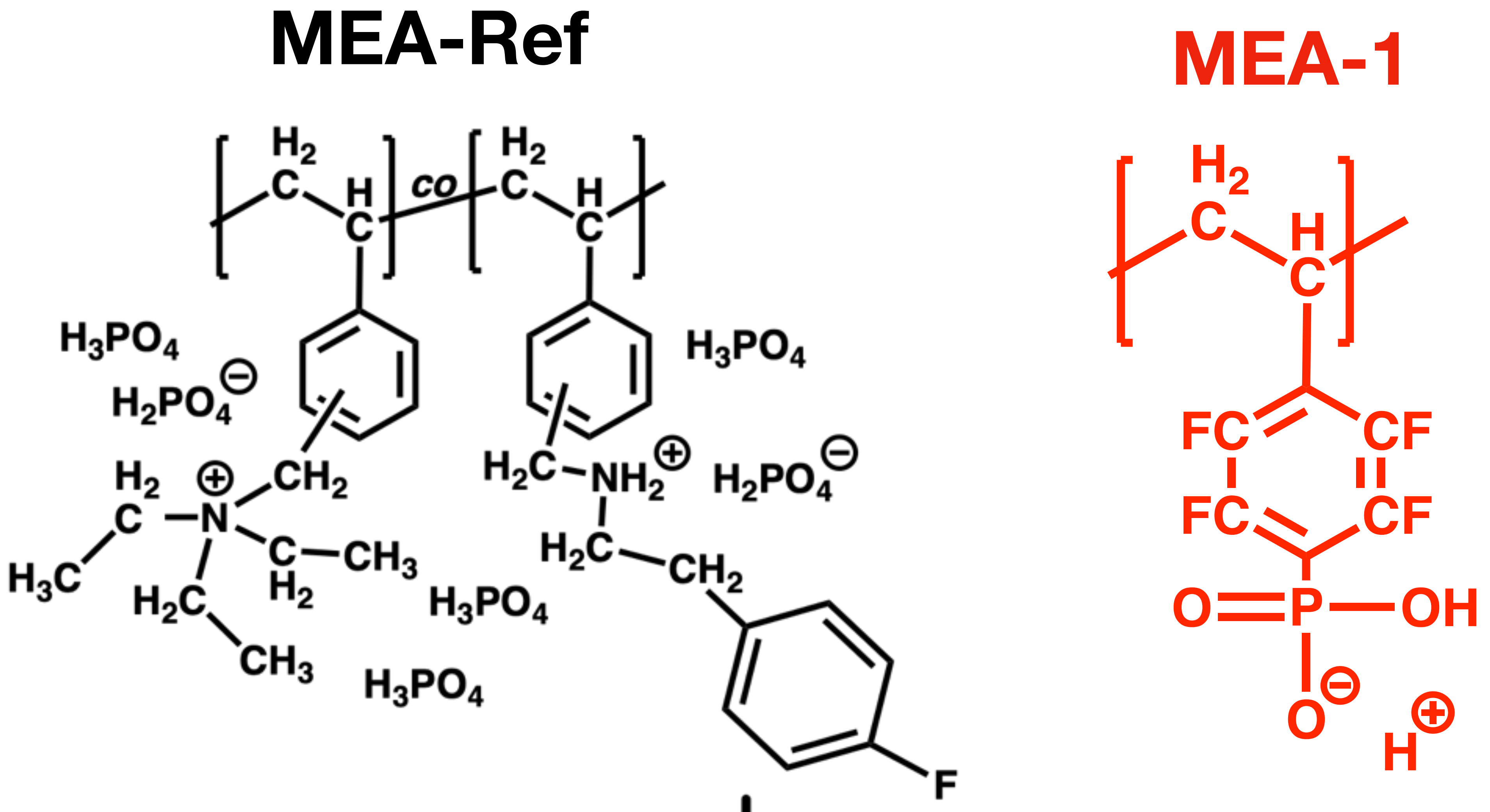

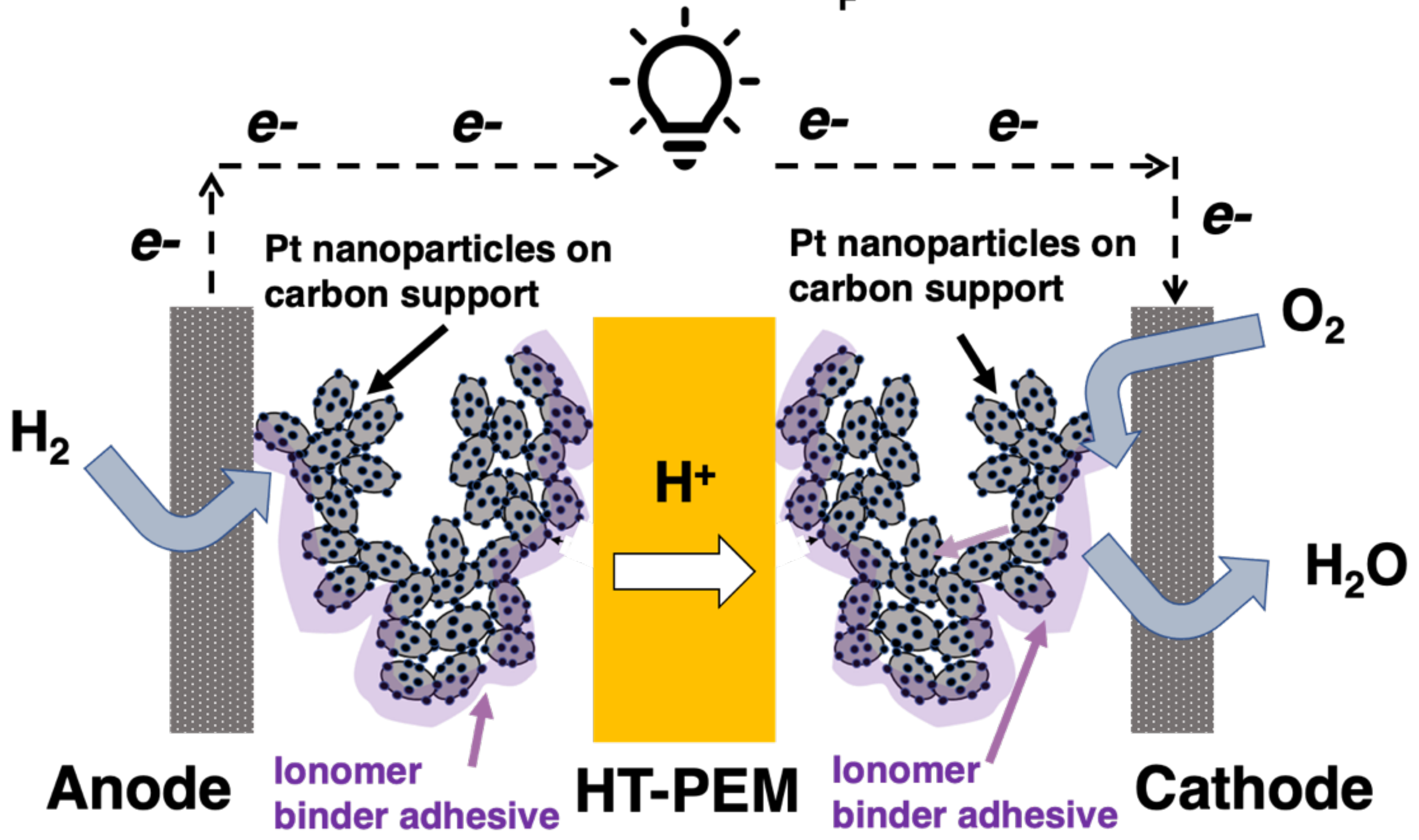

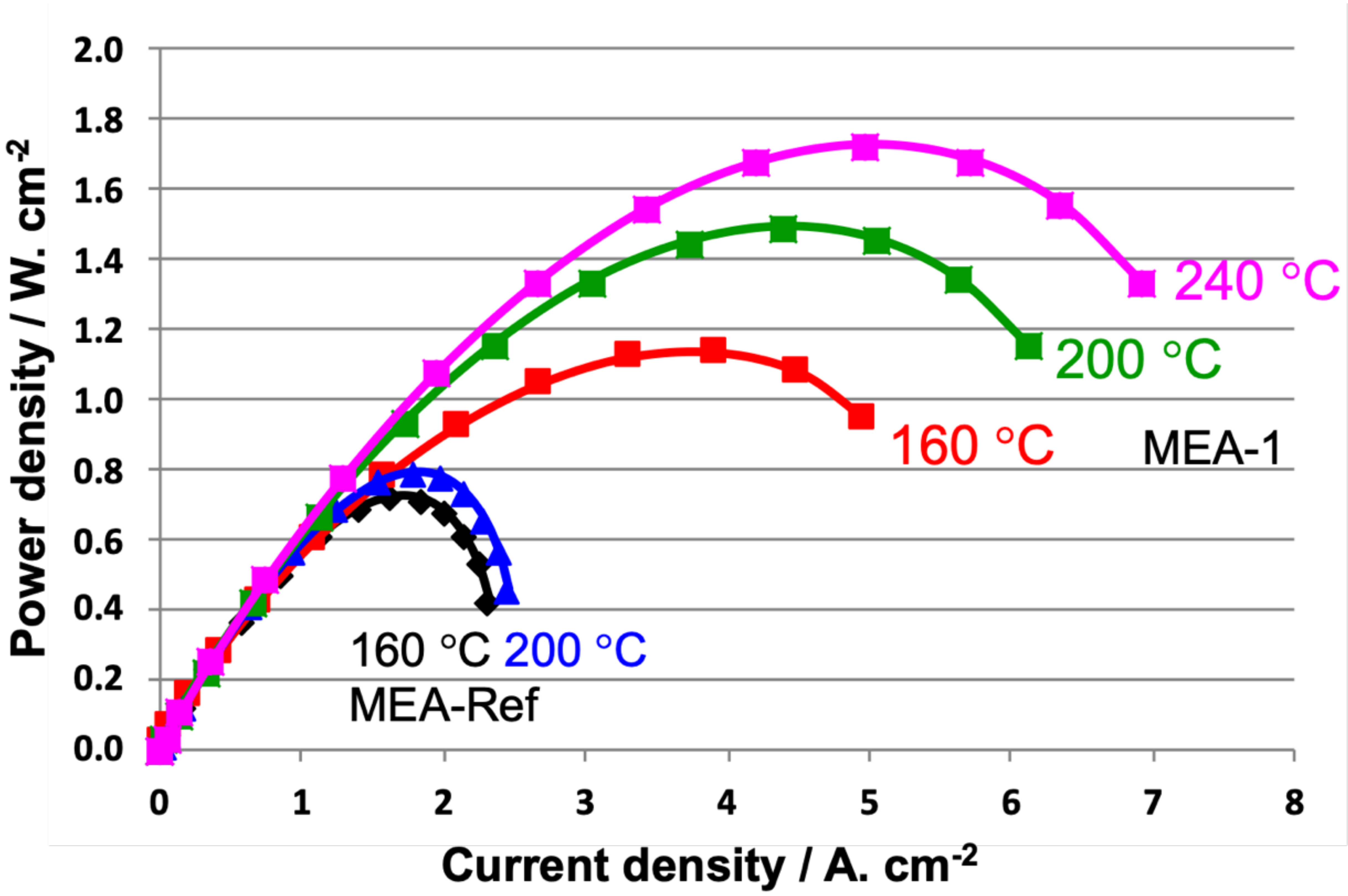

By switching the electrode binder, Los Alamos doubled its power density

V. Atanasov, J. Kerres, Y.S. Kim *et al., Nature Materials*, **2021** Y.S. Kim. *et al. Nature Energy*, **2016**; *et al. Energy Environ. Sci.*, **2018**

Synthesis of phosphonic acid ionomers

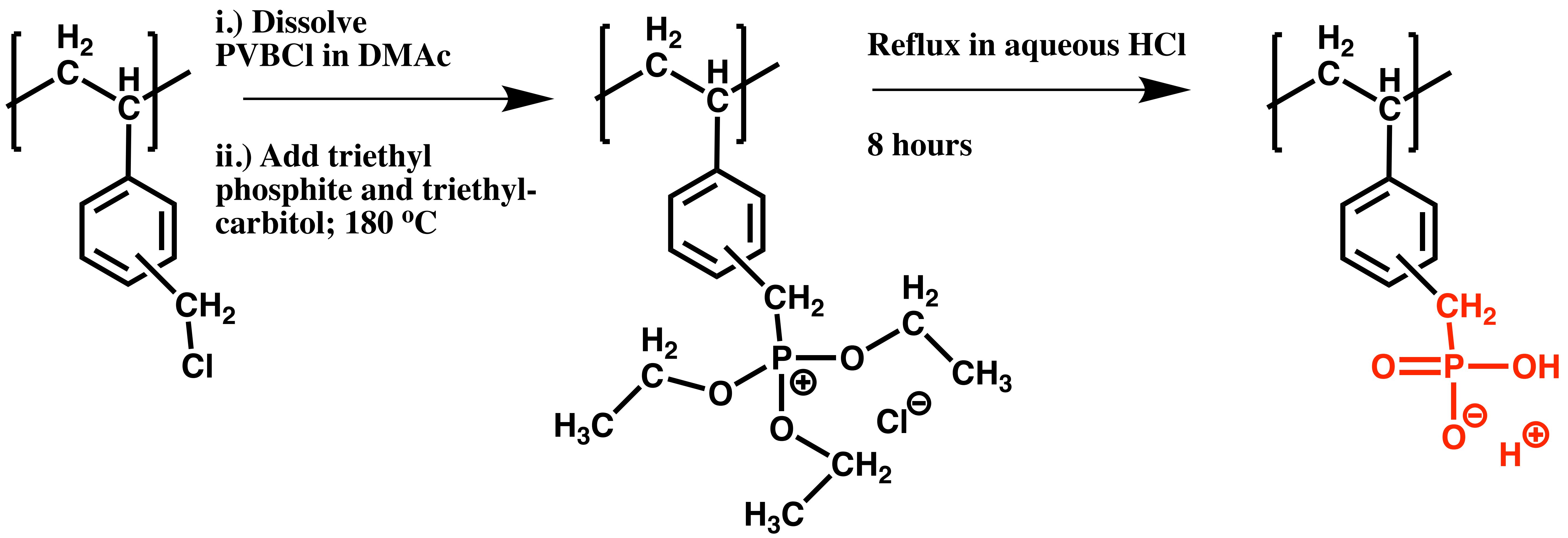

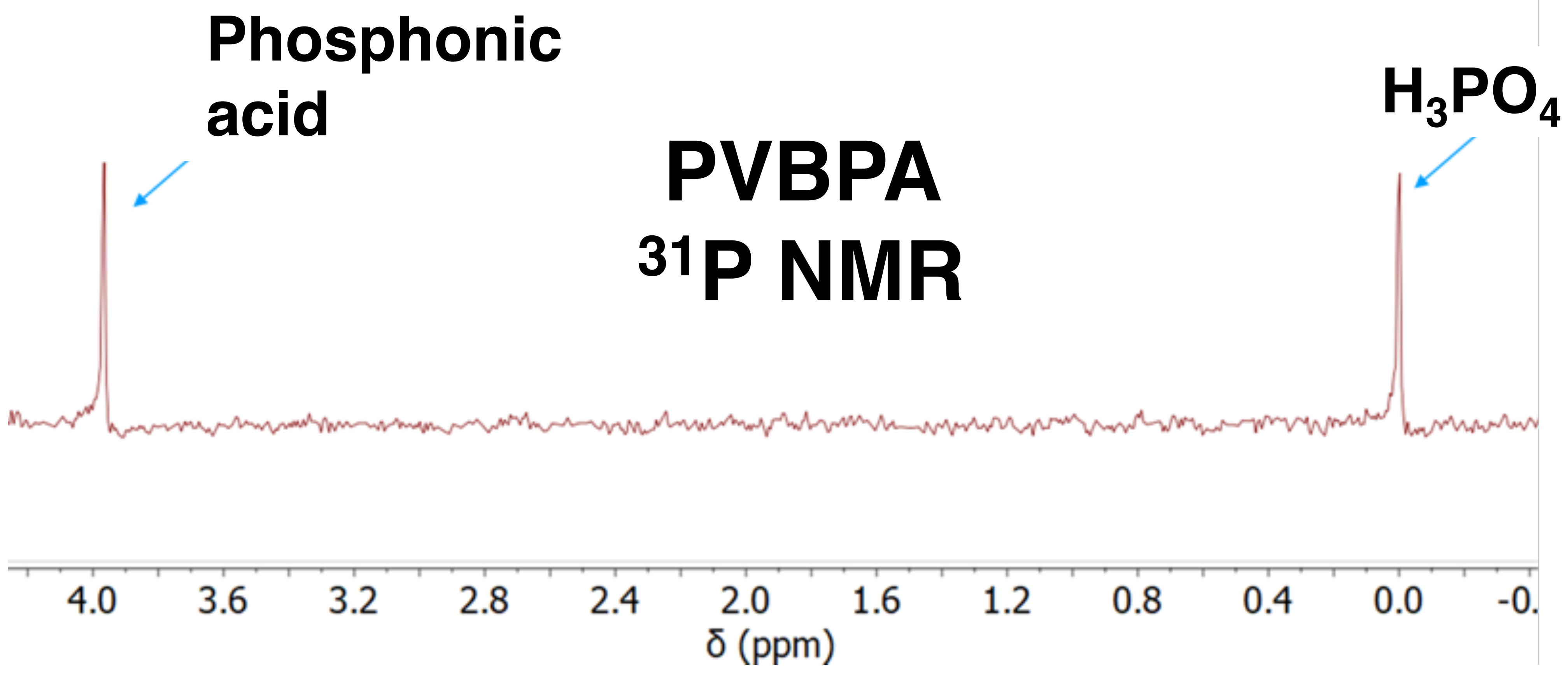

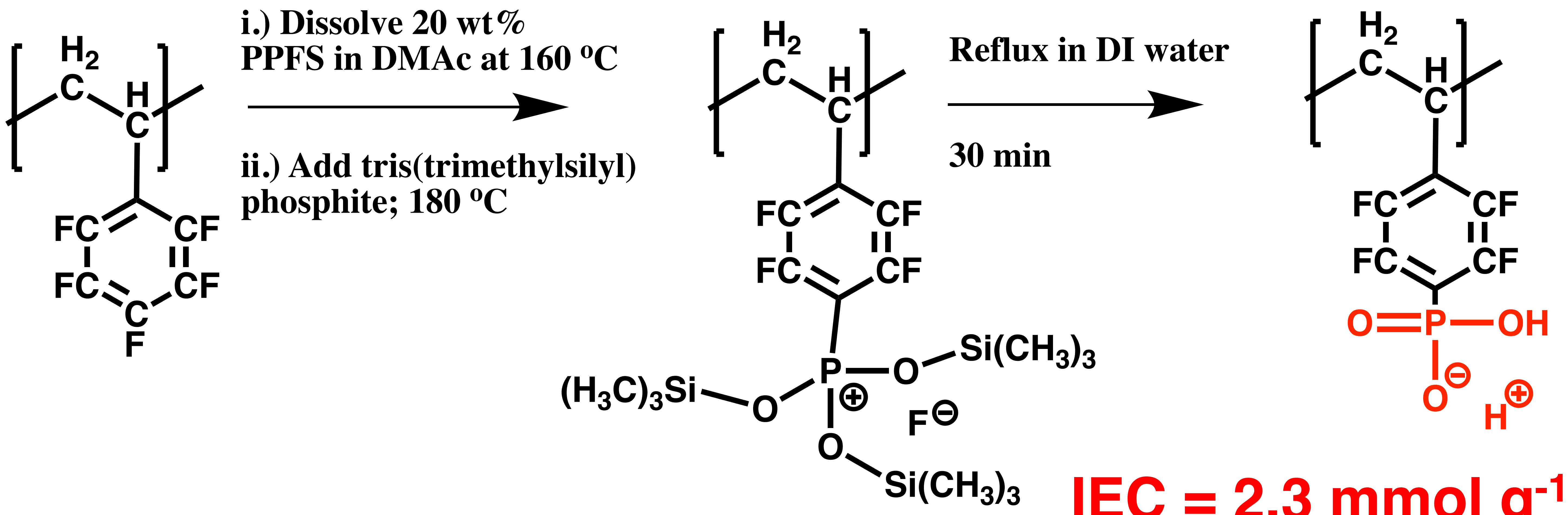

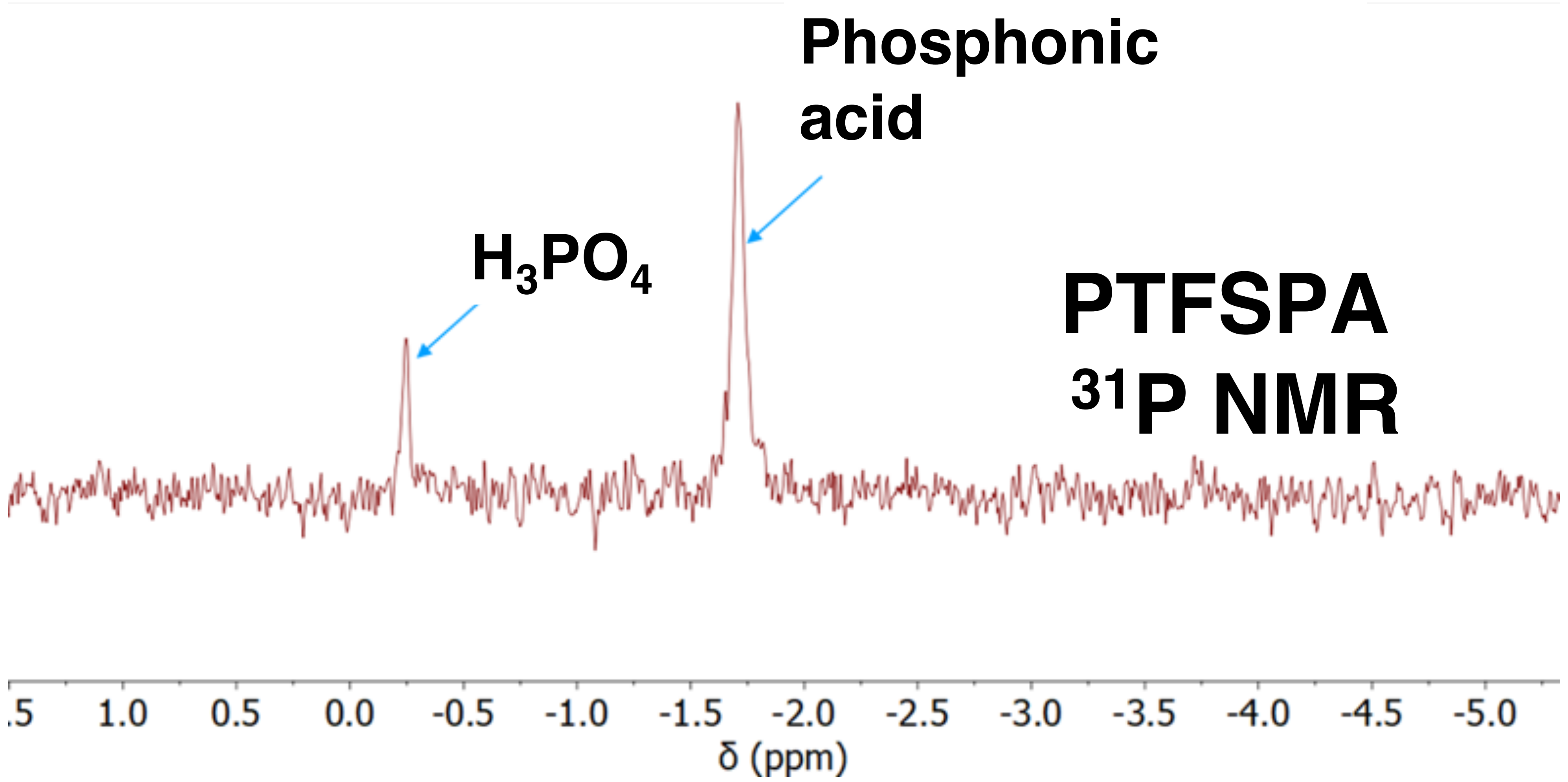

IEC = 2.3 mmol g^{-1} (titration)

V. Atanasov, J. Kerres, *et al., J. Power Sources*, **2017**

Properties of phosphonic acid ionomers

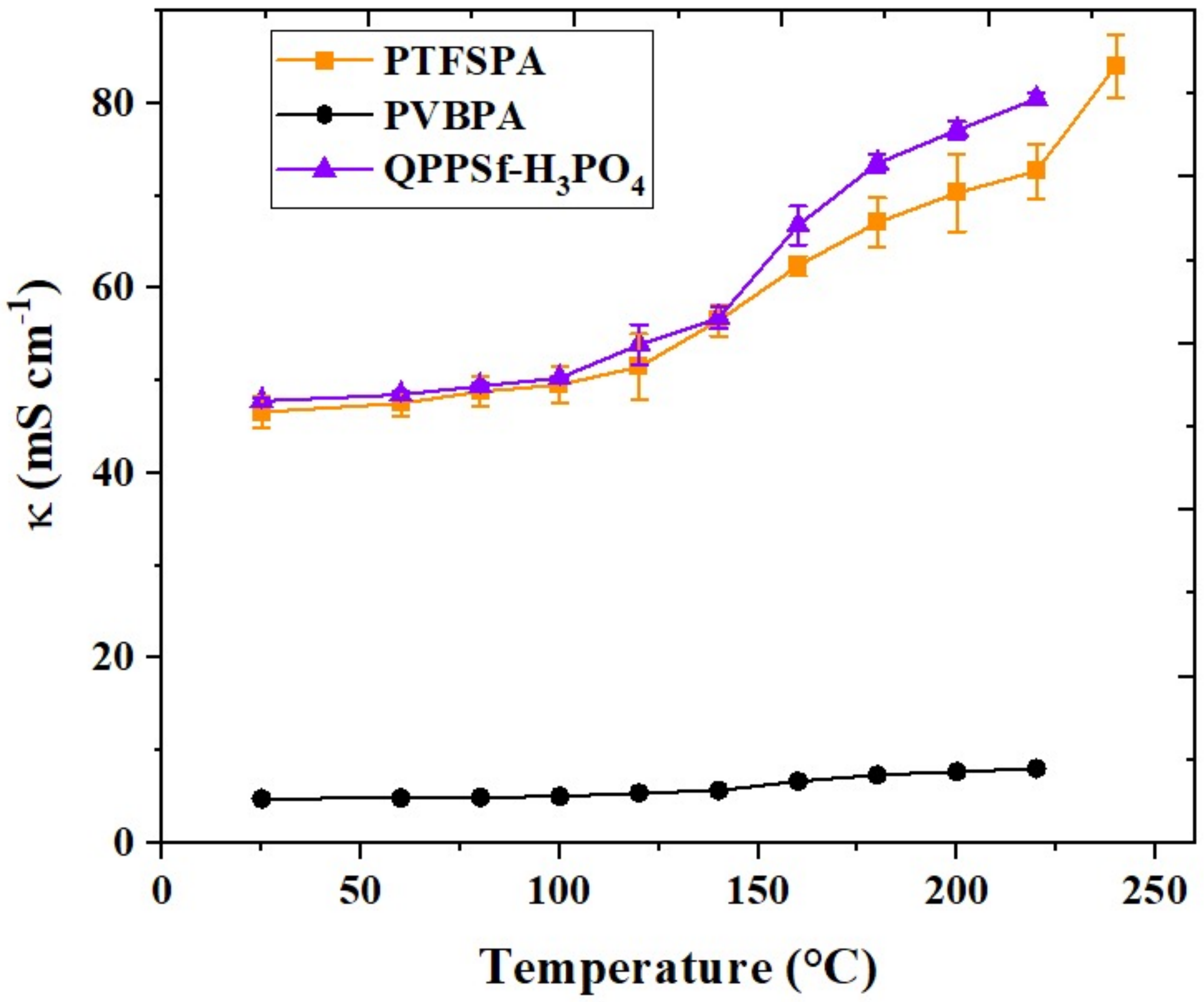

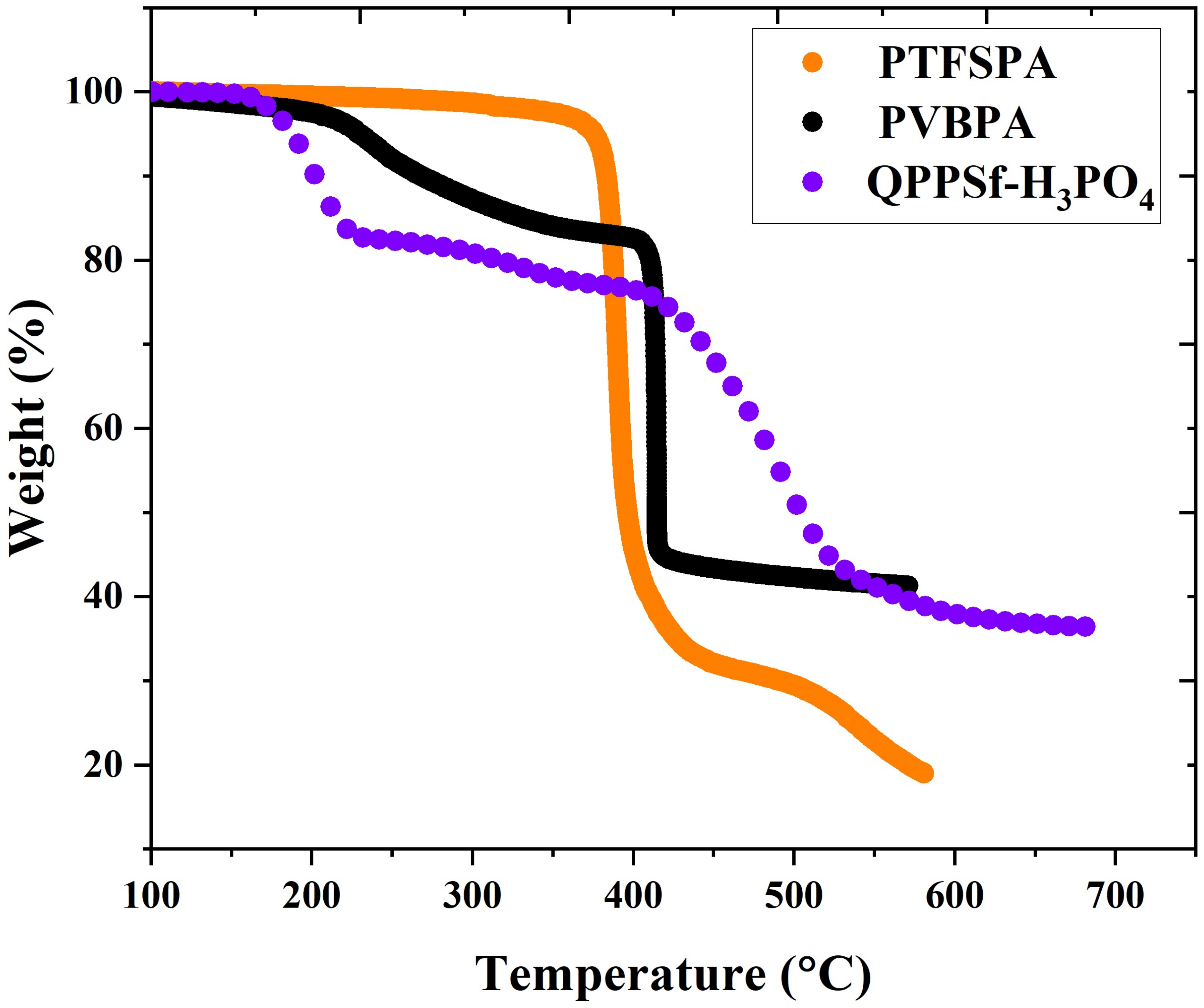

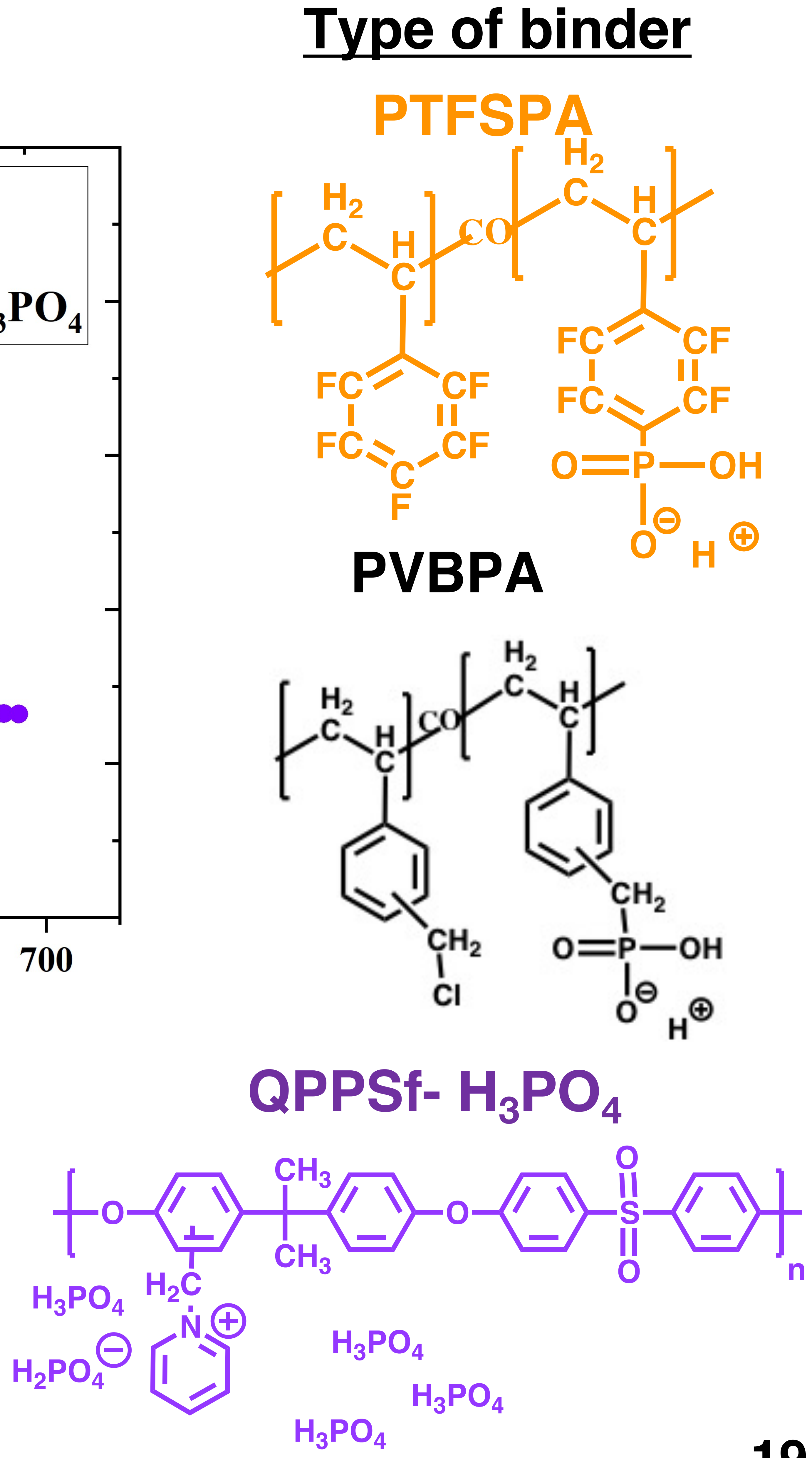

PTFSPA shows the same thin film conductivity as QPPSf-H_3PO_4 and has excellent thermal stability

G. Venugopalan, C.G. Arges, *Materials Advances (revision submitted)*

Our fuel cell data with phosphonic acid ionomer binders

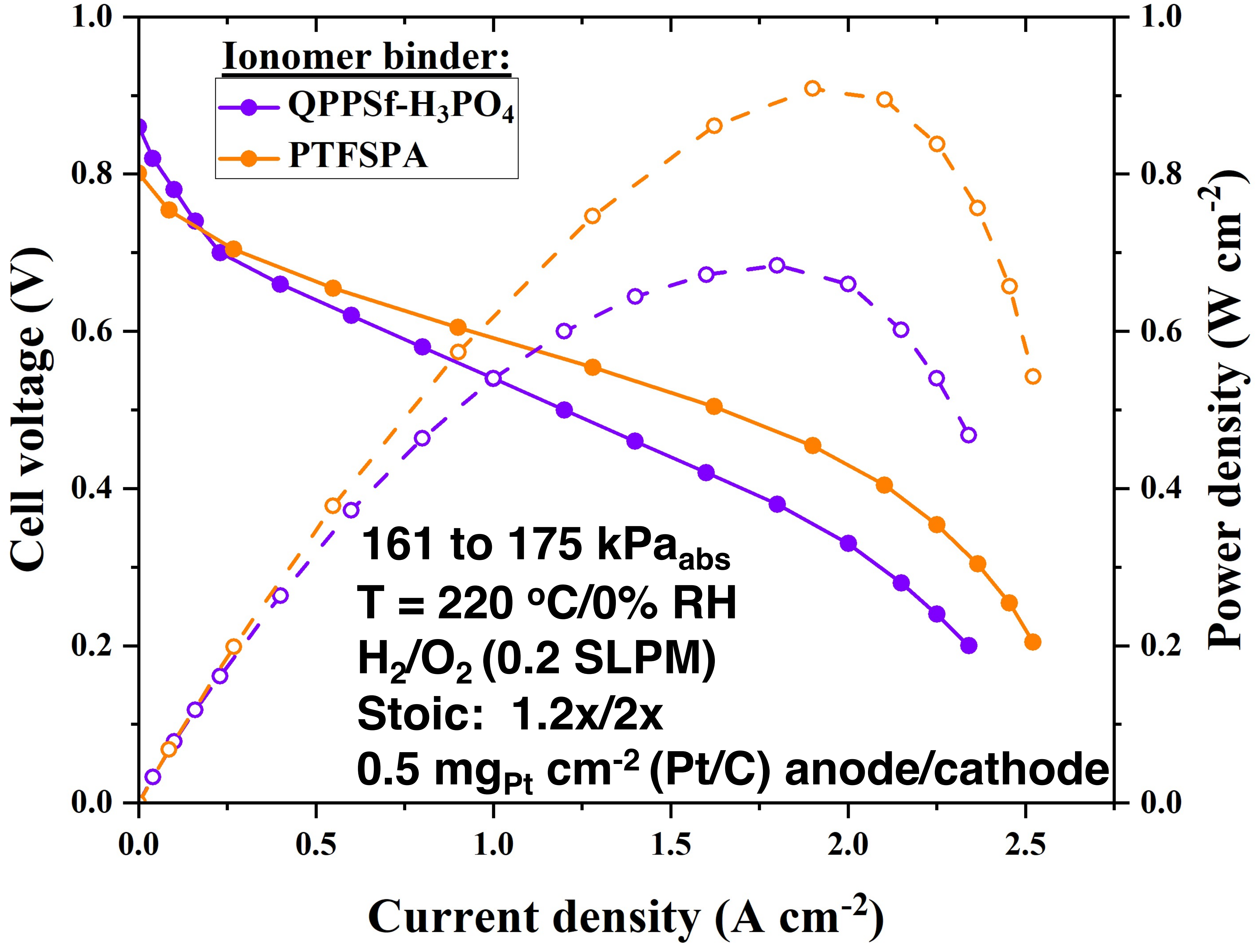

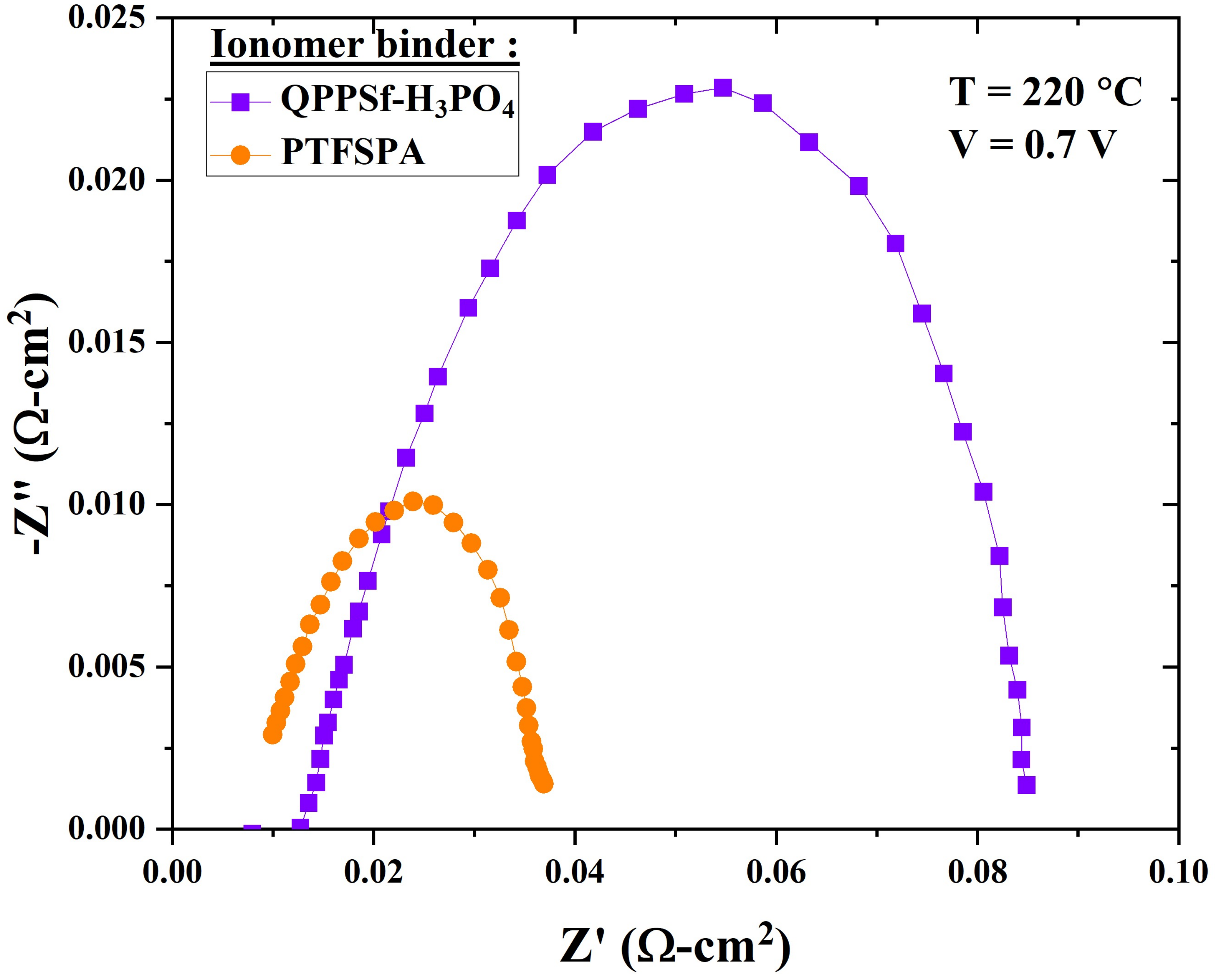

Type of binder

PTFSPA

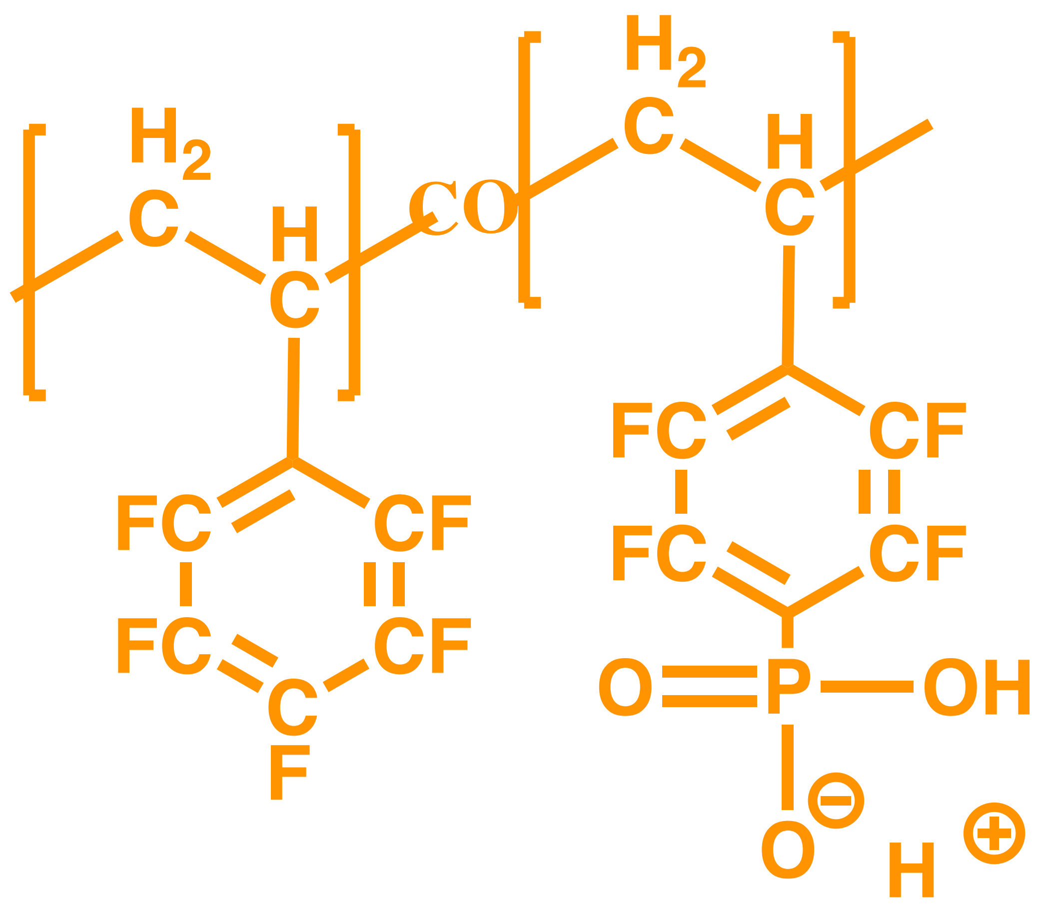

QPPSf- H_3PO_4

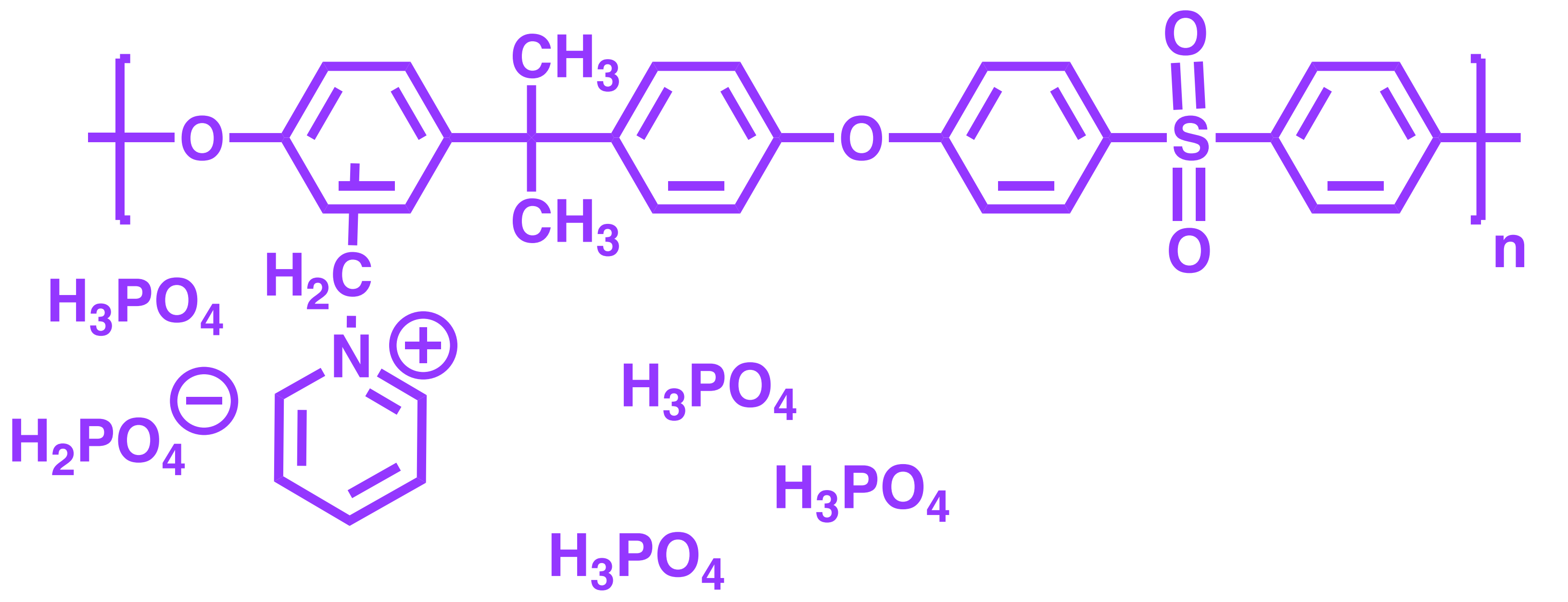

By switching the electrode binder only, fuel cell performance improved because of improved electrode kinetics

Presentation overview

High-temperature polymer electrolyte membranes (HT-PEMs) and binders for fuel cells

Studying the electrochemical properties of electrode ionomer binders as thin films

Future directions and concluding remarks

Property requirement differences: binders vs. membranes

Membrane

- Low gas (H_2 & O_2) permeability
- Mechanically robust
- Electron insulating

Membrane & Binder

- High ionic conductivity
- Chemically & thermally stable
- No excessive swelling

Binder

- Good gas (H_2 & O_2) permeability
- Solution processable (low boiling point & non-toxic solvents preferred)
- Small to negligible interaction with catalyst surface
- Electrically conductive is a plus

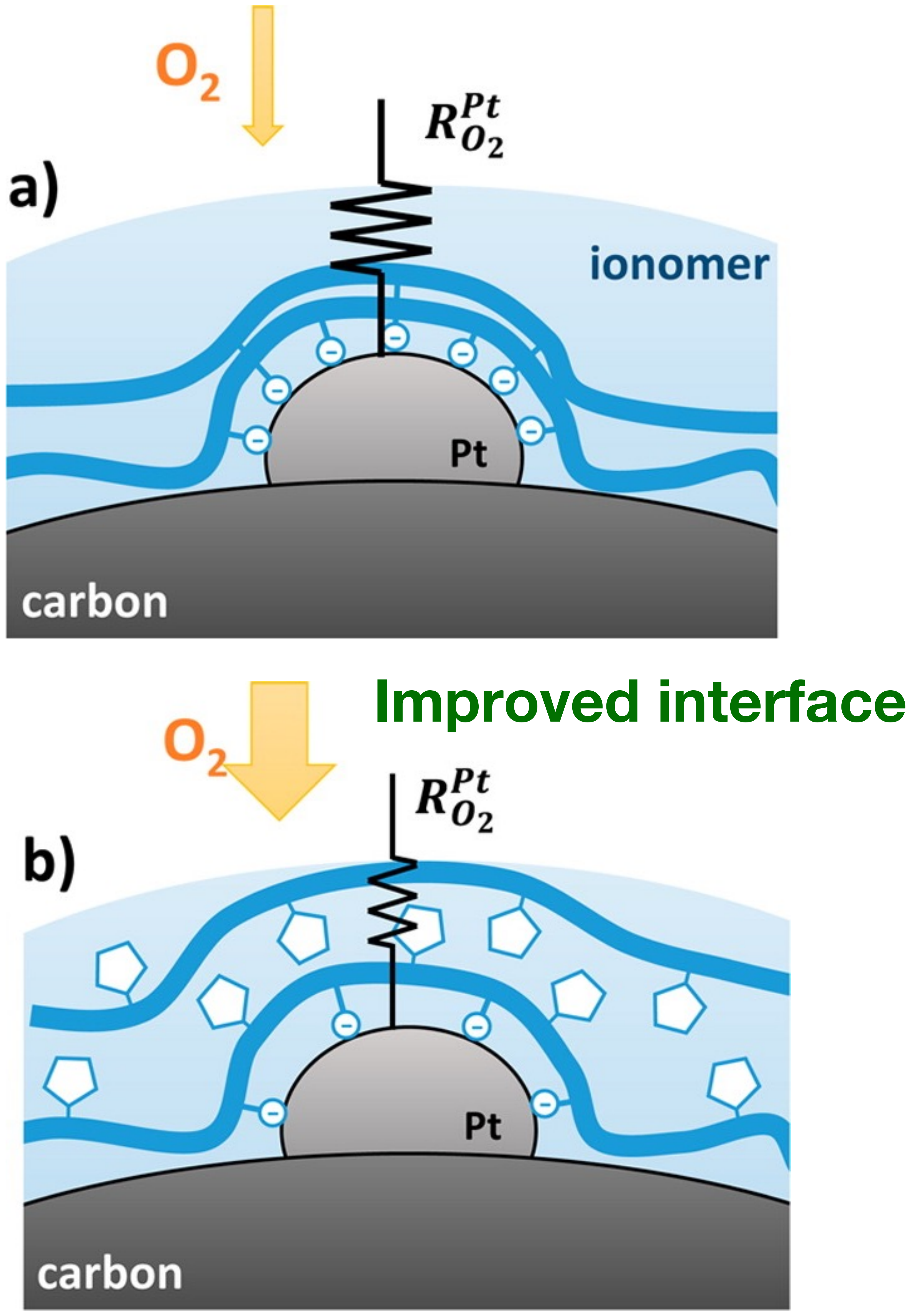

A. Kongkanand & M. Mathias, *J. Phys. Chem. Lett.*, **2016**

Motivation for studying thin film polymer electrolyte properties

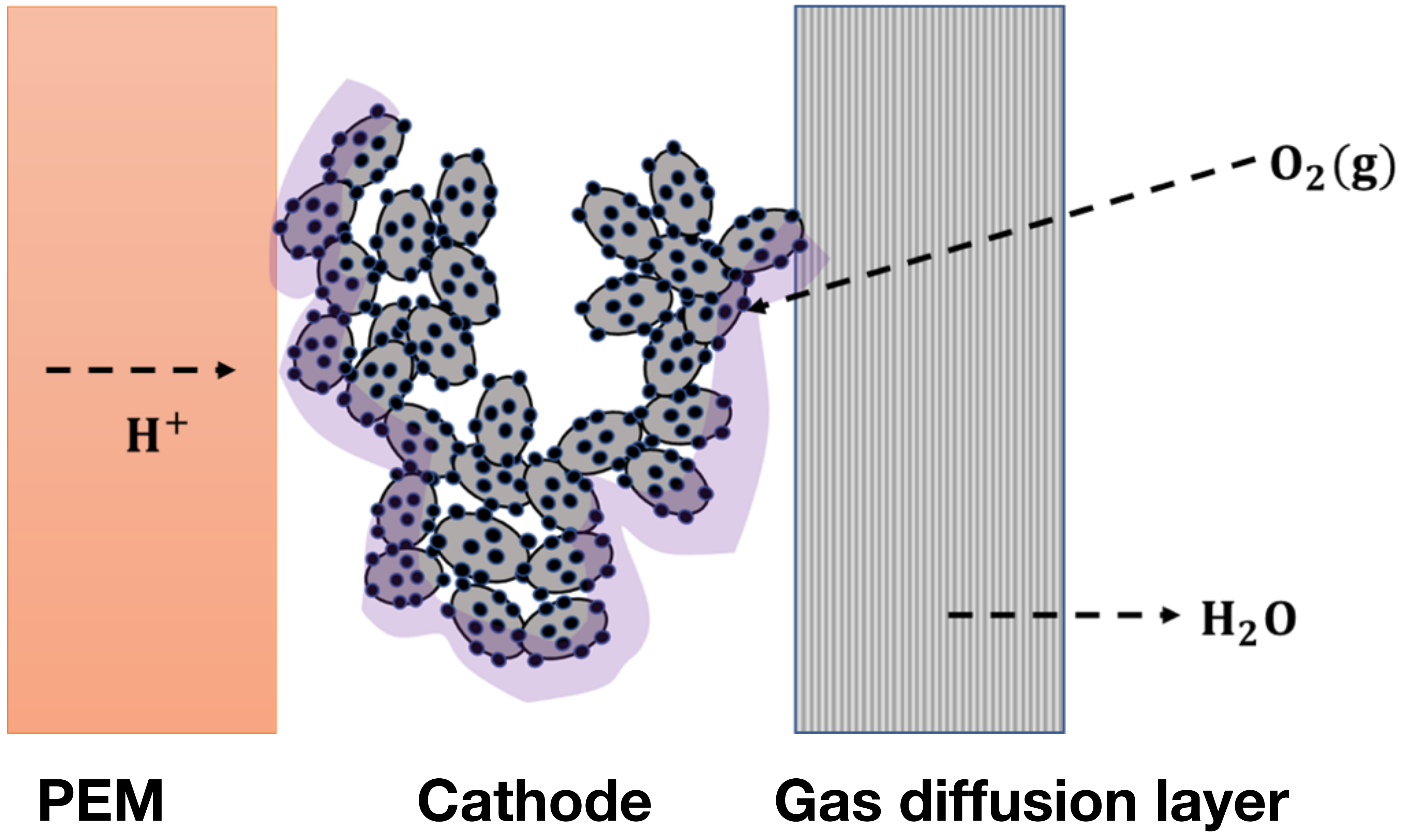

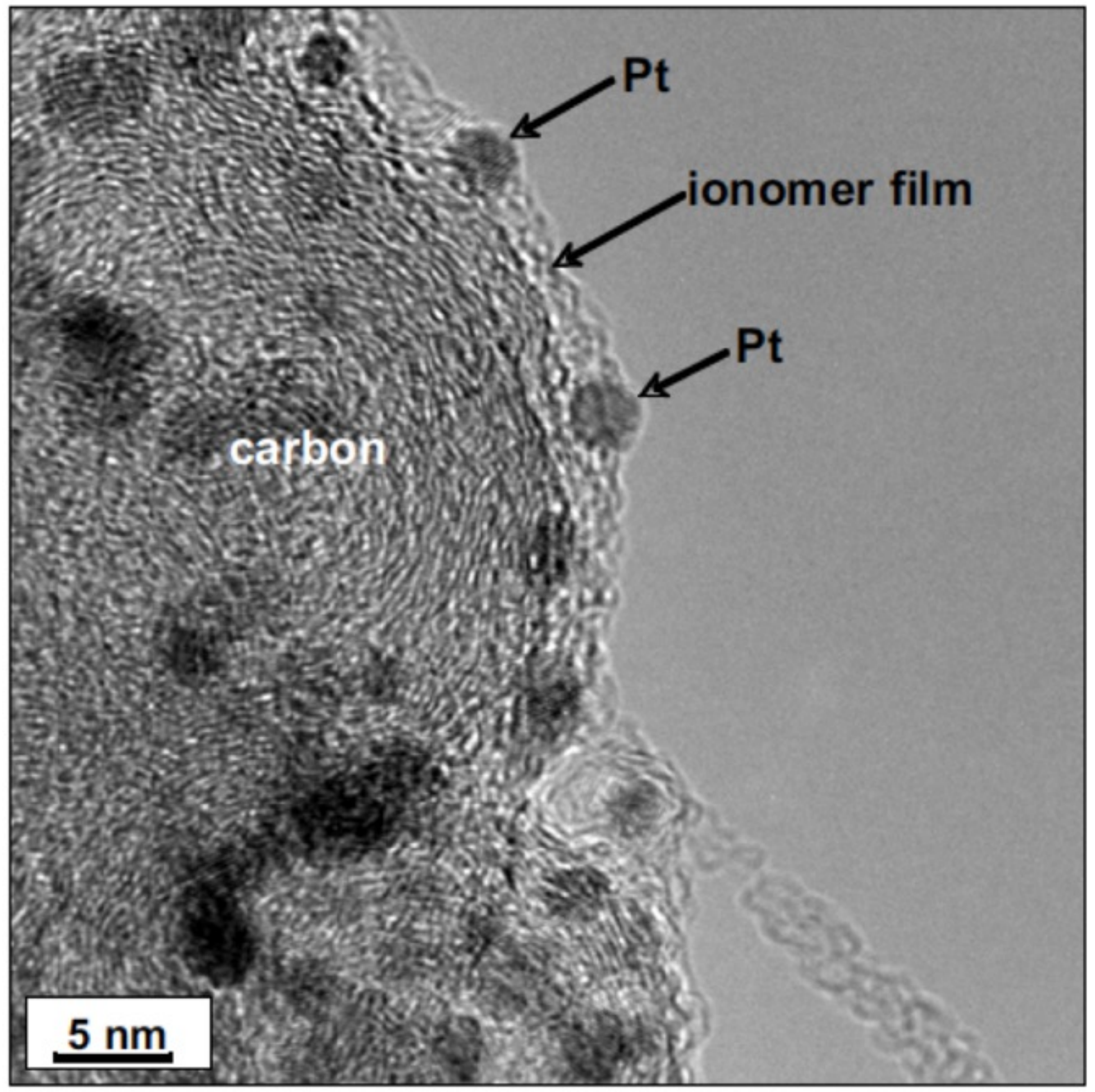

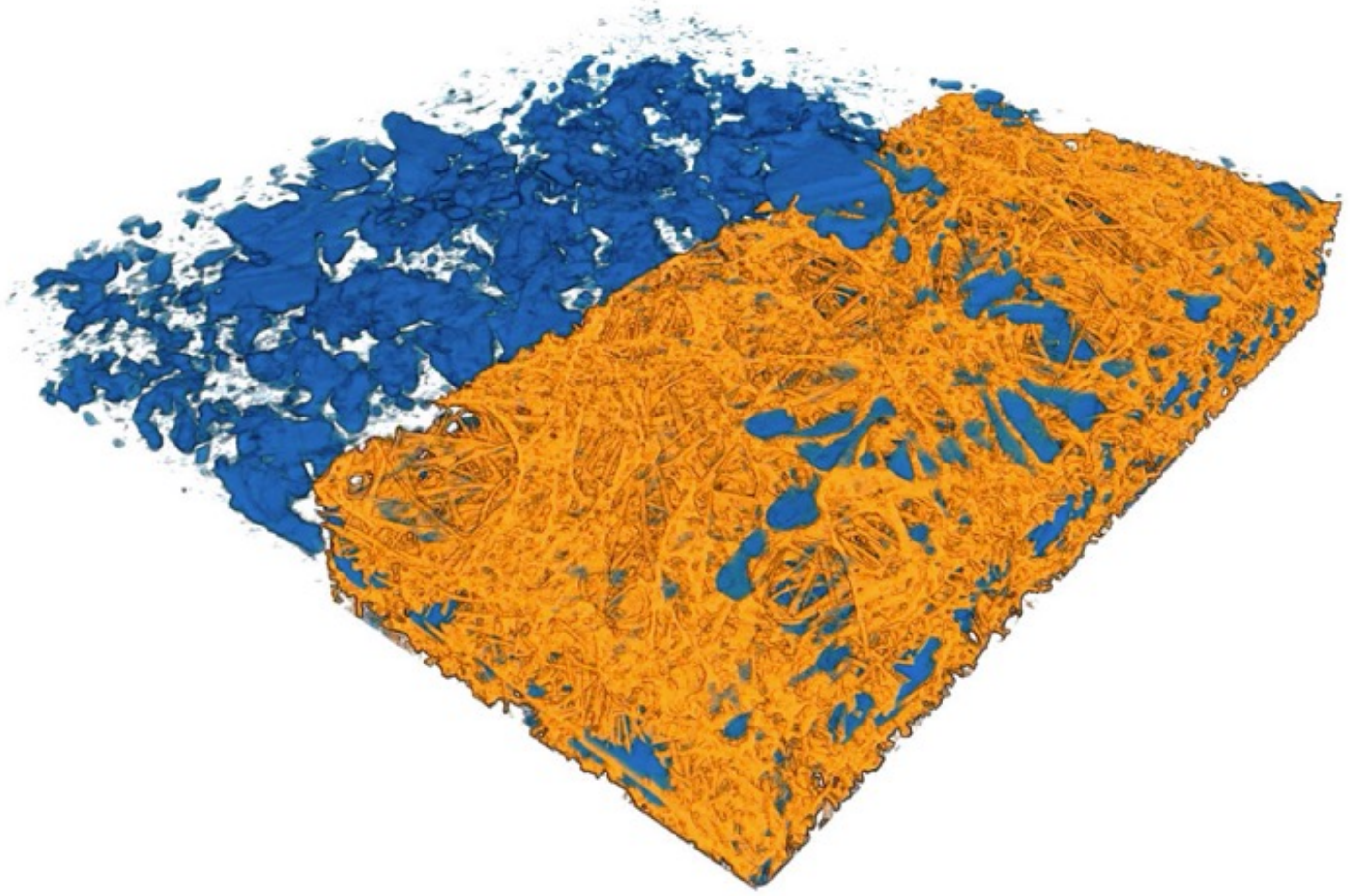

X-ray tomography of LT-PEMFC electrode

Porous electrodes have a *__complex structure.__* They are required to deliver electrons, reactants, and protons to the electrocatalyst surface for the redox reactions

K.L. More *et al.*, *ECS Trans.*, **2006**

I. Zenyuk *et al.*, *Solid-State Ionics.*, **2019**

Electrochemical properties of thin film Nafion®

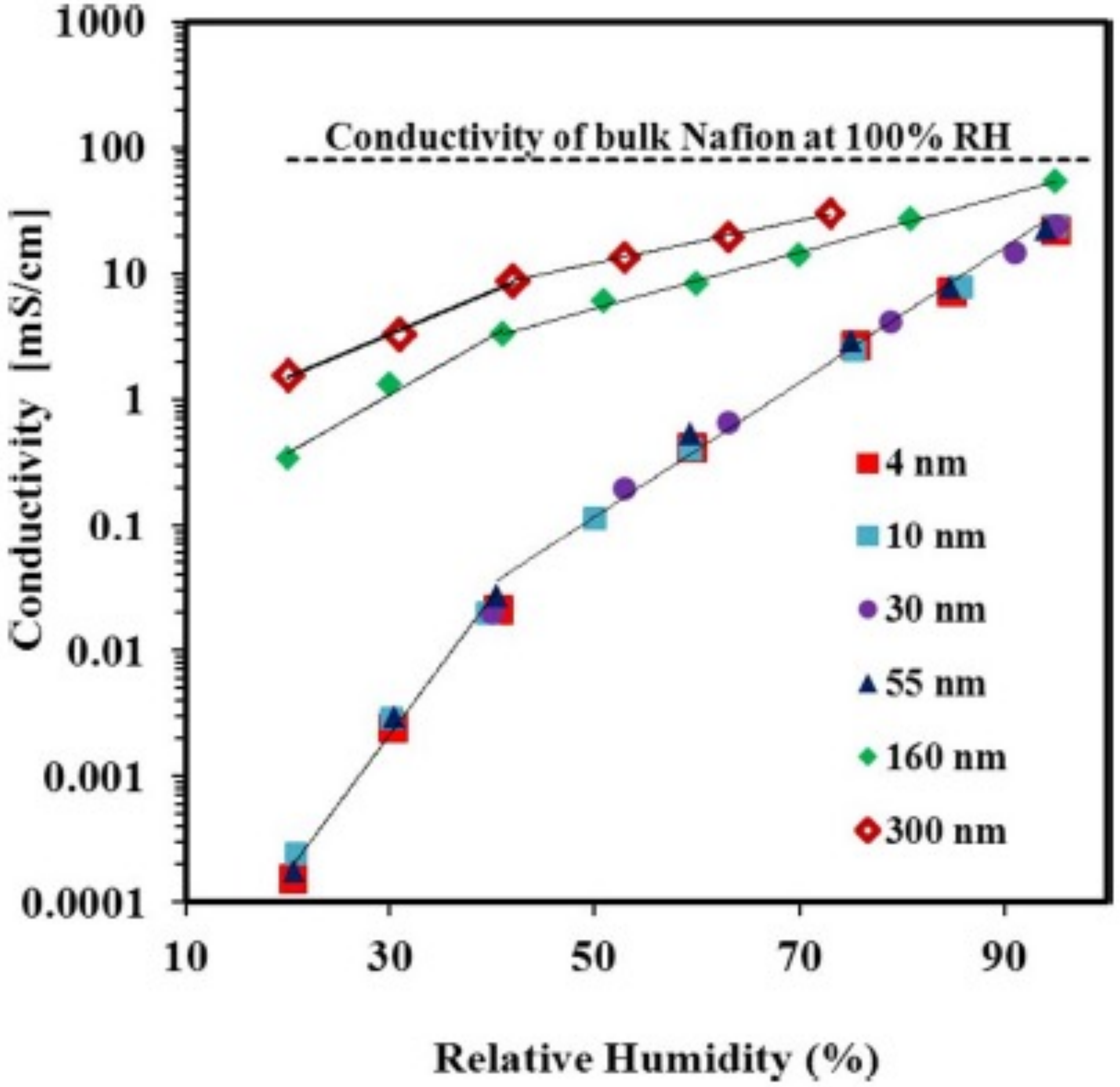

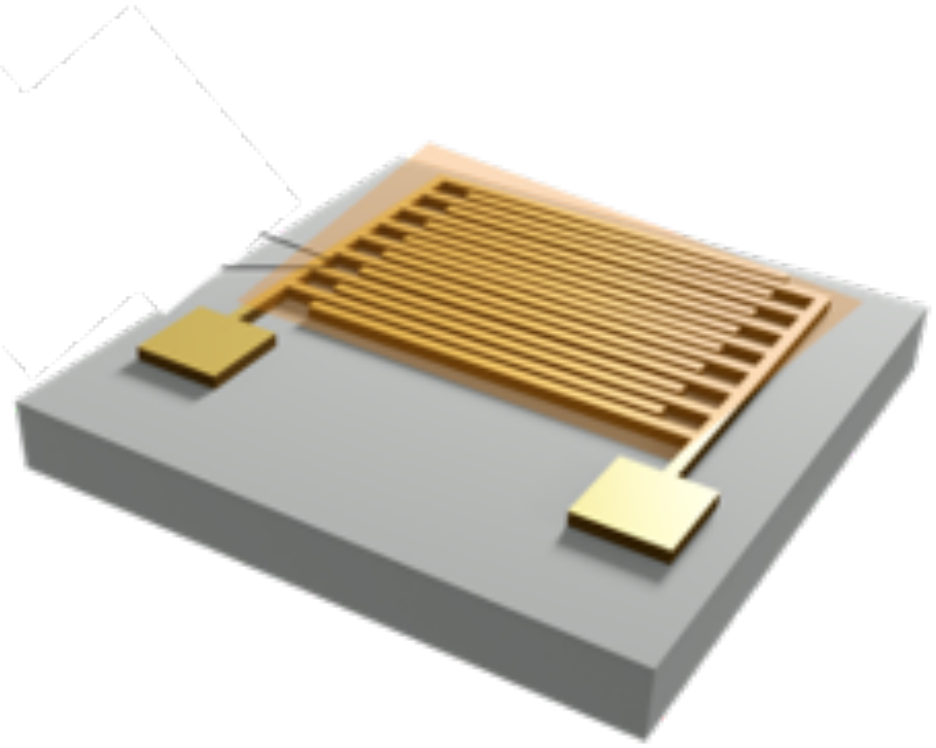

Interdigitate electrode (IDE)

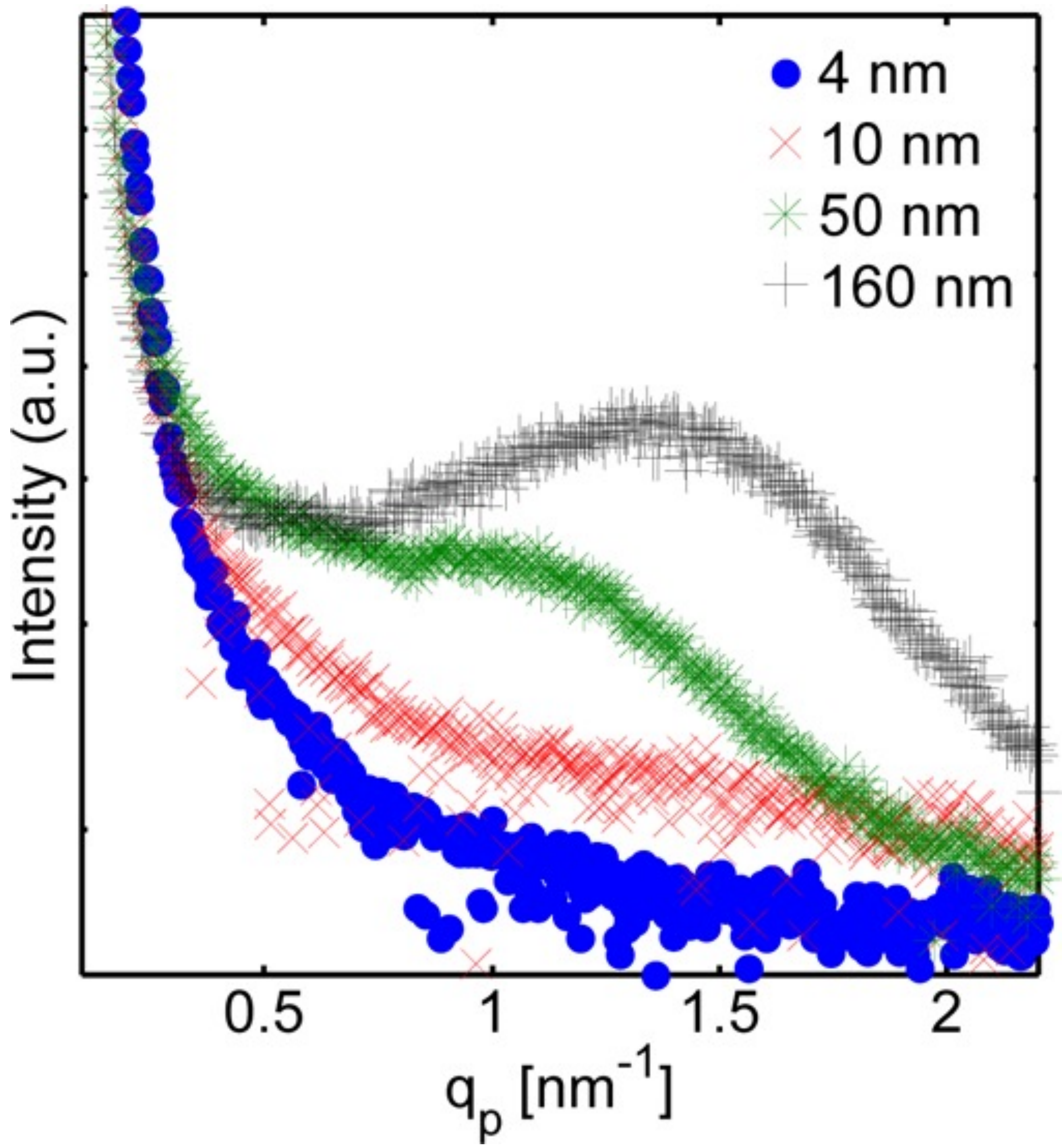

Nafion®, when confined as a thin film, cannot self-assemble into percolated pathways compromising conductivity

D.K. Paul *et al.*, *J. Electrochem. Soc.*, **2014**

M.A. Modestino *et al.*, *Macromolecules*, **2013**

Thin film conductivity of high-temperature polymer electrolytes

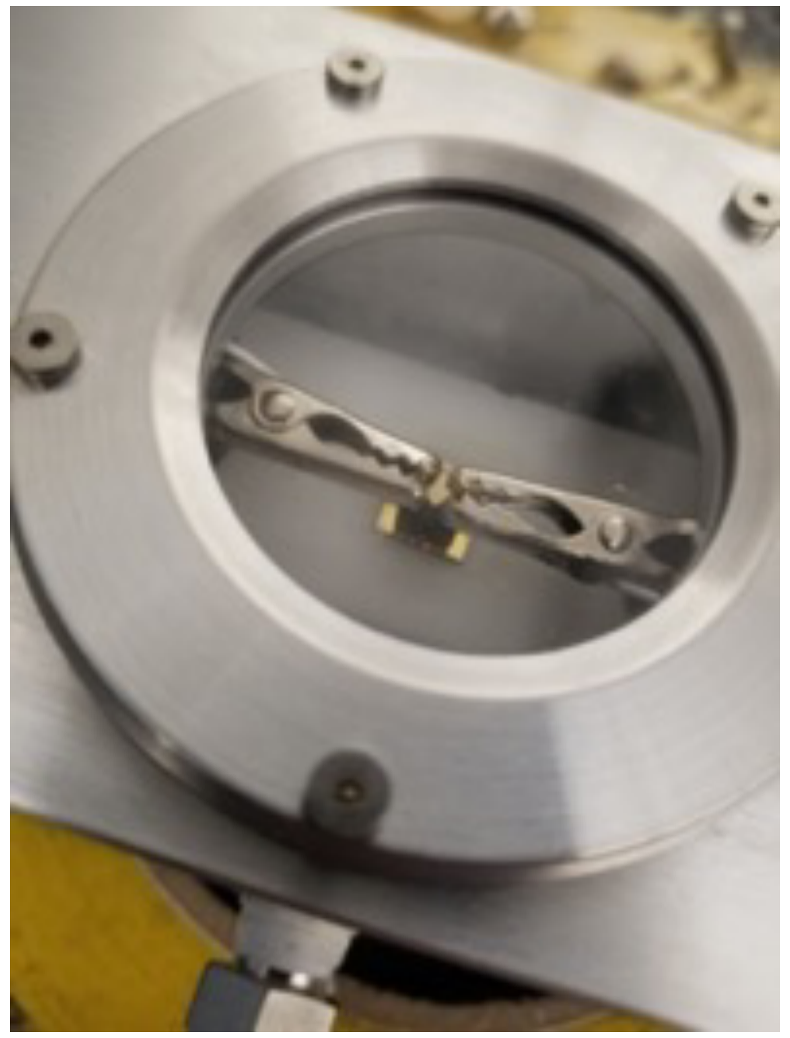

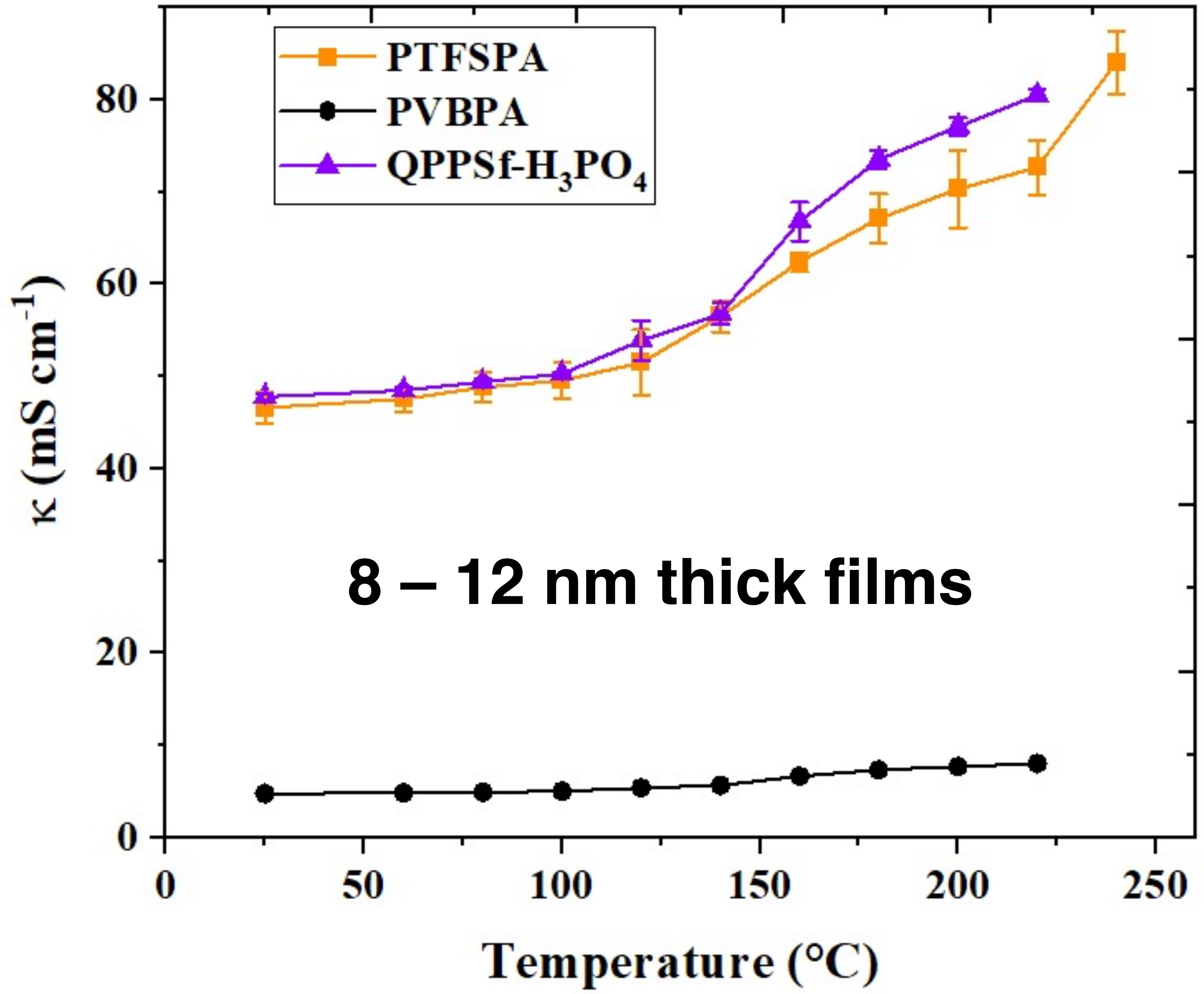

Fabrication of IDEs
Subarna Kole
ChE PhD candidate

PTFSPA

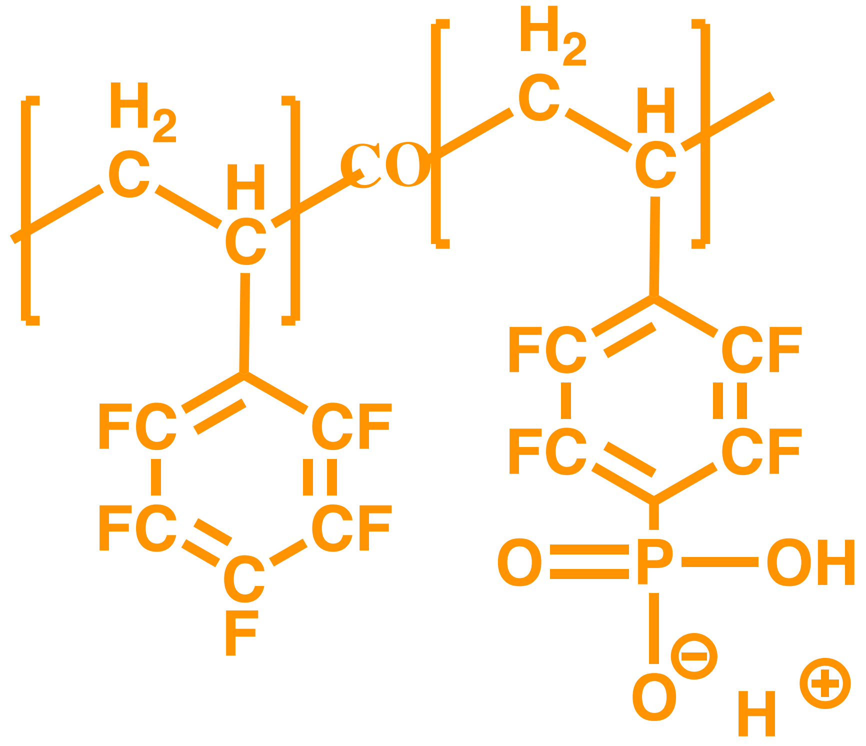

PVBPA

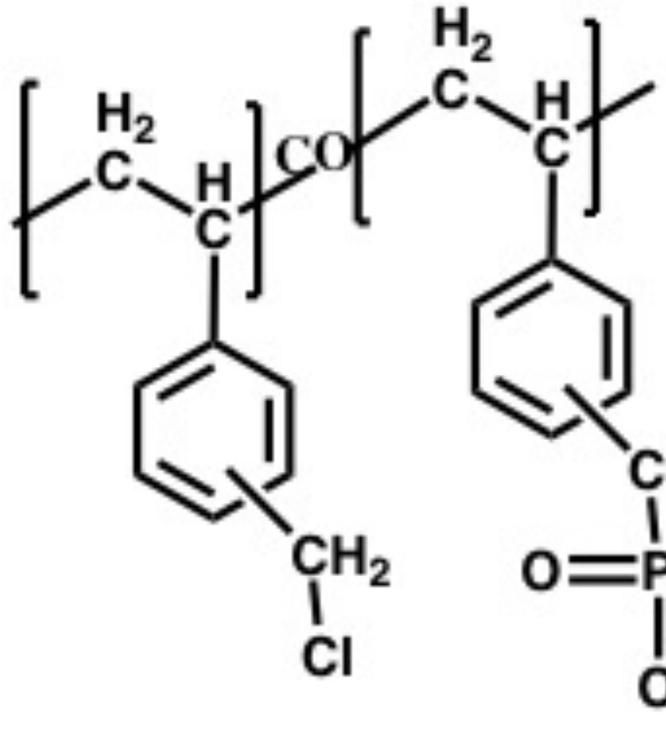

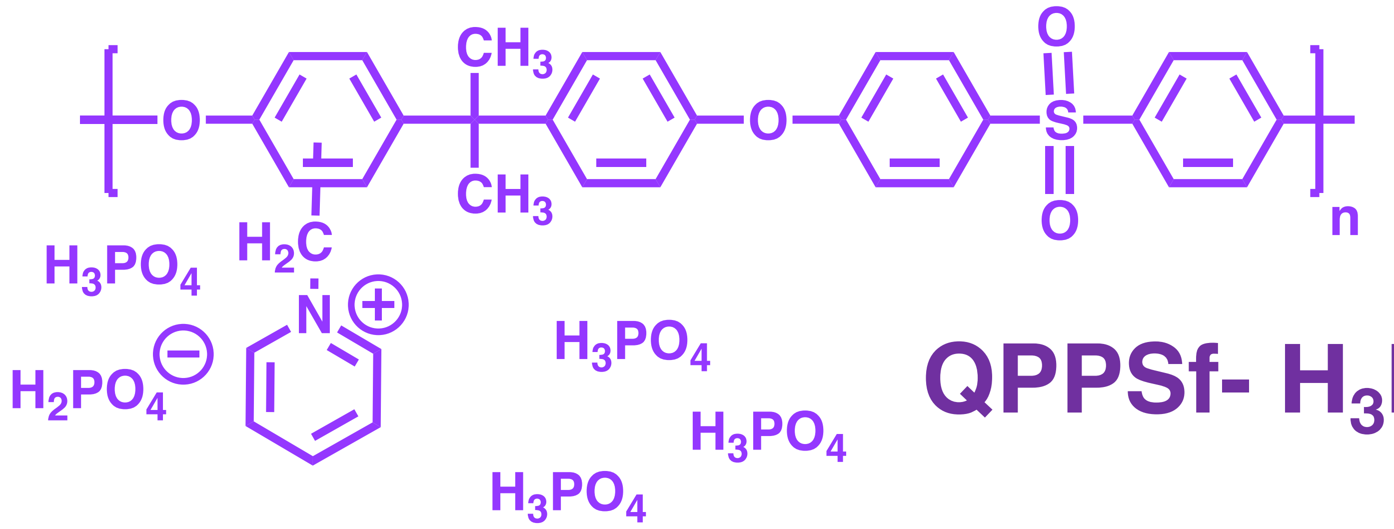

QPPSf- H_3PO_4

Higher ionic conductivity over Nafion® because these polymer electrolytes do not require self-assembled ionic domains for facile proton conductivity

Can we measure how the polymer electrolyte binder affects reaction kinetics and gas permeability?

Can we do it without using liquid supporting liquid electrolyte and fabricating membrane electrode assemblies?

Ionic conductivity often has a relatively small impact on fuel cell performance

Luis Briceno-Mena
PhD candidate

Prof. José Romagnoli

Current distribution analysis for fuel cells

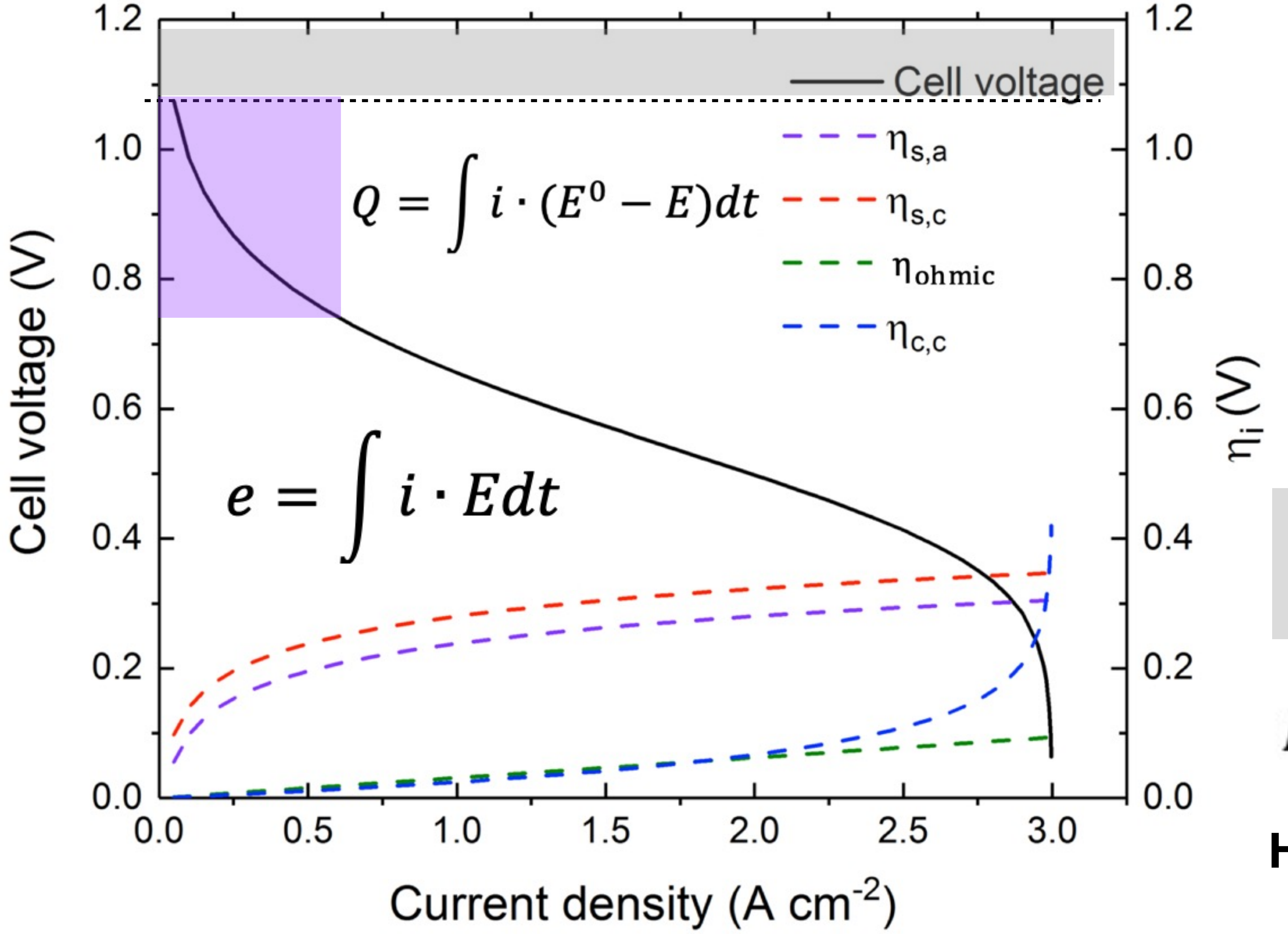

$$i = -\frac{n}{s_i} F N_i$$ **Faraday's Law**

Cell polarization relationship between voltage & current

$$E(i) = E_{oc} - \eta_{act} - \eta_{con} - \eta_{ohm}$$

$$\Delta G^o = -nFE^o$$

Cell voltage is informed from thermodynamics

$$E_{oc} = 1.23 - 0.9 \times 10^{-3}(T - 298.15) + \frac{RT}{2F}\ln\left(P_{H_2}\sqrt{P_{O_2}}\right)$$

H_3PO_4 uptake in electrodes $m_{io} = 0.0902 IEC_{io} + 0.0352$

$$\eta_{act} = \frac{RT}{\alpha_{an}F}\ln\left(\frac{i}{i_0^{an}(1-\theta_{CO})^2}\right) + \frac{RT}{\alpha_{cat}F}\ln\left(\frac{i}{i_0^{cat}}\right)$$

Reaction kinetics for the electrodes (Butler-Volmer)

Exchange current density (i_o) ~ rxn rate coeff.

$$i_0^{an} = a_C L_C \left(\frac{P_{H_2} H_{H_2}^{CL}}{C_{H_2}^0}\right)^{0.5} \exp\left(-\frac{E_C^{H_2}}{R}\left(\frac{1}{T_{an}} - \frac{1}{T_{ref}^0}\right)\right) i_{0-ref}^{an} \exp(-\eta(1 - m_{io}))$$

$$i_0^{cat} = a_C L_C \left(\frac{P_{O_2} H_{O_2}^{CL}}{C_{O_2}^0}\right) \exp\left(-\frac{E_C^{O_2}}{R}\left(\frac{1}{T_{cat}} - \frac{1}{T_{ref}^0}\right)\right) i_{0-ref}^{cat} \exp(-\eta(1 - m_{io}))$$

CO coverage on catalyst

$$\theta_{CO} = 19.9 \exp(-7.69 \times 10^{-3} T_{an}) + 0.085 \ln\left(\frac{y_{CO}}{y_{H2}}\right)$$

L. Briceno-Mena, G. Venugopalan, J.A. Romagnoli, C.G. Arges, *Patterns (Cell Press)*, **2021**

Current distribution analysis for fuel cells

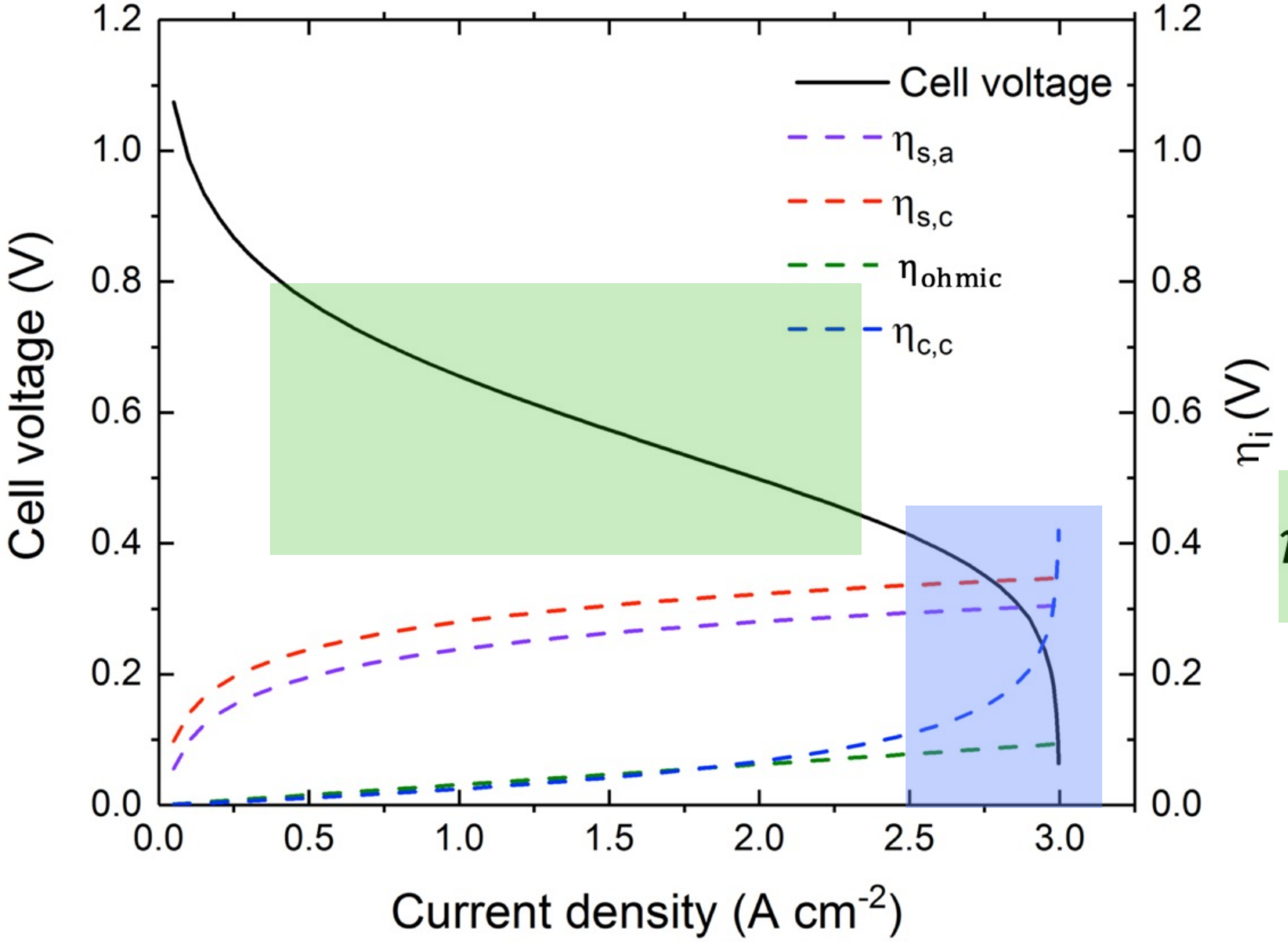

$$i = -\frac{n}{s_i} F \frac{m_i}{A \cdot Mw_i \cdot t} = -\frac{n}{s_i} F N_i$$

Current is measure of chemical species flux

$$E(i) = E_{oc} - \eta_{act} - \eta_{con} - \eta_{ohm}$$

$$\eta_{ohm} = i\left(\frac{\delta_{mem}}{\kappa_{mem}} + \frac{\delta_{io}}{\kappa_{io}}\right)$$

Ohmic drop arises from ion transport mass transfer resistance

Concentration polarization (mass-transfer controlled behavior)

$$\eta_{con} = -B\left(\ln\left(1 - \frac{i}{i_{lim}^{an}}\right) + \ln\left(1 - \frac{i}{i_{lim}^{cat}}\right)\right)$$

$$i_{lim}^{cat} = \frac{K_{an} D_{H_2}^{CL} P_{H_2}}{T\delta_{CL}} (1 - \theta_{CO})^2 \qquad i_{lim}^{cat} = \frac{K_{cat} D_{O_2}^{CL} P_{O_2}}{T\delta_{CL}}$$

Diffusion coefficient

$$D_{O_2}^{CL} = (1.0 \times 10^{-6}) \exp\left(-\frac{4500\, m_{io}^2 - 10000 m_{io} + 4010}{T}\right)$$

$$D_{H_2}^{CL} = 2 D_{O_2}^{CL} \qquad K_{an} = 0.5 K_{cat}$$

L. Briceno-Mena, G. Venugopalan, J.A. Romagnoli, C.G. Arges, *Patterns (Cell Press)*, **2021**

Versatile materials for nanostructure templating - BCP self-assembly

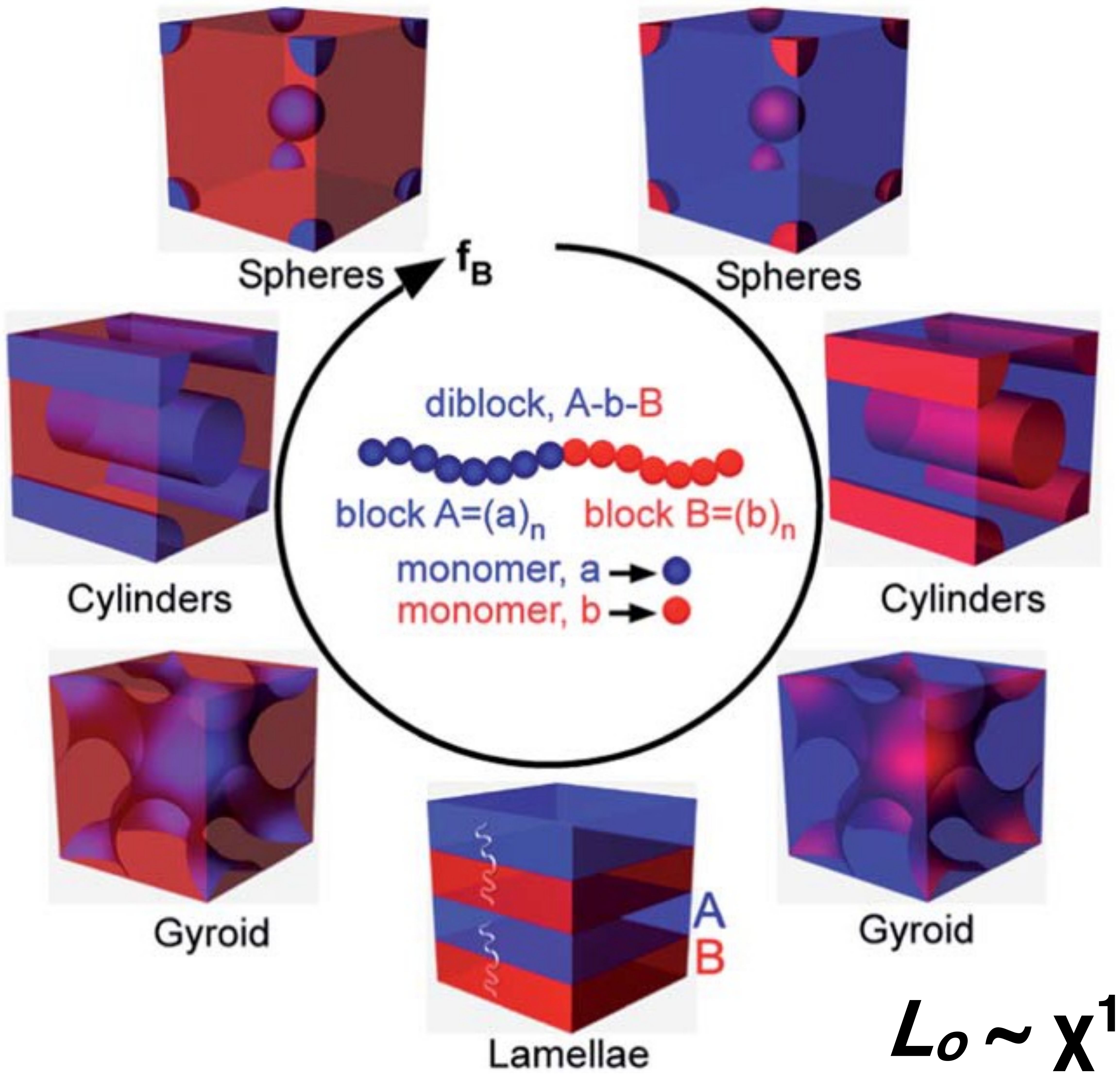

$L_o \sim \chi^{1/6}N^{2/3}$

C. Osuji *et al.*, *Soft Matter*, **2014**

Self-consistent field theory phase diagram

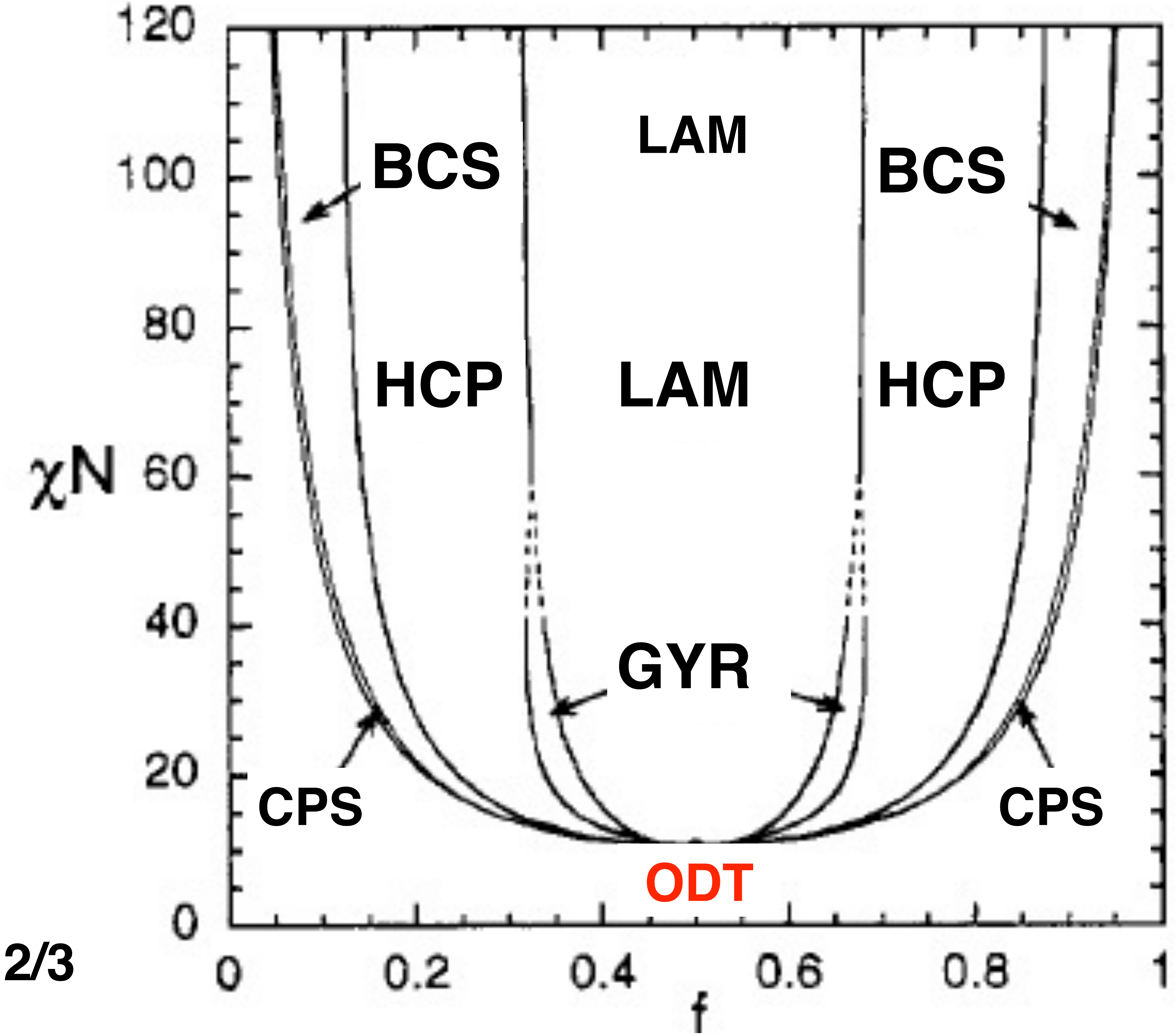

L. Leibler, *Macromolecules*, **1980**

Probing reaction kinetics and gas transport at electrocatalyst-thin film ionomer interfaces

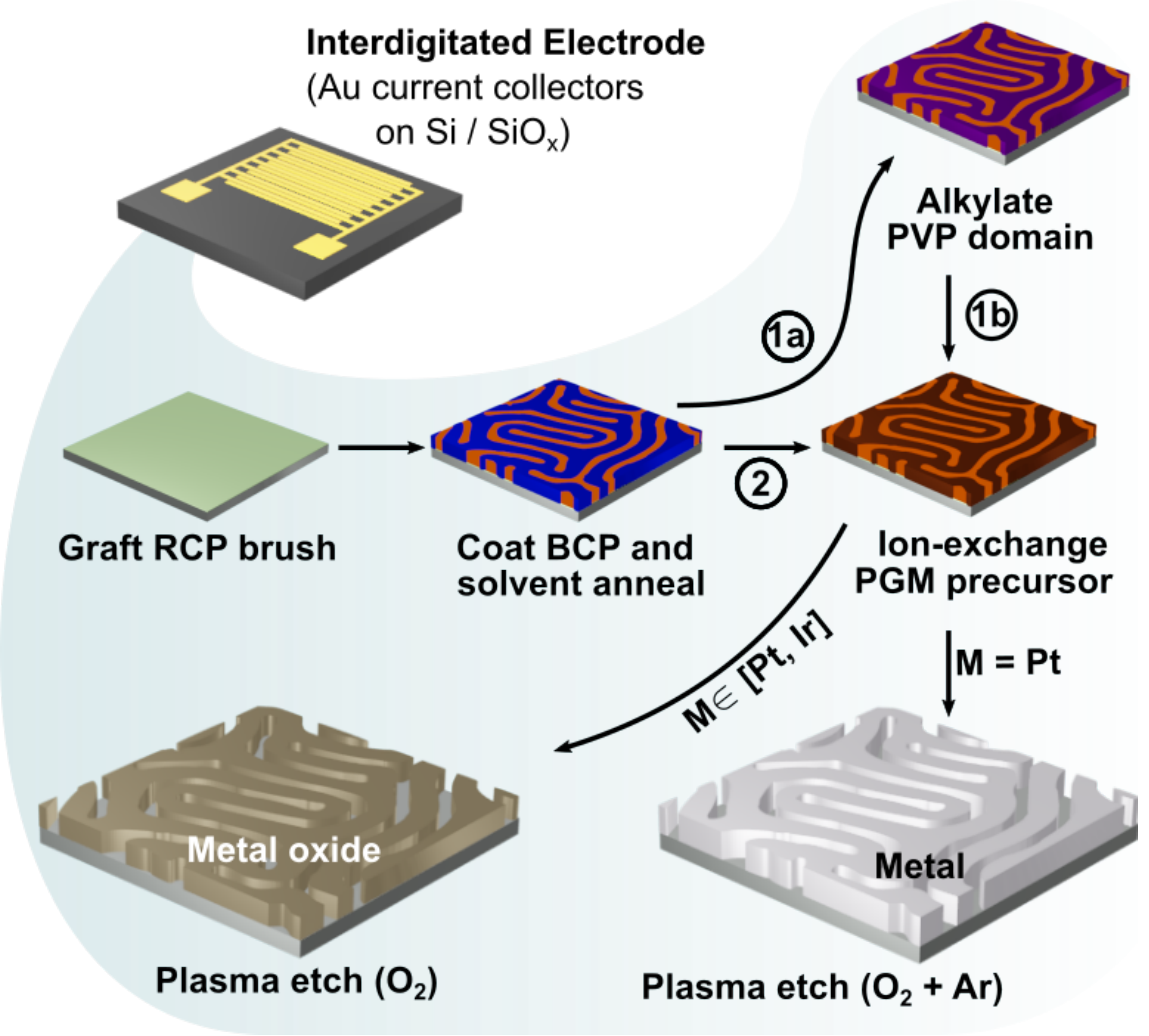

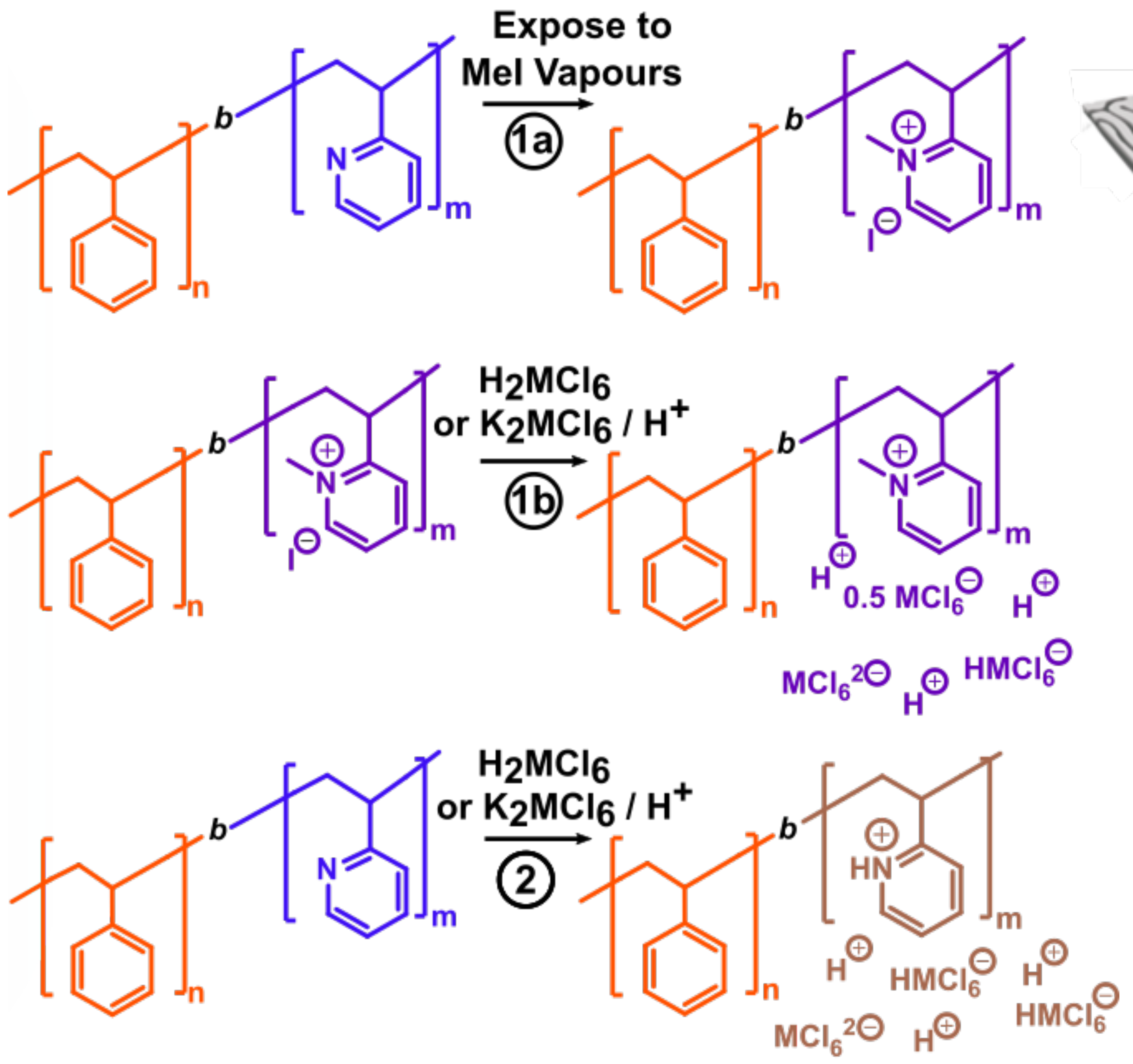

Platinum nanowires on Au current collectors

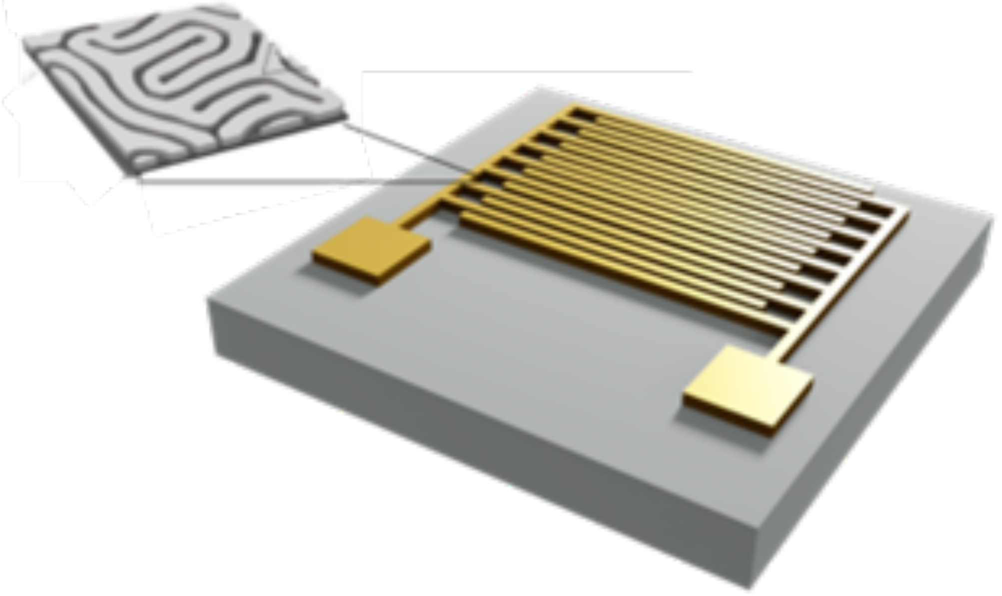

Deepra Bhattacharya
PhD candidate

D. Bhattacharya, C.G. Arges, *Small*, **2021** *(accepted, doi: 10.1002/smll.202100437)*

PGM nanostructures from self-assembled BCP templates

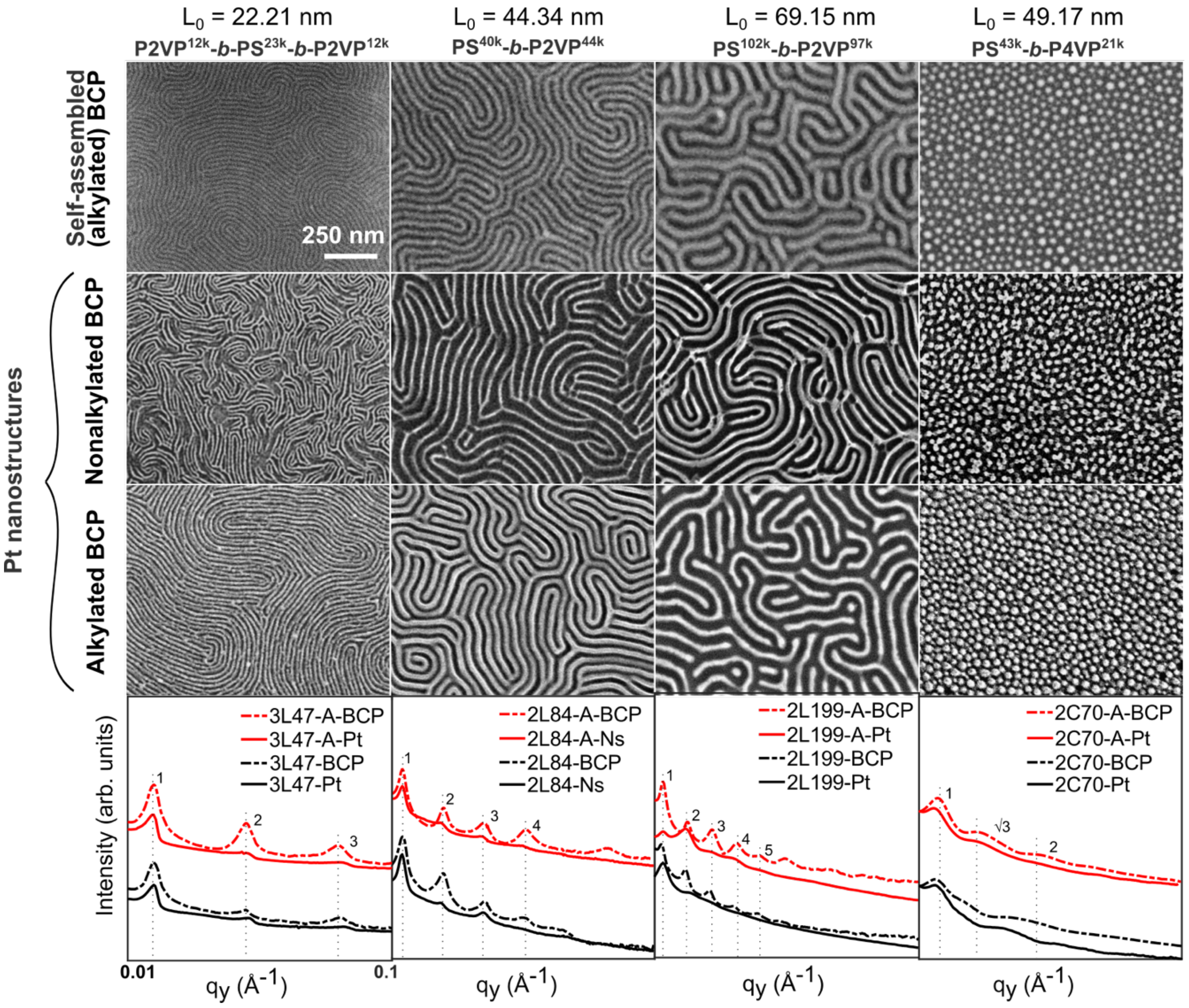

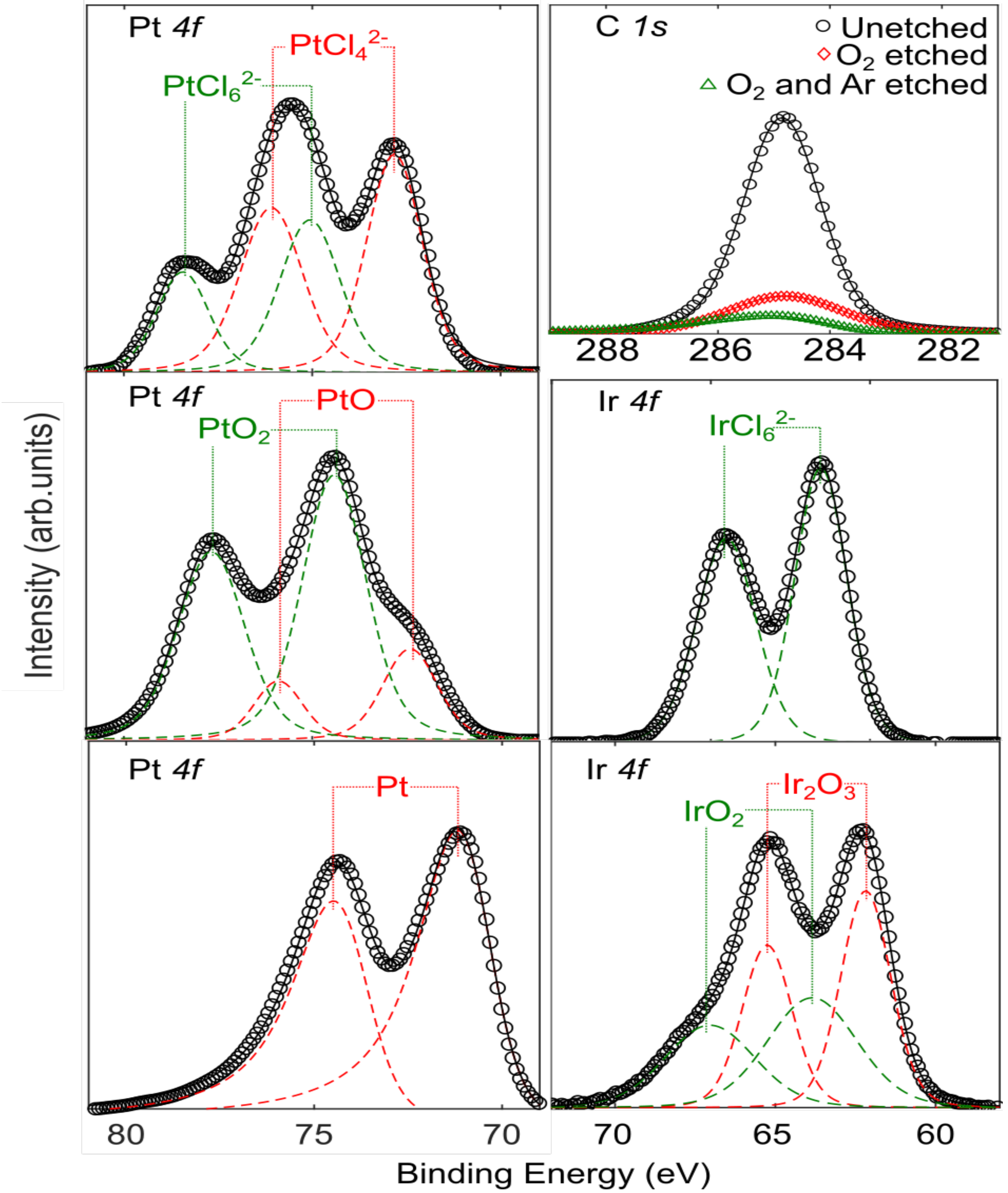

D. Bhattacharya, C.G. Arges, *Small*, **2021** *(accepted, doi: 10.1002/smll.202100437)*

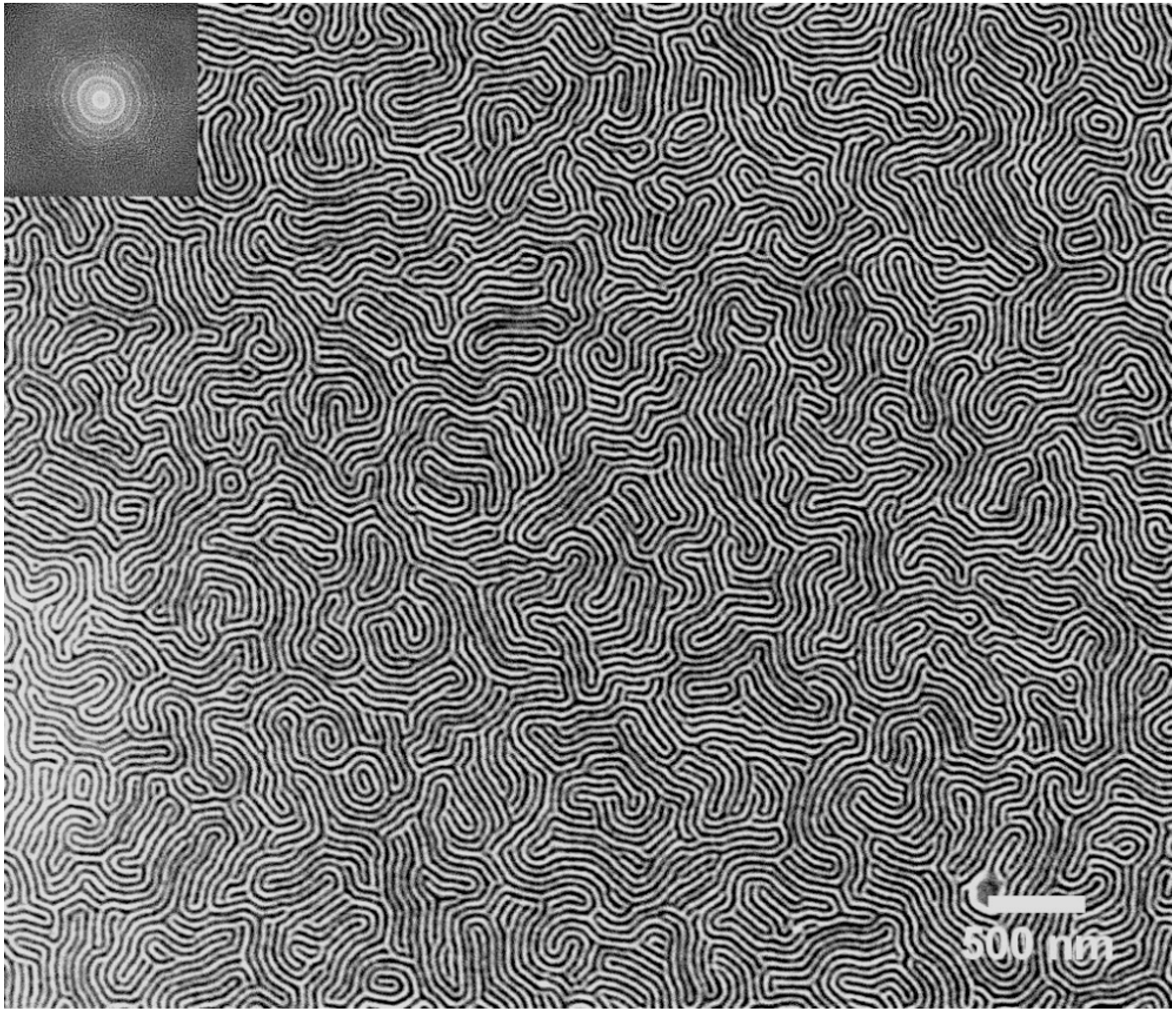

High density platinum nanowires (22 nm diameter)

6 µm x 6 µm micrograph

PGM nanostructures – surface area

Filter and binarize

Analyze 2D area of the structures

Height (h) from AFM topography images

P2VP^{12k}-*b*-PS^{23k}-*b*-P2VP^{12k} | **PS^{40k}-*b*-P2VP^{44k}** | **PS^{102k}-*b*-P2VP^{97k}** | **PS^{40k}-*b*-P4VP^{44k}**

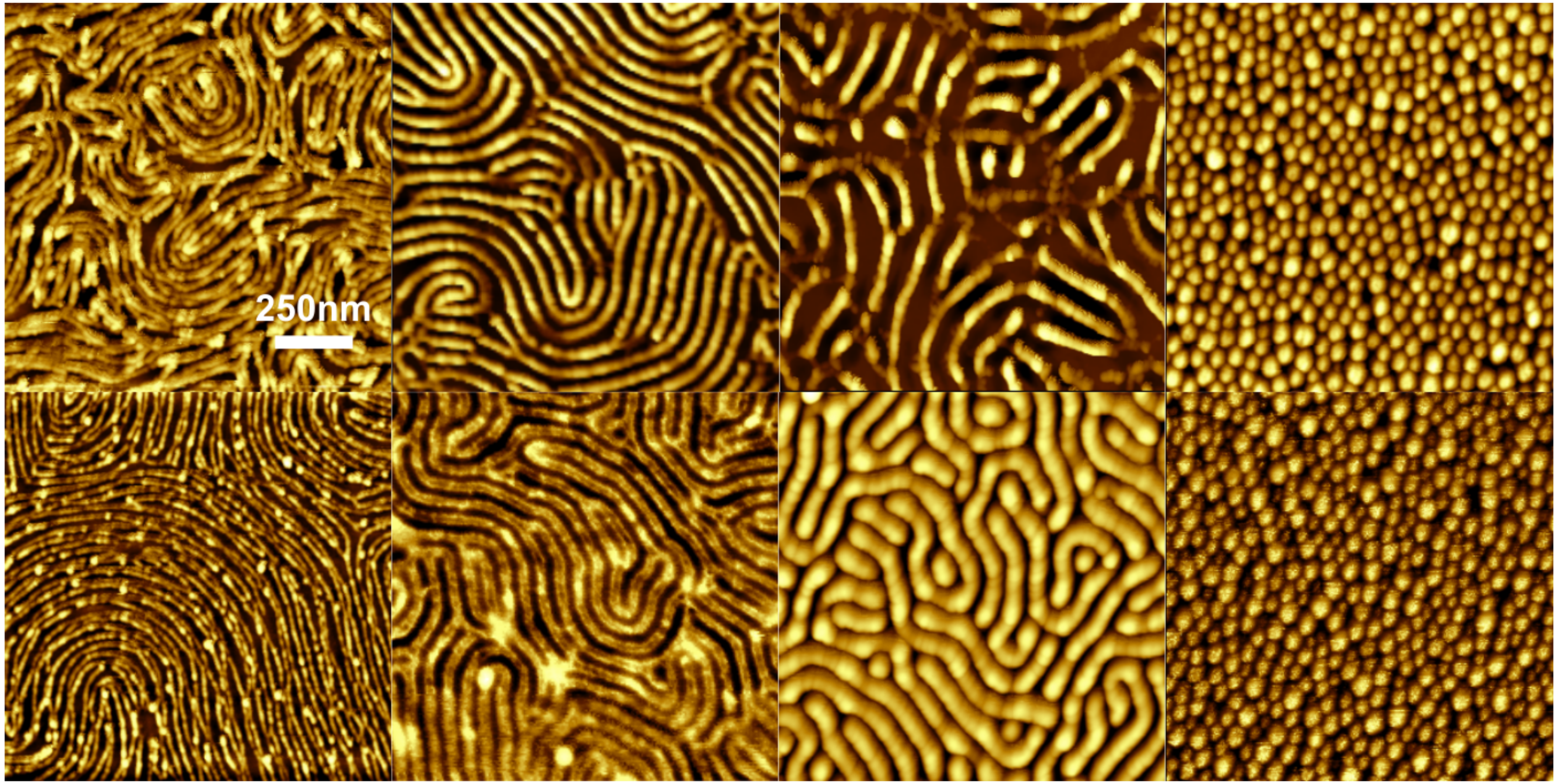

Surface coverage (φ), area covered by the nanowires (A), perimeter (p) from image analysis

$$S = ph + \varphi A$$

D. Bhattacharya, C.G. Arges, *Small*, **2021** *(accepted, doi: 10.1002/smll.202100437)*

Water electrolysis on IDEs

Droplet of 0.1 M $HClO_4$

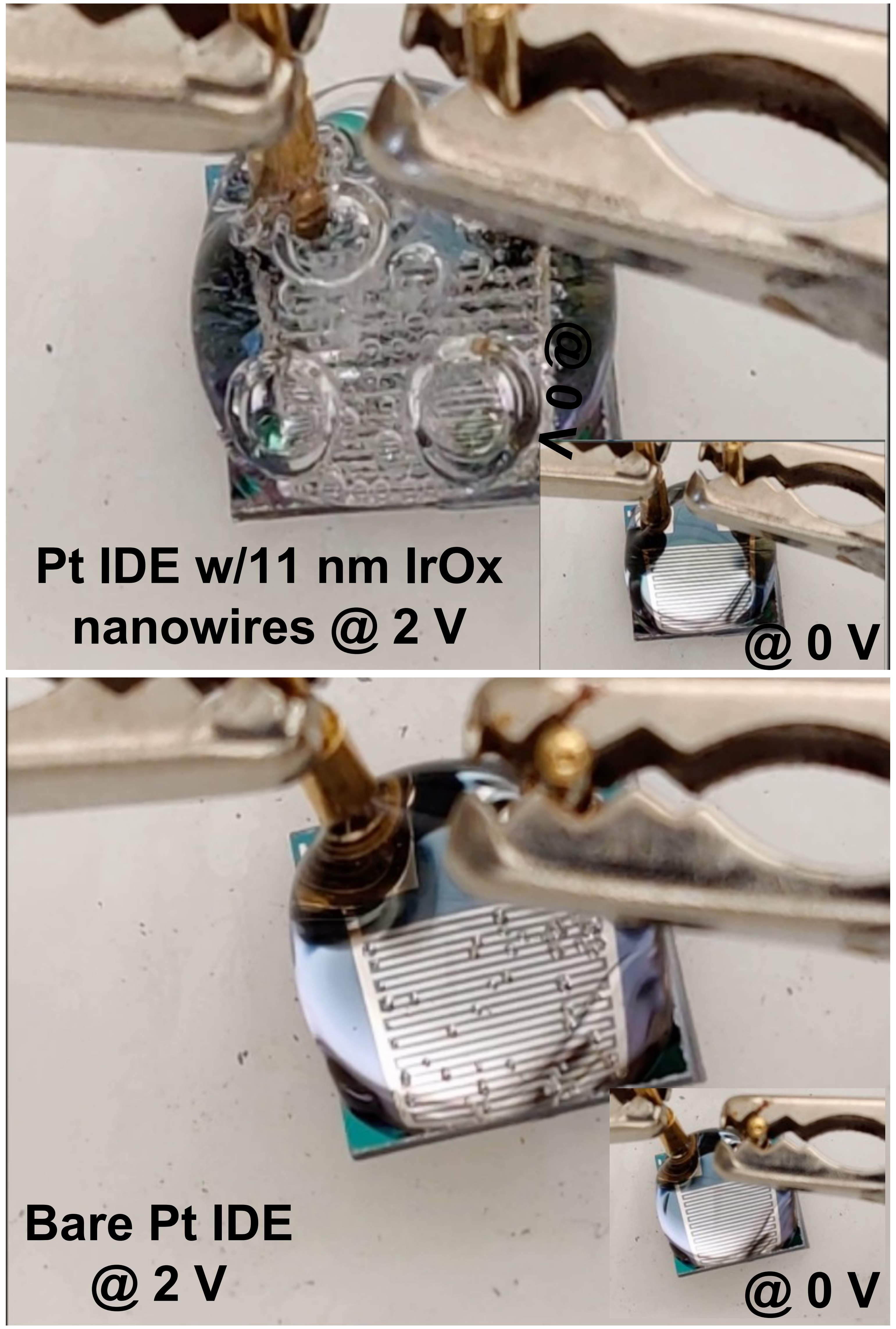

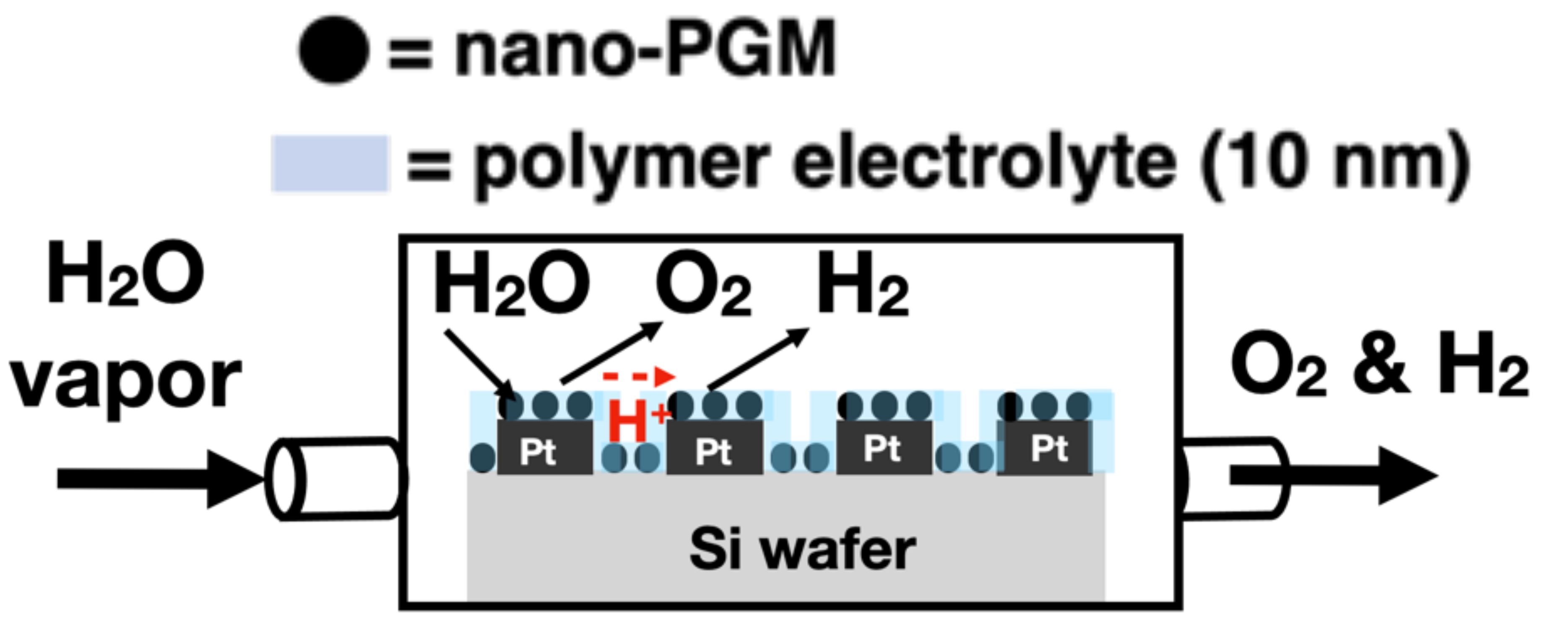

$H_2O \longrightarrow 2H^+ + 2e^- + \frac{1}{2}O_2$ (E^0 = 1.23 vs SHE)

$2H^+ + 2e^- \longrightarrow H_2$ (E^0 = 0 vs SHE)

Differences in reactivity were observed depending on the PGM type

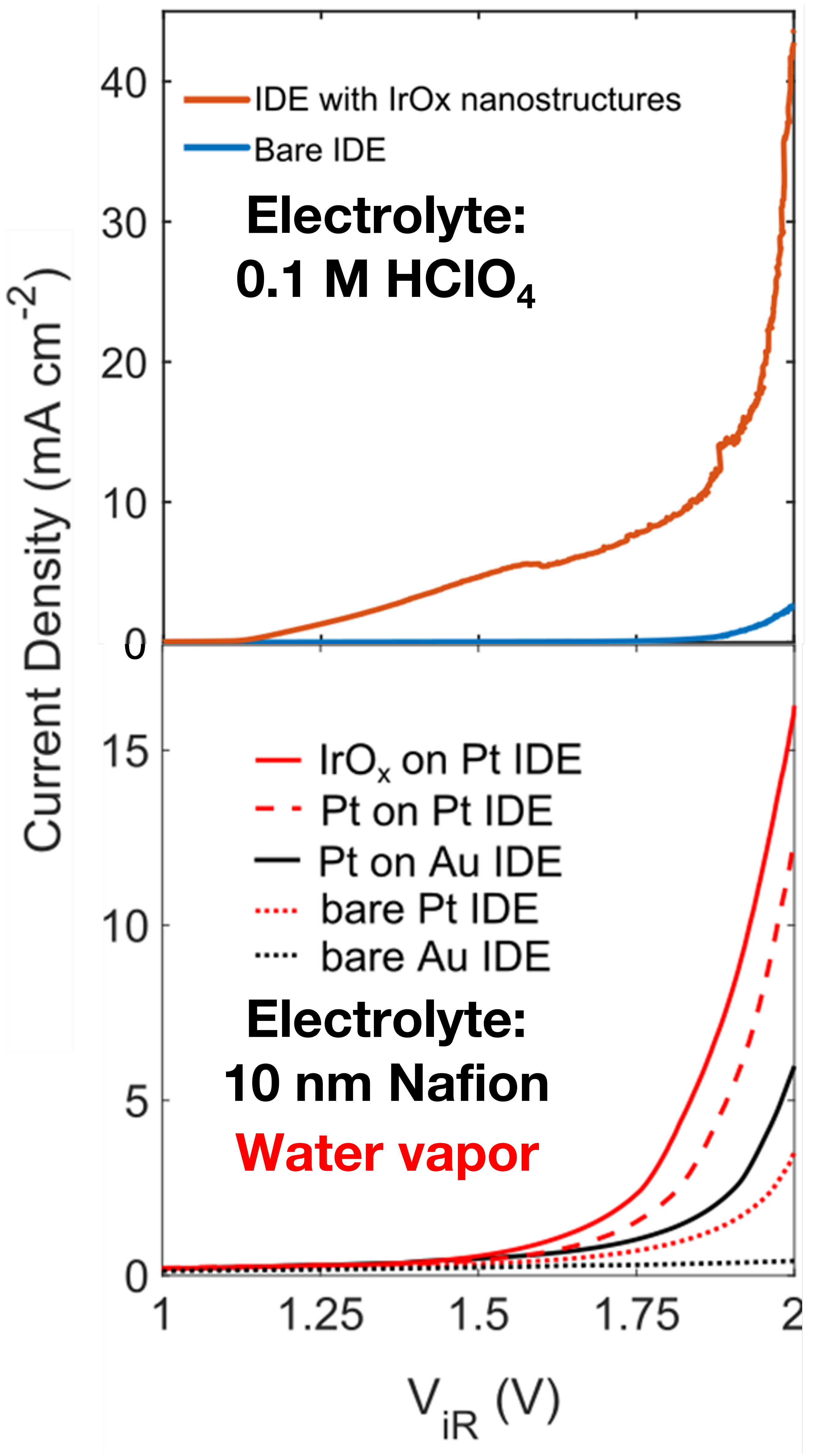

D. Bhattacharya, C.G. Arges, *Small*, **2021** *(accepted, doi: 10.1002/smll.202100437)*

Hydrogen pump on IDEs with Nafion® thin films

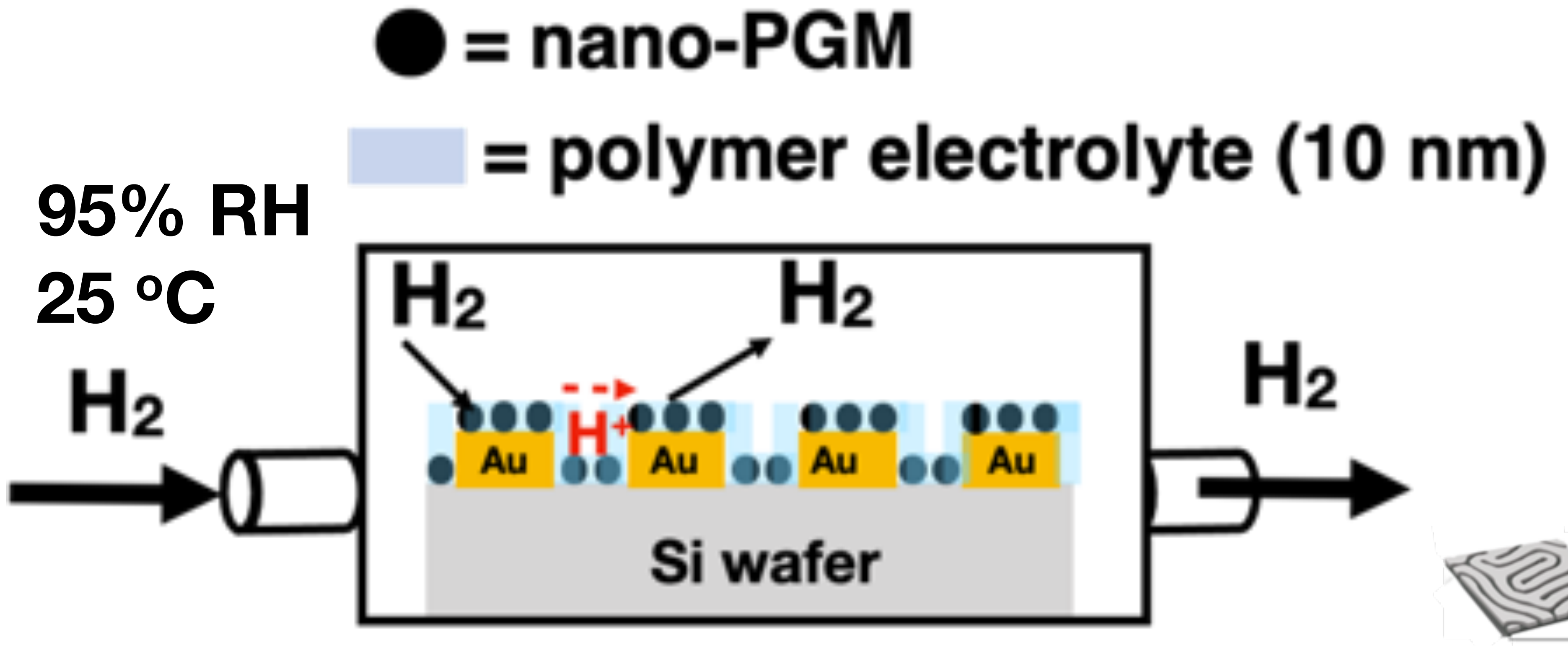

$H_2 \longrightarrow 2H^+ + 2e^-$ ($E^0 = 0$ vs SHE)

$2H^+ + 2e^- \longrightarrow H_2$ ($E^0 = 0$ vs SHE)

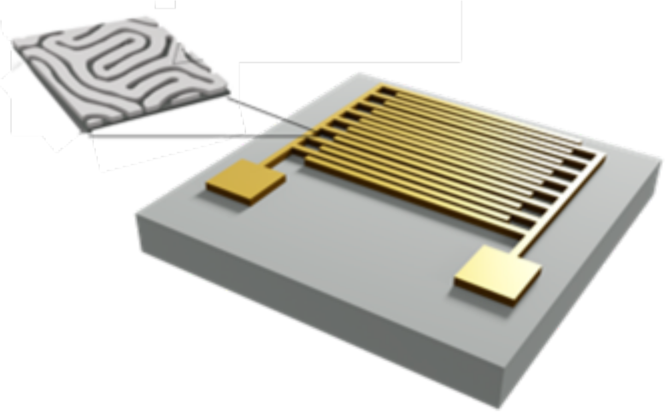

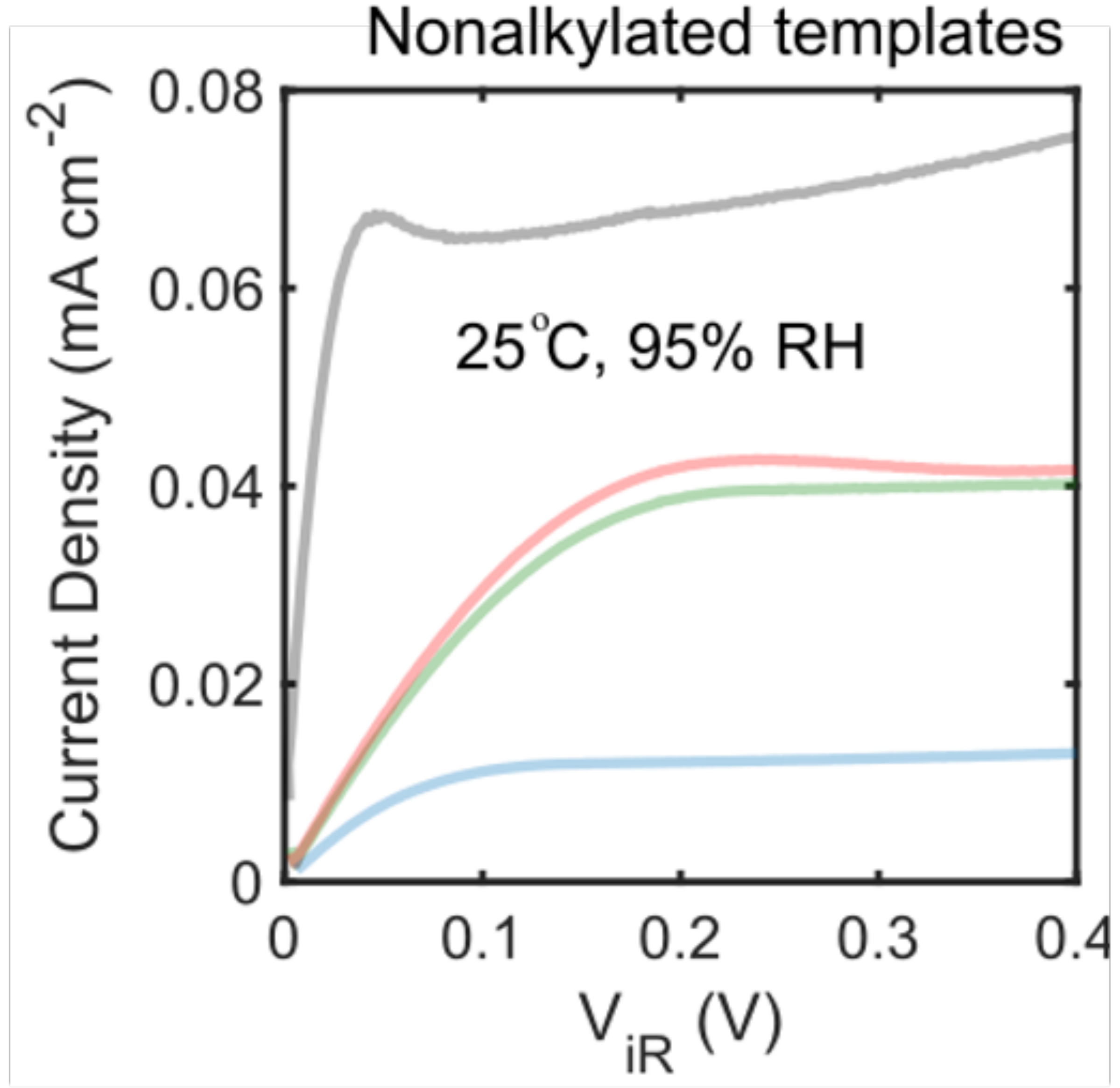

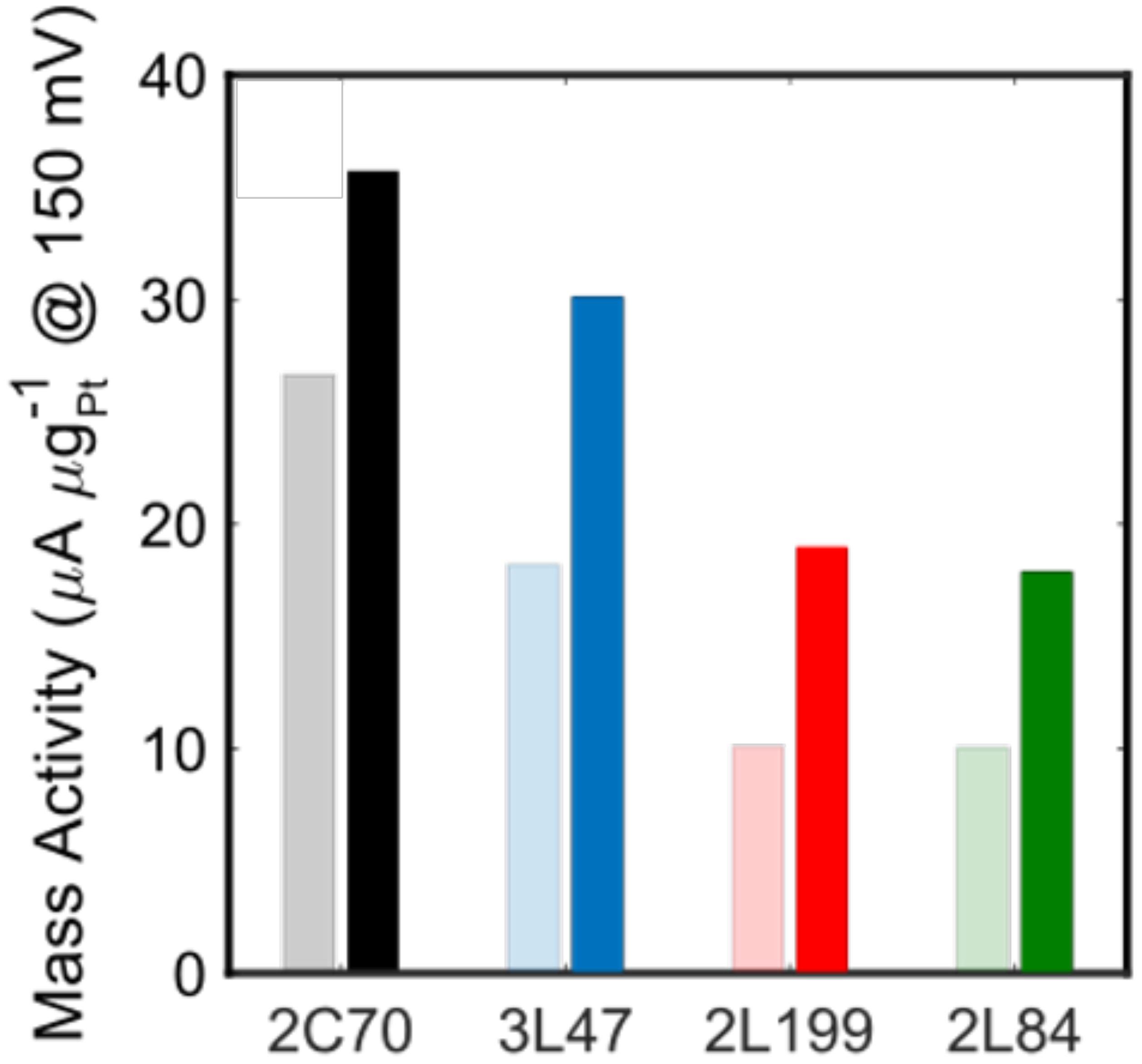

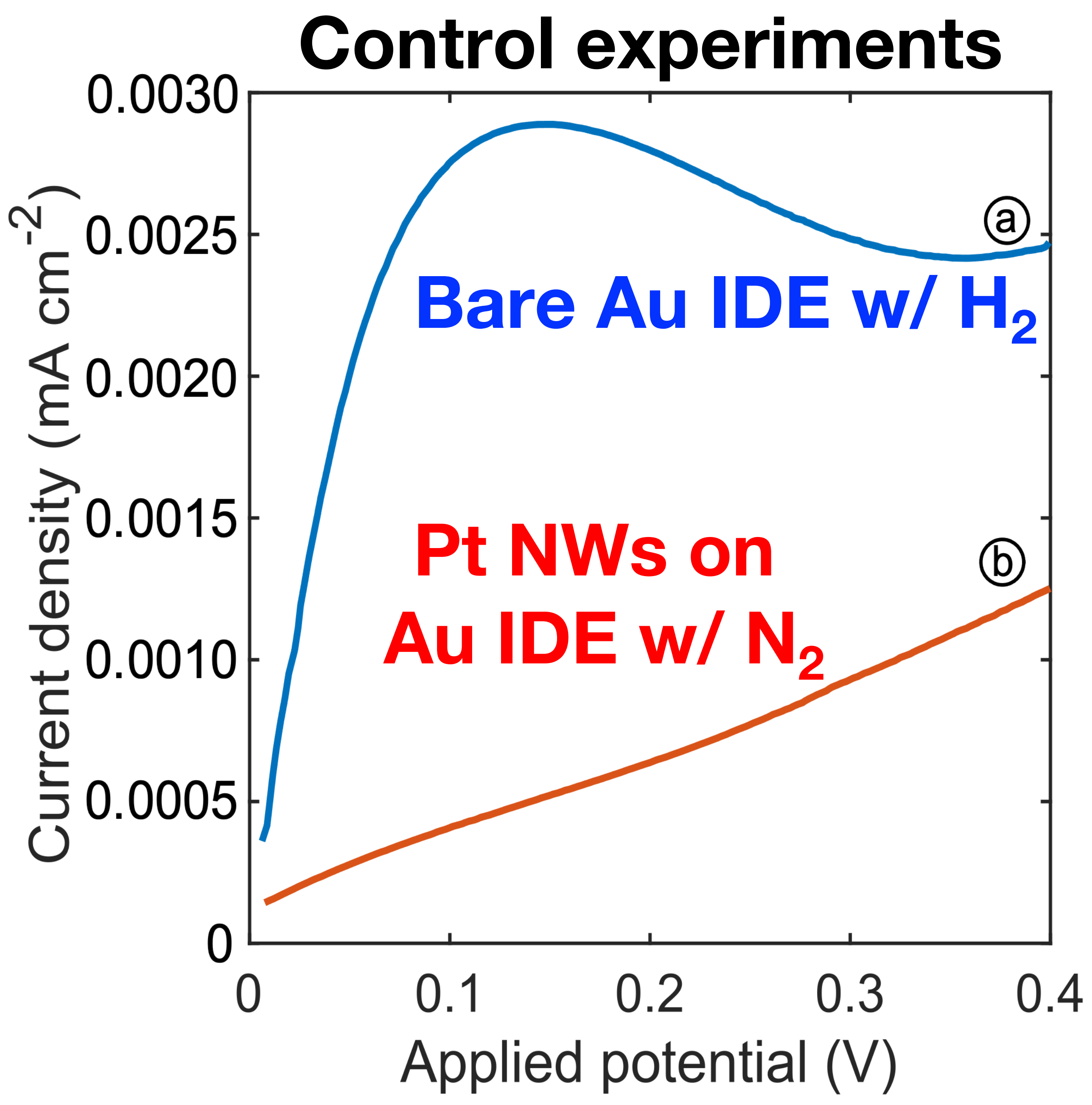

Reactivity differences between Pt meso-structures can be discerned

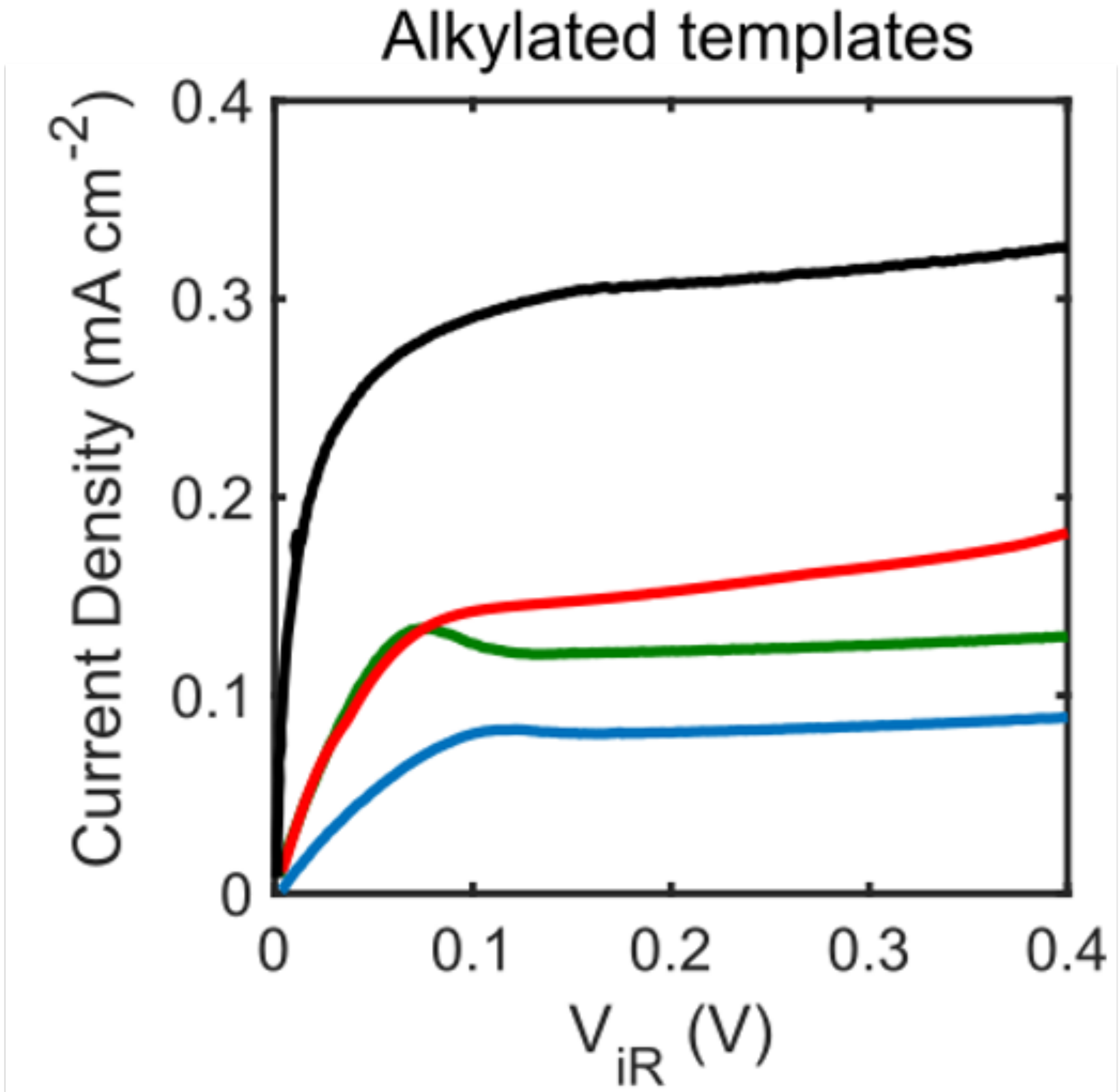

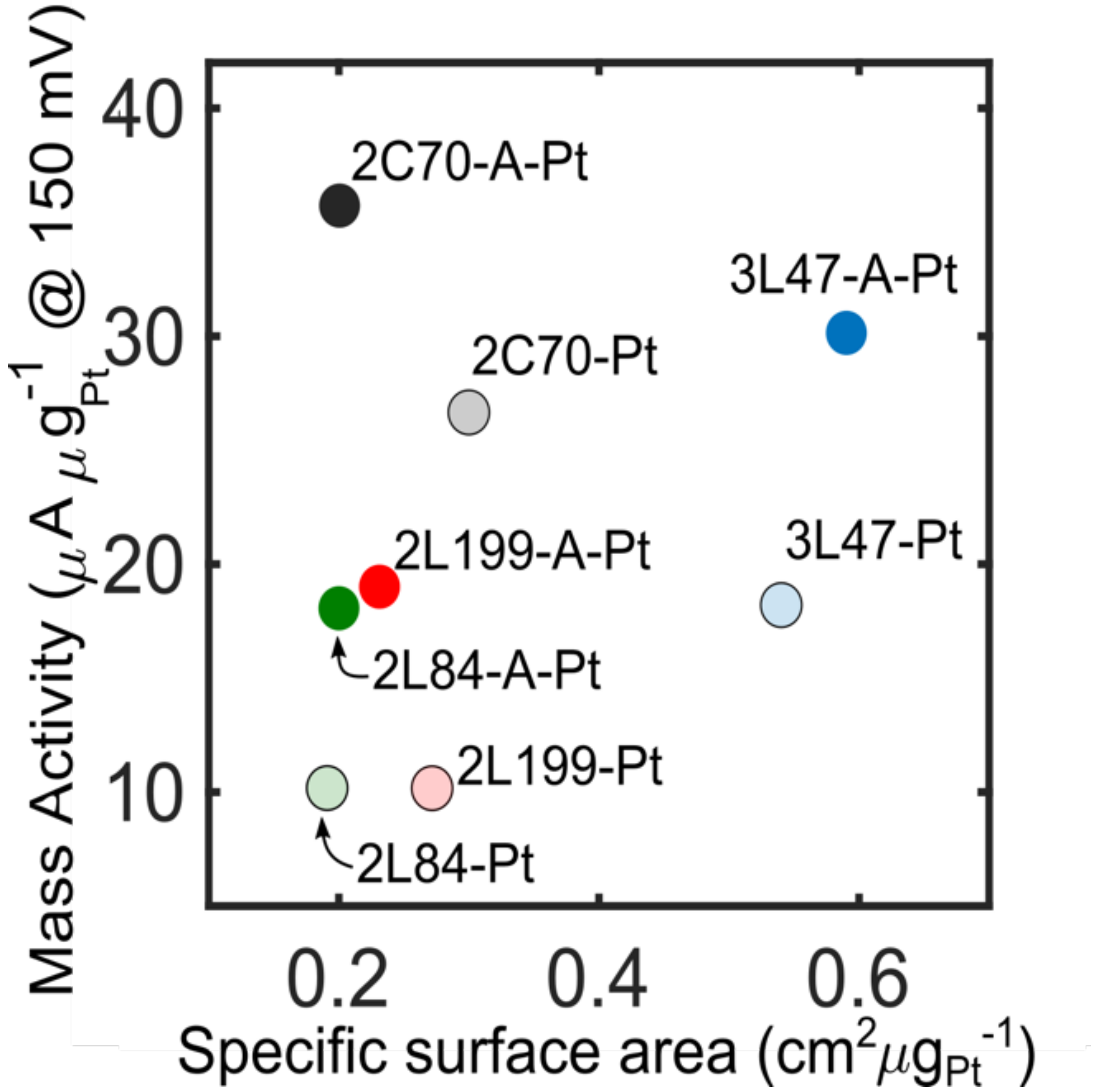

D. Bhattacharya, C.G. Arges, *Small*, **2021** *(accepted, doi: 10.1002/smll.202100437)*

Using the IDE platform to assess how thin film polymer electrolytes affect reactant transport and HOR/HER kinetics

H_2 pump w/ high-temperature thin film polymer electrolytes on IDEs

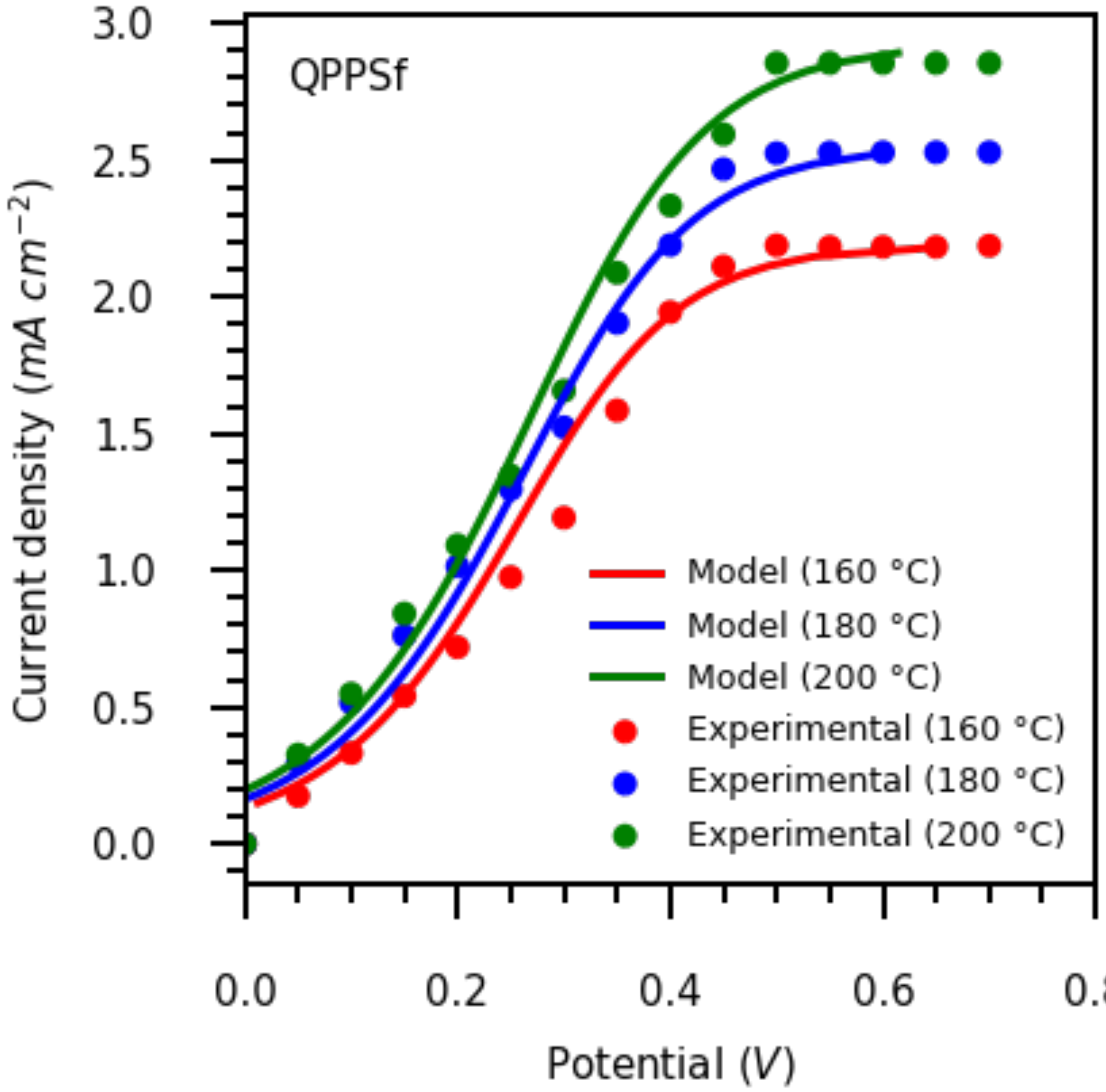

Platinum loading:
9 $\mu g_{Pt}\ cm^{-2}$

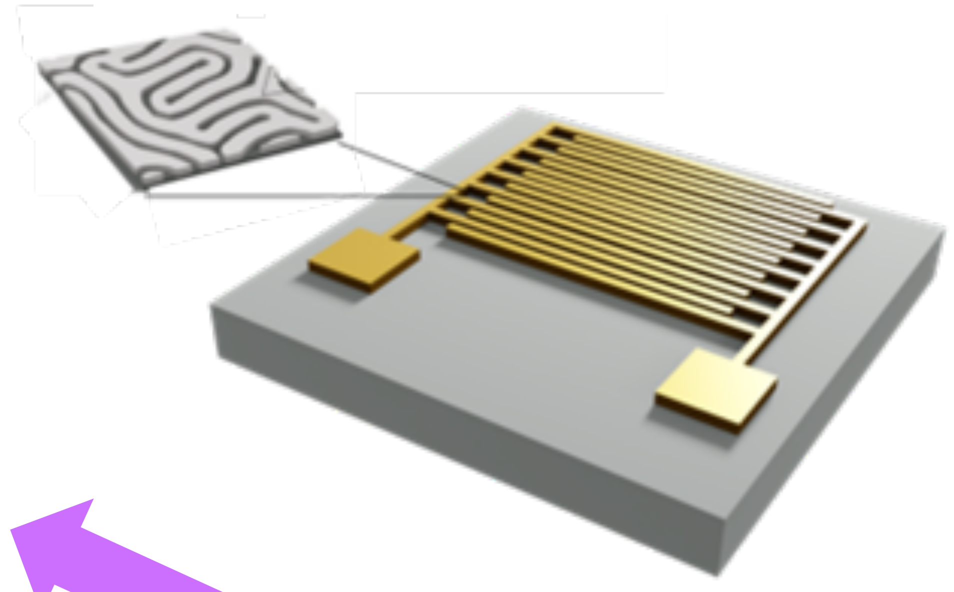

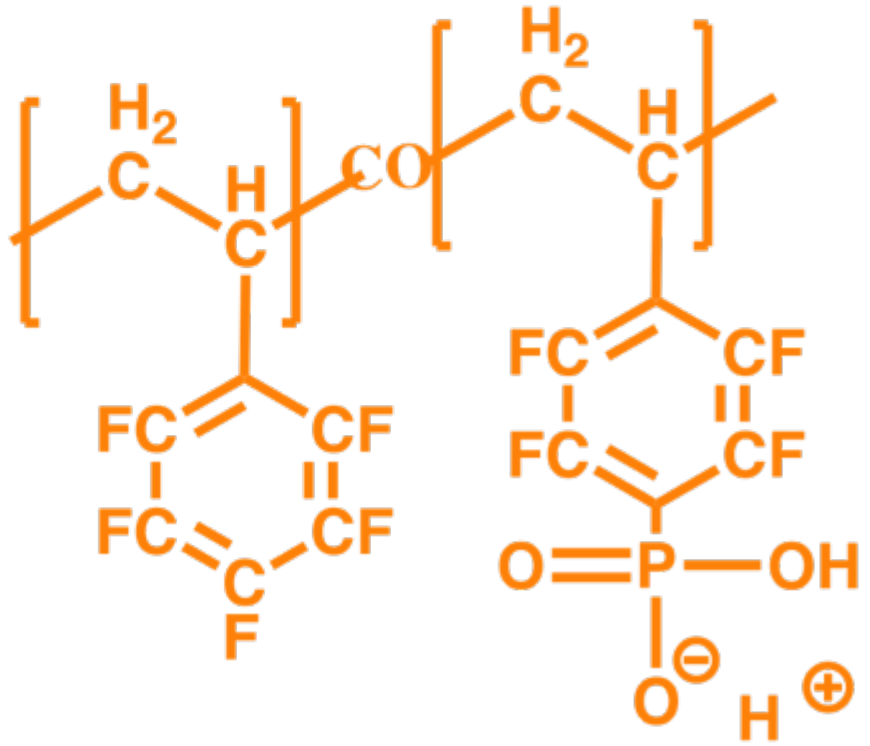

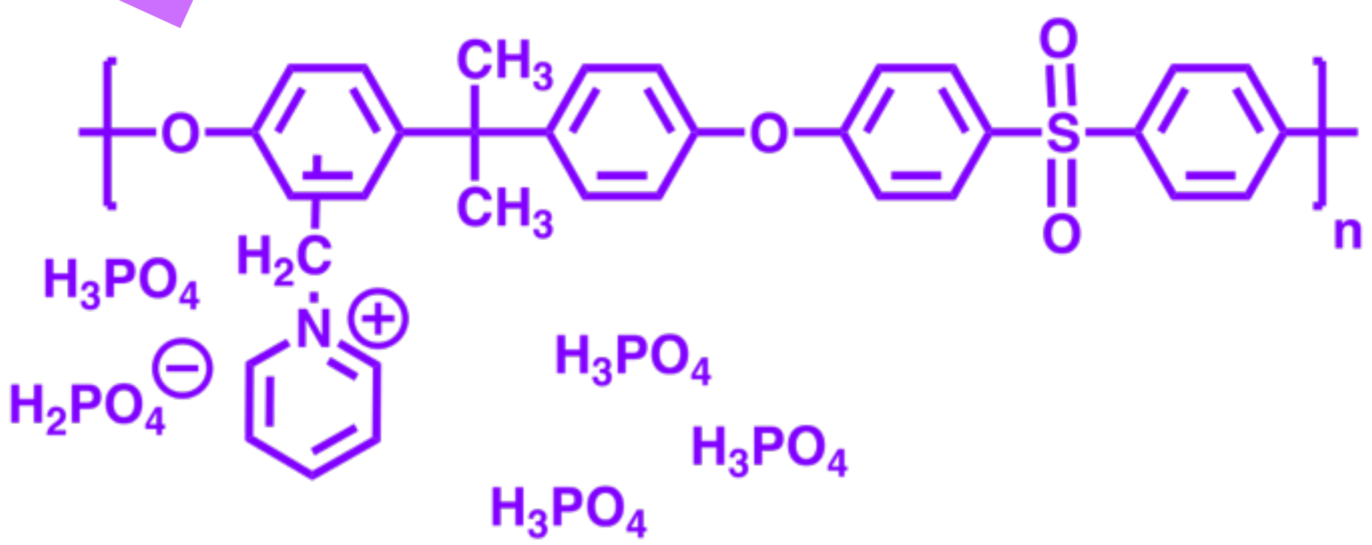

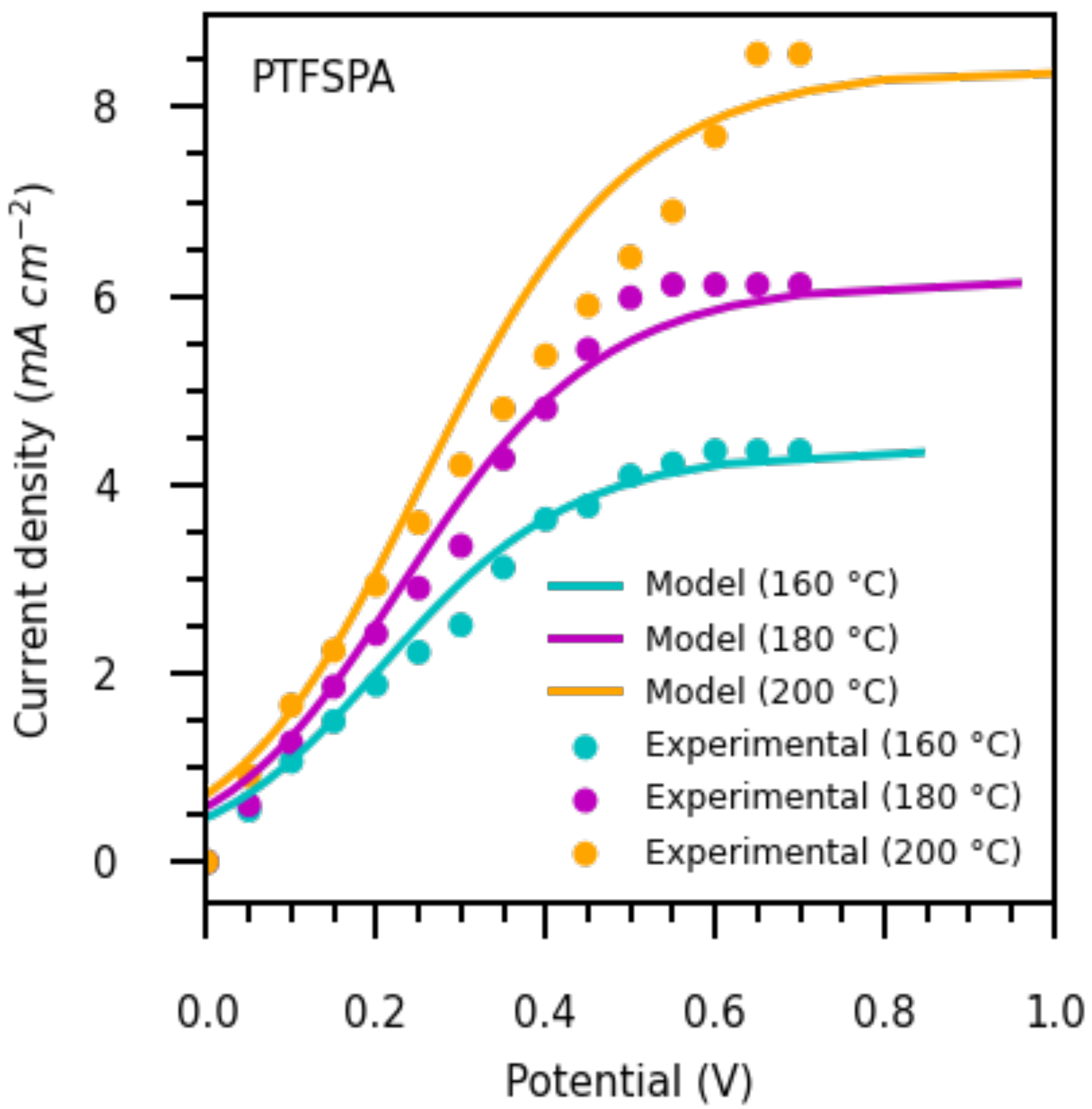

$$E(i) = E_o + \frac{RT}{(\alpha_{an}+\alpha_{ca})F} ln\left(\frac{i}{i_0}\right) + i\left(\frac{\delta_{io}}{\kappa_{io}^{+}}\right) - B\left(ln\left(1-\frac{i}{i_{lim}}\right)\right)$$

Thermo **Rxn kinetics** **Ohmic** **Mass transfer**

Adjustable parameters
γ, *B*, and *$i_{0\text{-}ref}$*

$$i_0 = a_C L_C \left(\frac{C_{H_2} H_{H_2}}{C_{H_2}^0}\right)^{0.5} \exp\left(-\frac{E_C^{H_2}}{R}\left(\frac{1}{T}-\frac{1}{T_{ref}^0}\right)\right) i_{0-ref} \exp(-\gamma(1-m_{io}))$$

$$i_{lim} = nFP_{H_2}\frac{C_{H_2}}{\delta} \qquad P_{H_2} = D_{H_2}H_{H_2}$$

H_2 pump with HT-ionomer thin films on IDEs

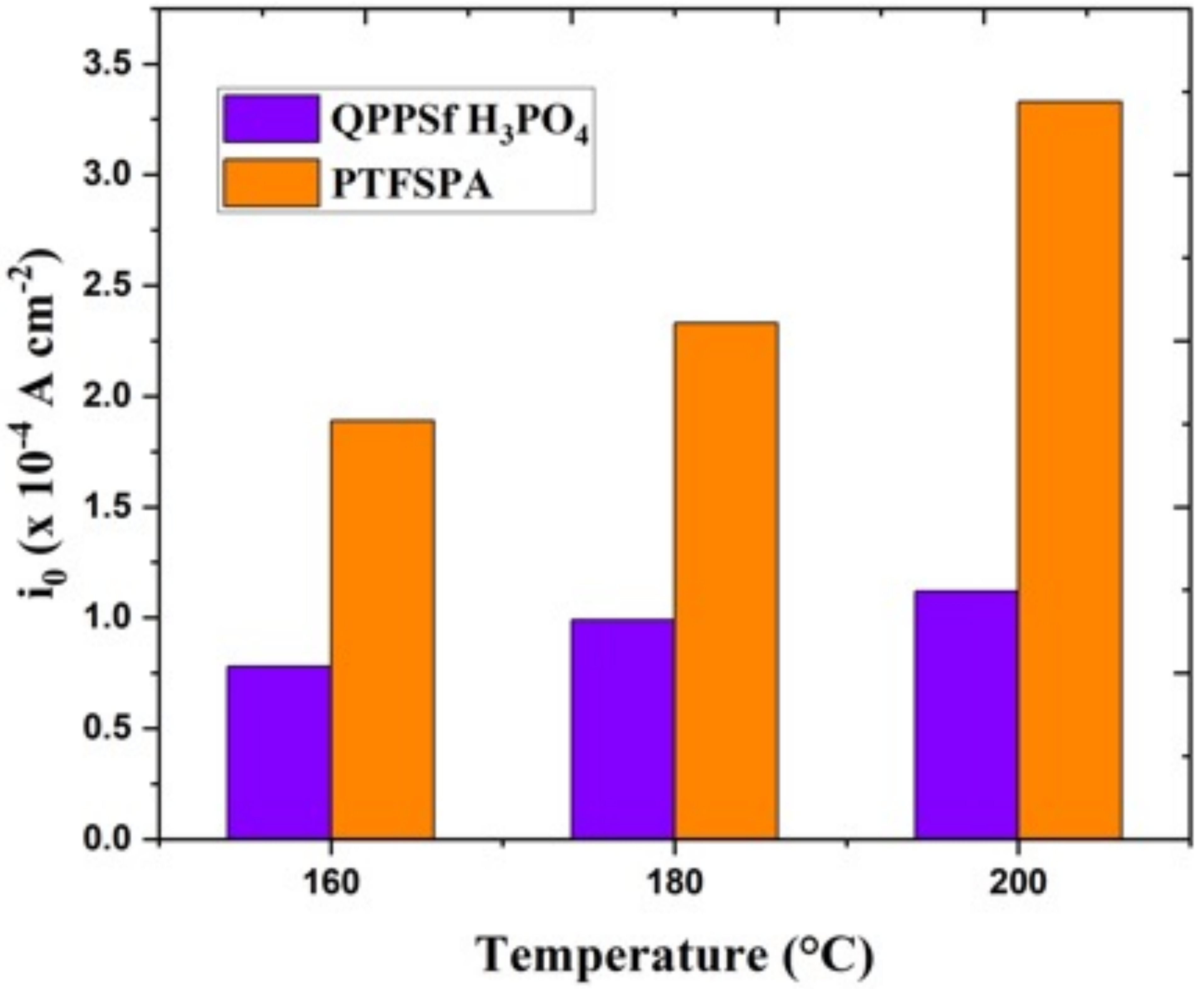

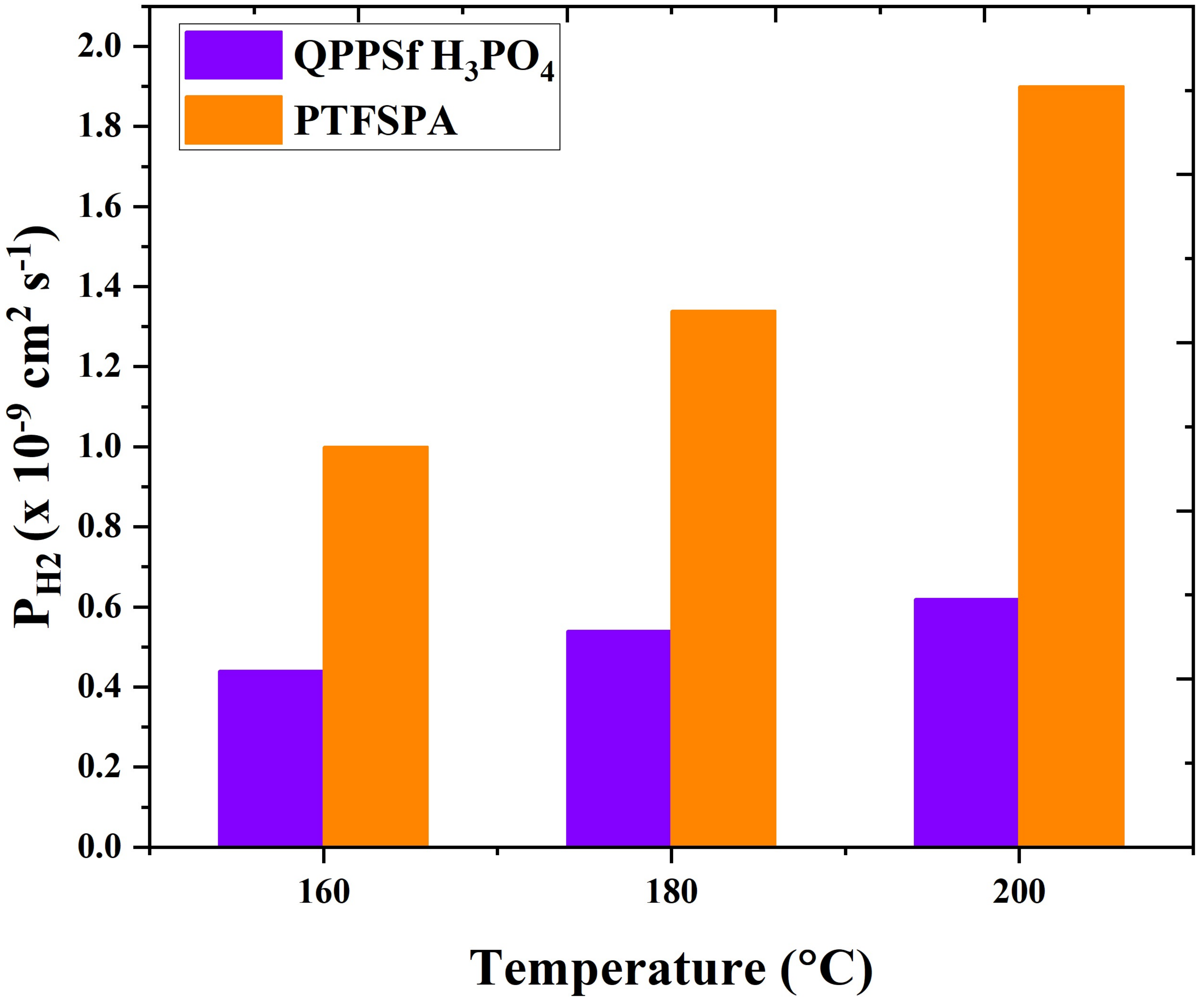

Removal of H_3PO_4 enhances reaction kinetics and gas permeability

G. Venugopalan, C.G. Arges, *Materials Advances (revision submitted)*

IDE data for informing fuel cell polarization

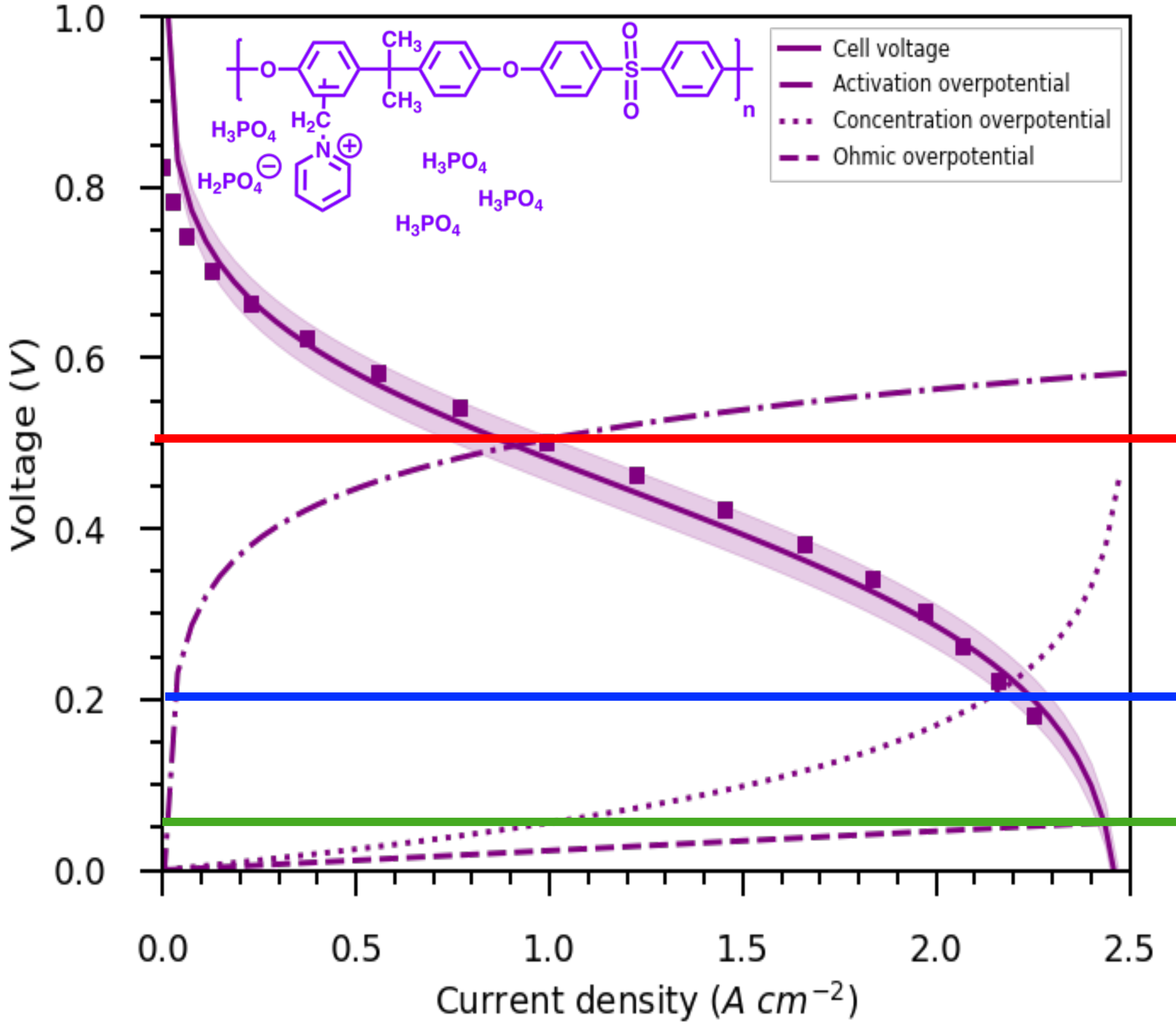

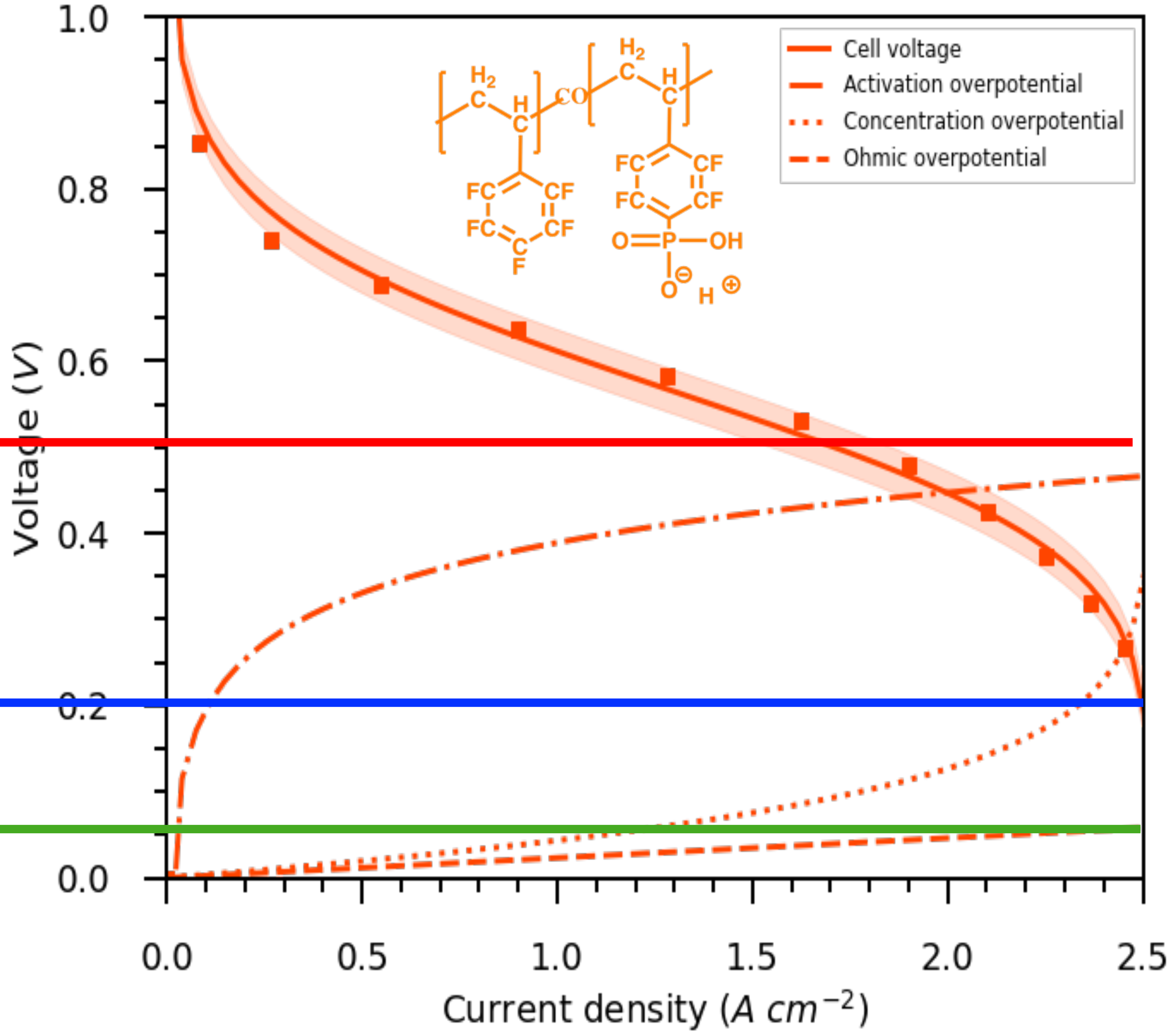

Adjustable parameters *γ* and *B*

Membrane electrode assembly (MEA) H_2 pump data with different binders

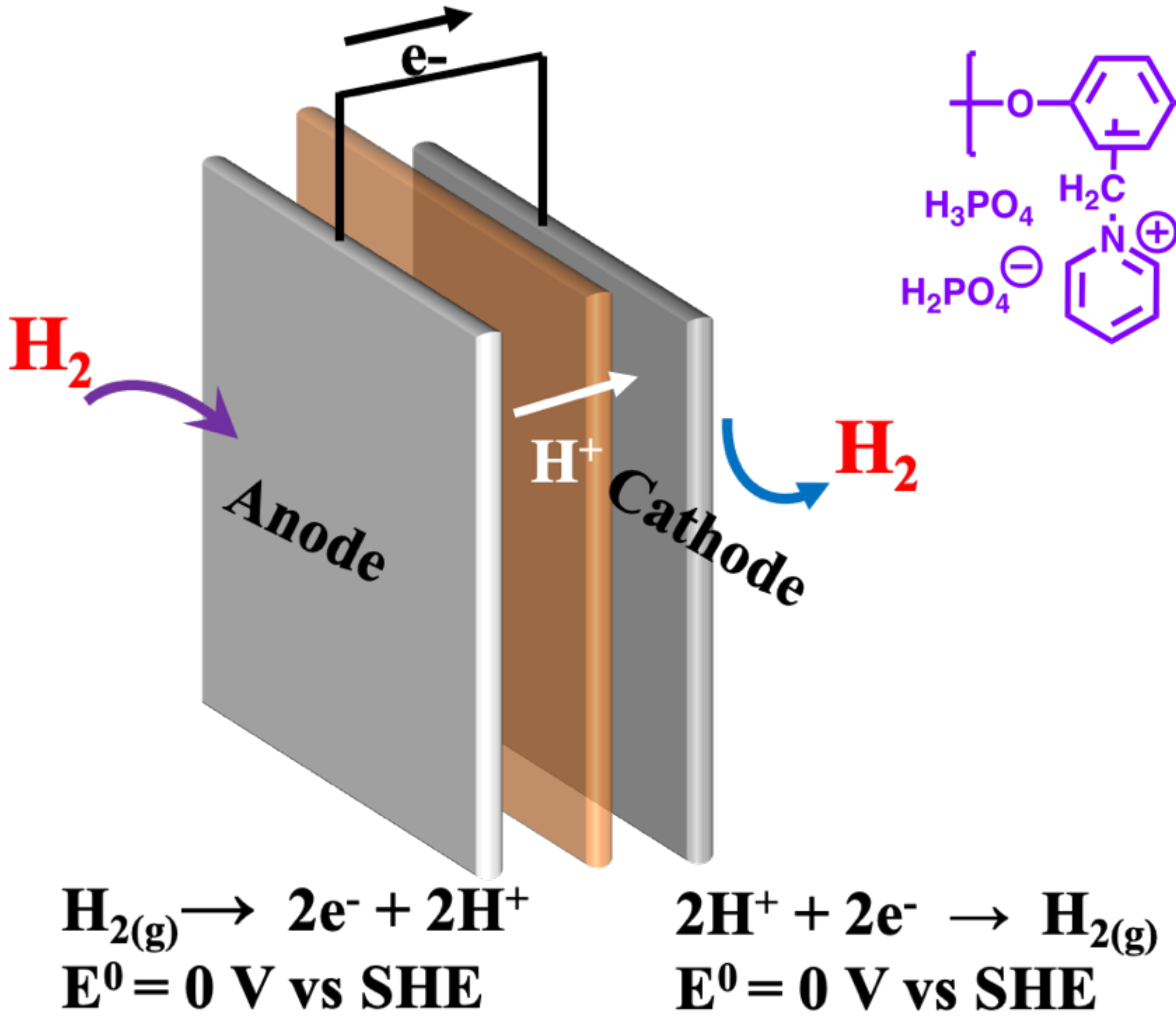

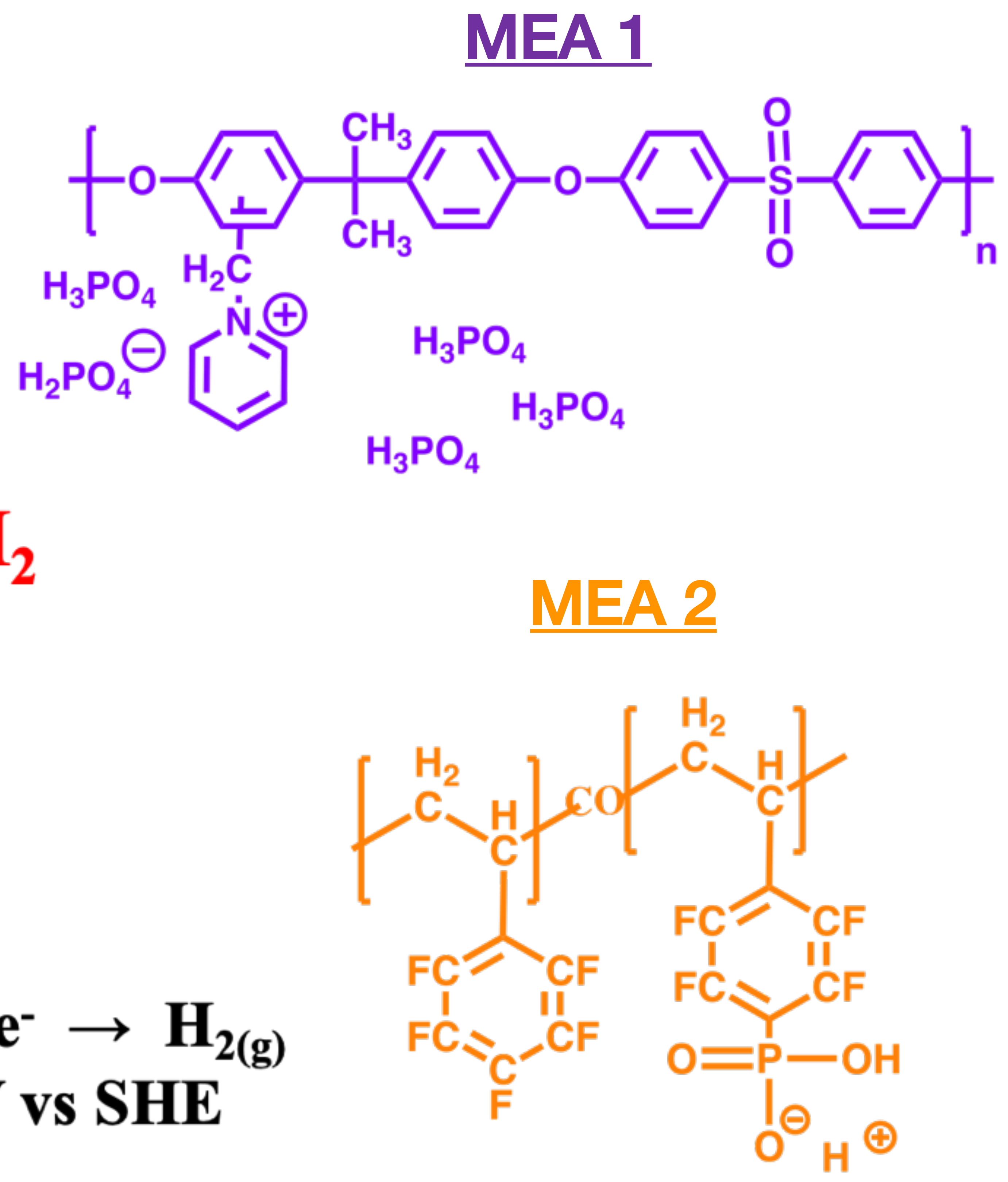

0.5 mg_{Pt} cm^{-2} for each electrode

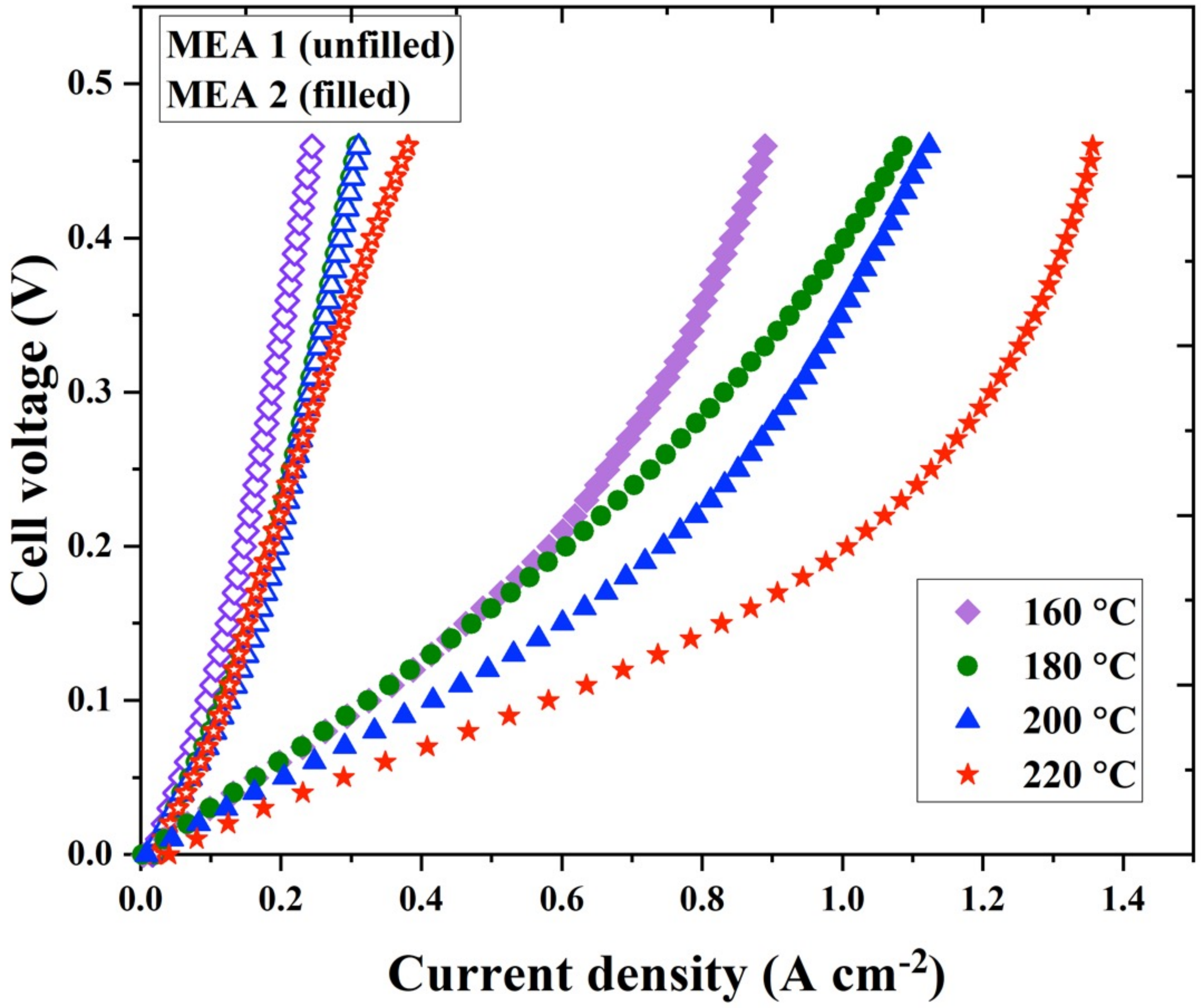

G. Venugopalan, C.G. Arges, *Materials Advances (revision submitted)*

Best HT-PEM H_2 pump data

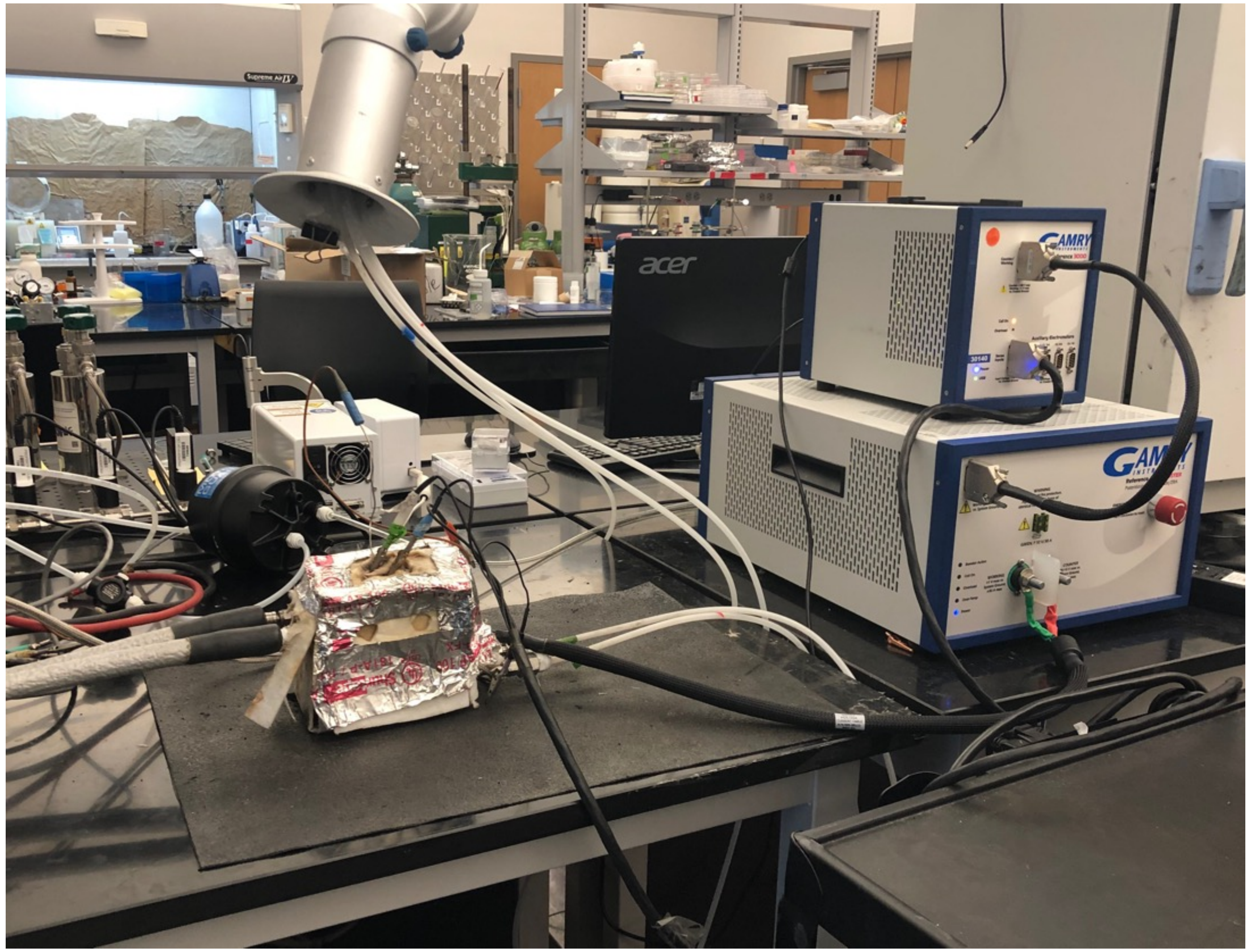

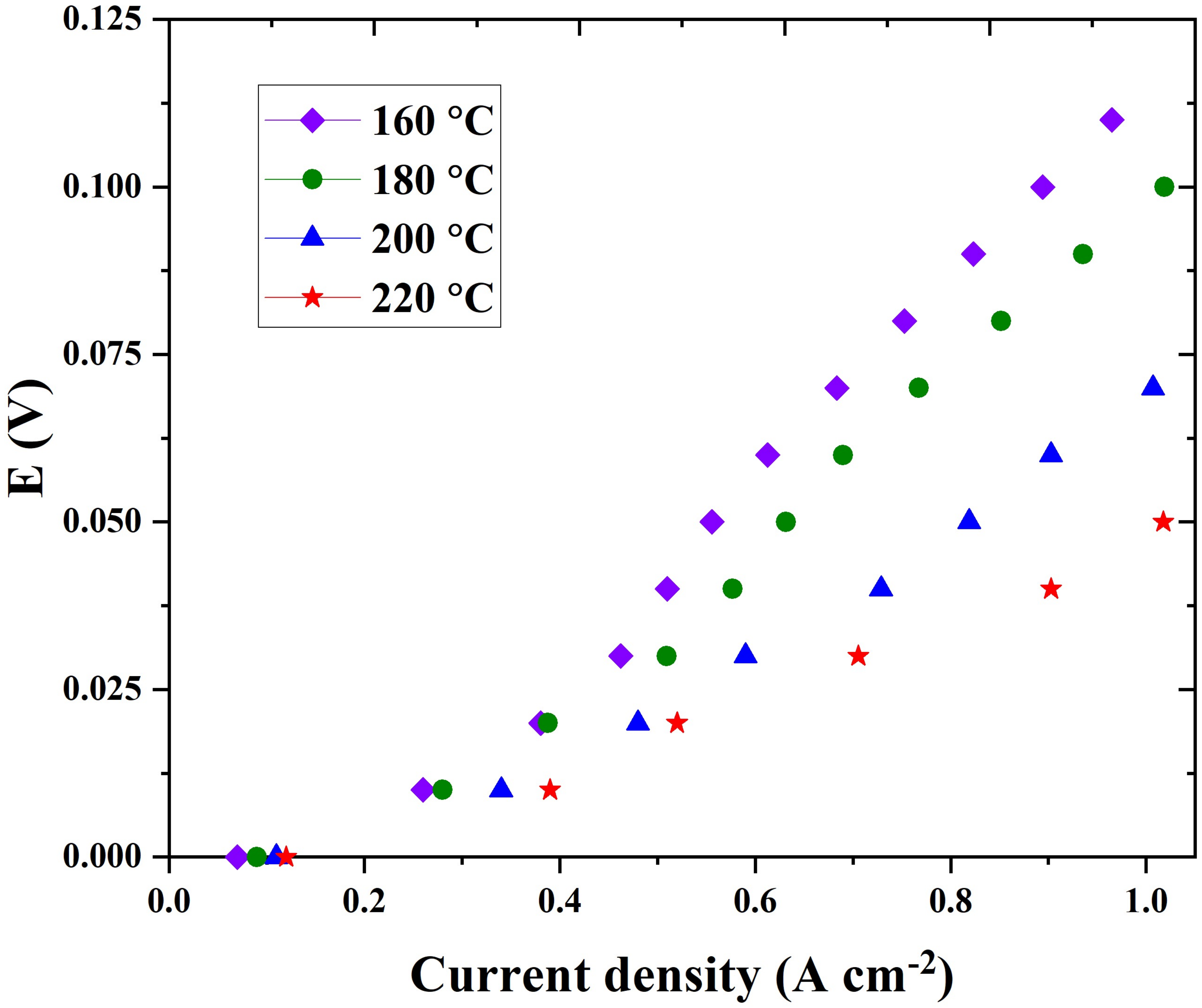

1 A cm^{-2} at 50 mV

G. Venugopalan, C.G. Arges, *Materials Advances (revision submitted)*

Correlating IDE data to MEA H_2 pump data

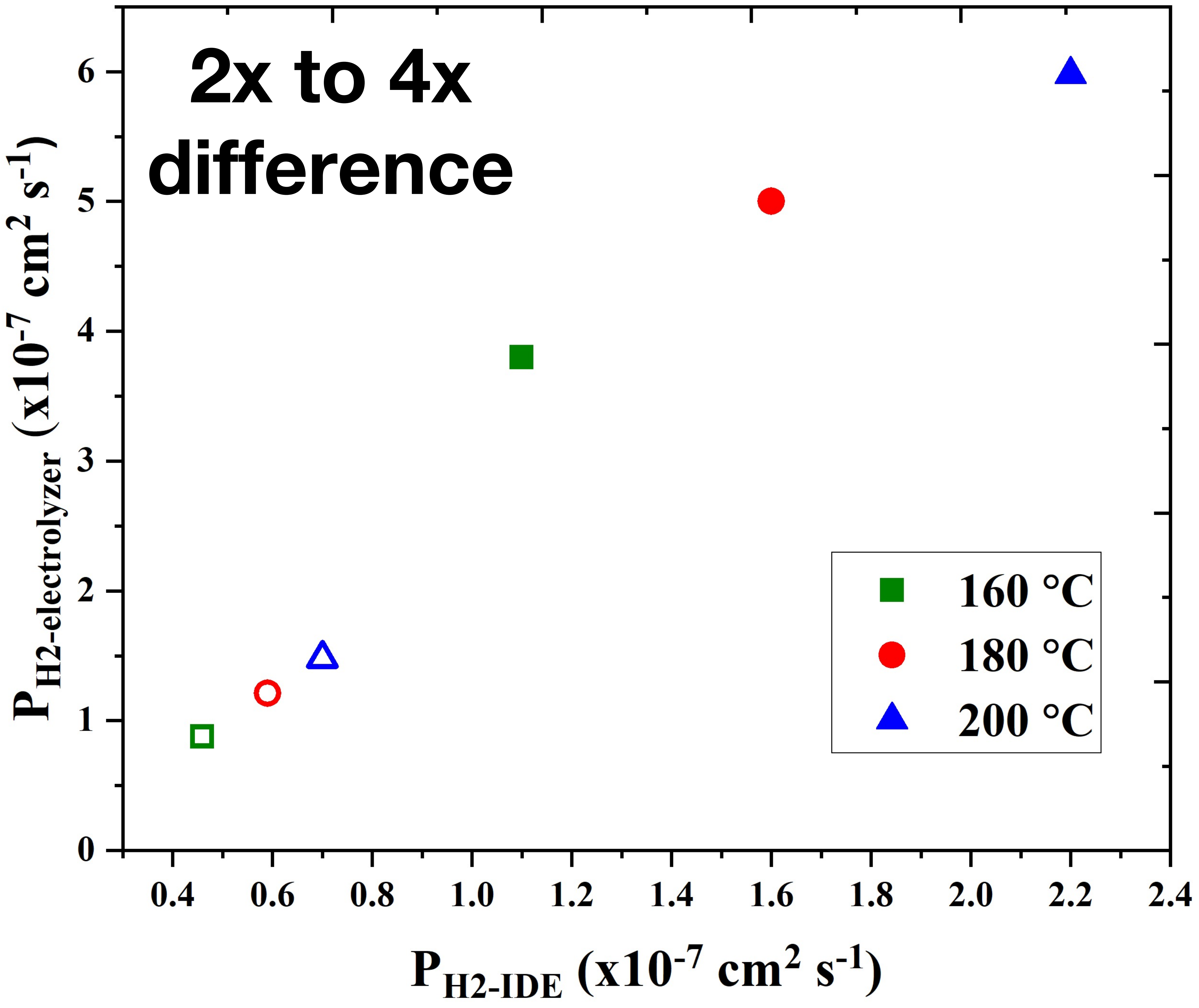

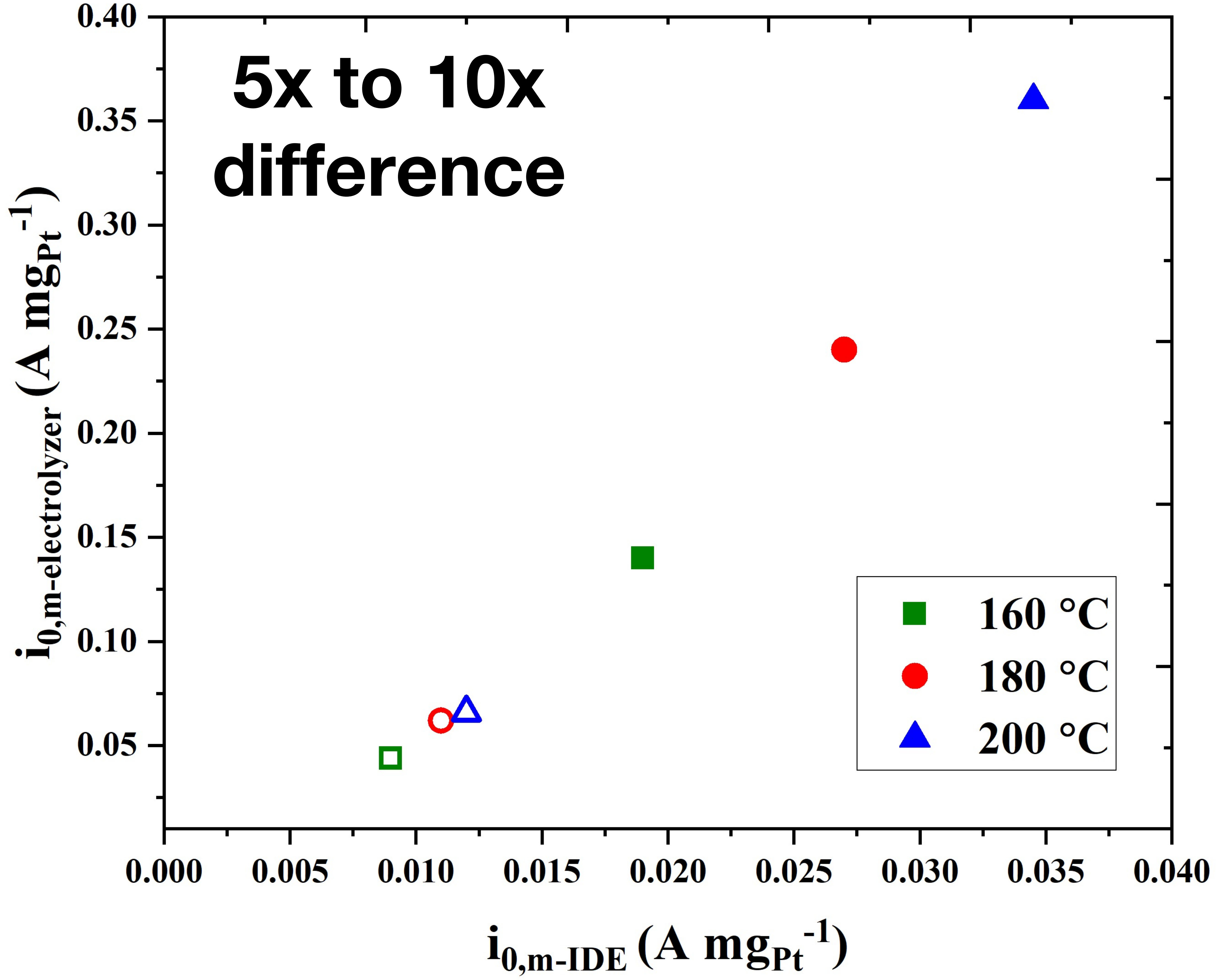

IDEs are a high-throughput, cost-effective platform for downselecting electrode ionomer binders for MEAs.

They use 100x less PGM, a small amount of binder, and do not require a bulk membrane and cell testing hardware.

G. Venugopalan, C.G. Arges, *Materials Advances (revision submitted)*

Broader use of hydrogen in the U.S. economy: H_2@Scale

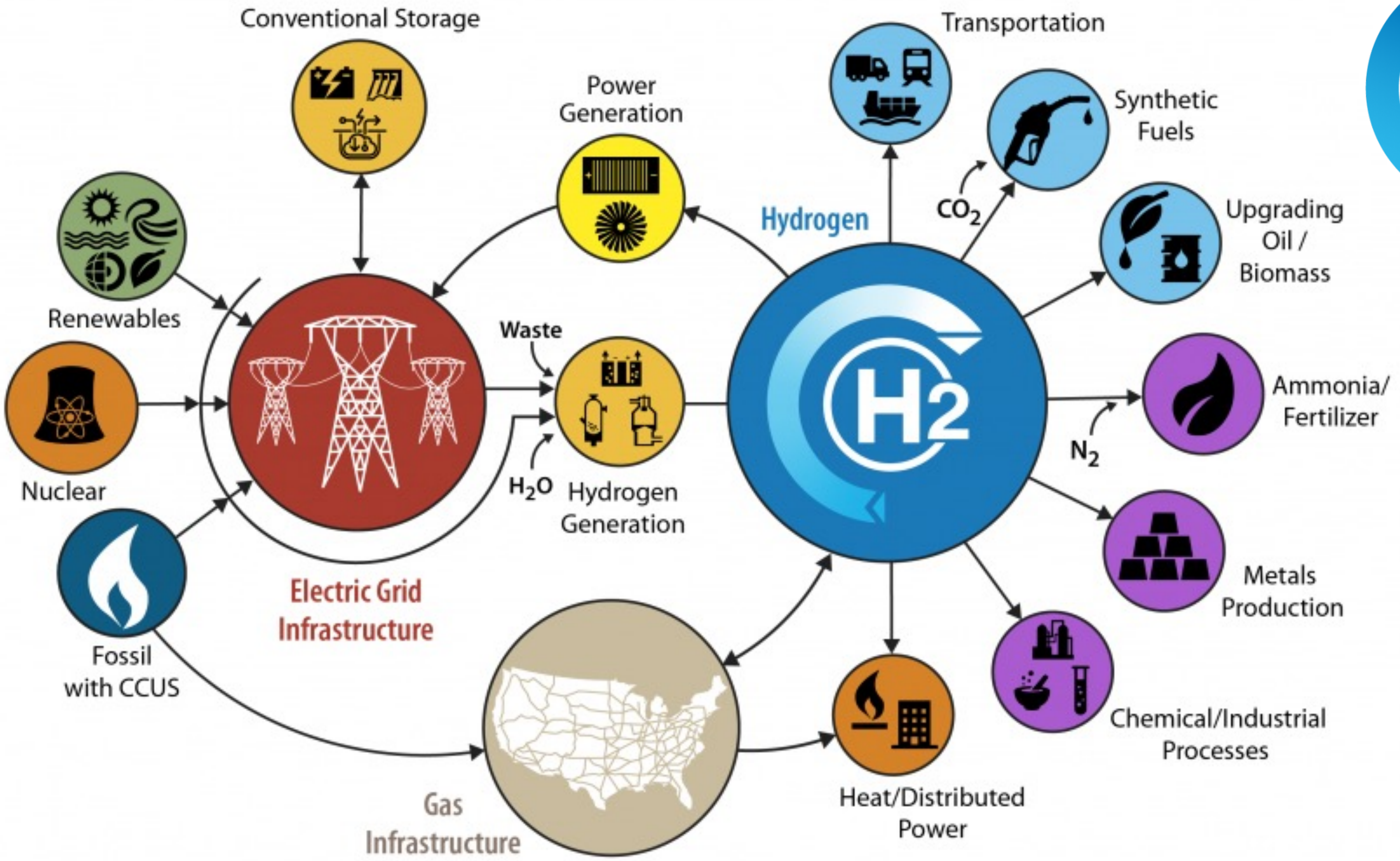

H2@Scale℠
U.S. Department of Energy

Presentation overview

High-temperature polymer electrolyte membranes (HT-PEMs) and binders for fuel cells

Studying the electrochemical properties of electrode ionomer binders as thin films

Future directions and concluding remarks

Machine Learning (ML) & data framework analysis approach

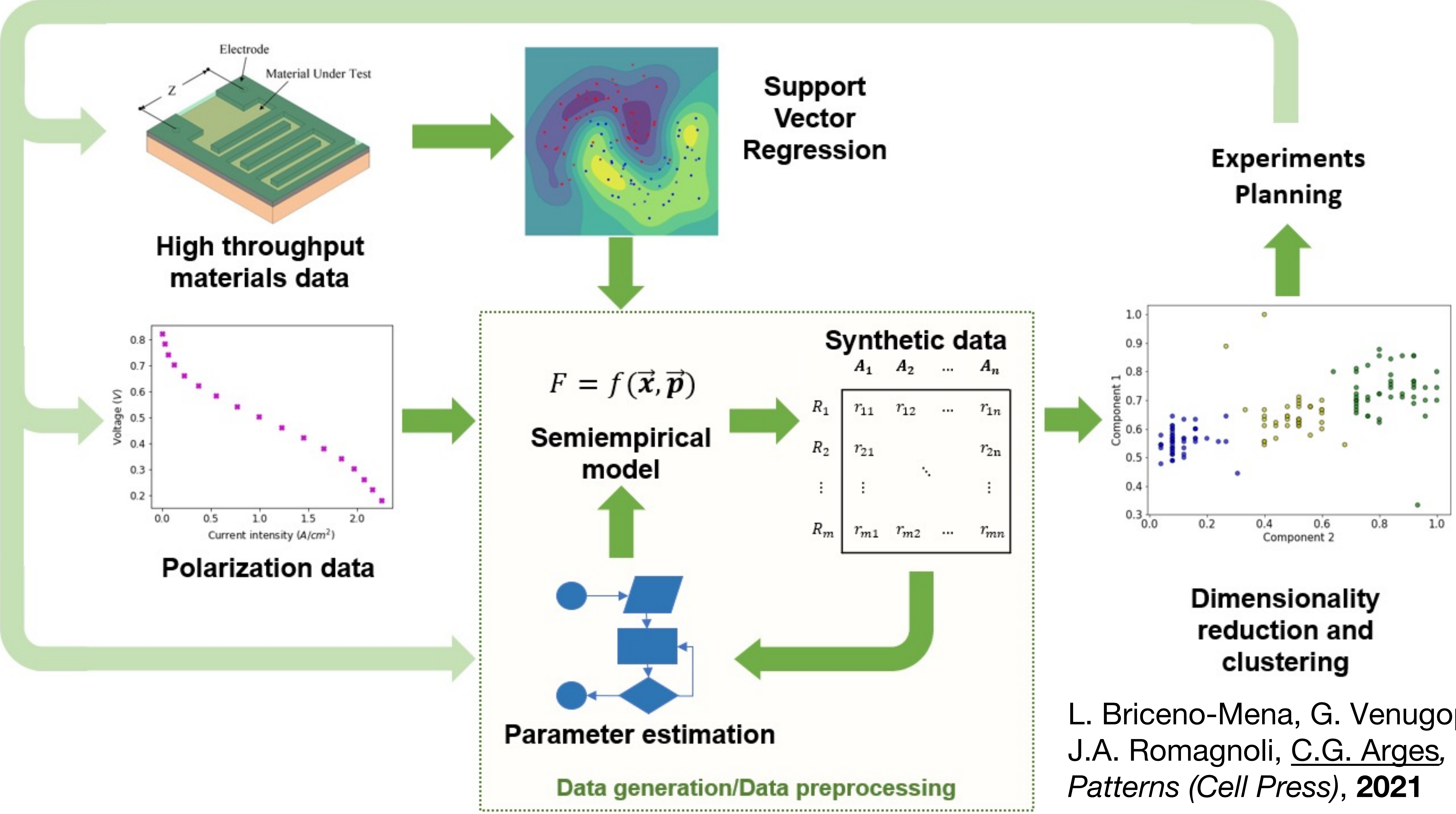

L. Briceno-Mena, G. Venugopalan, J.A. Romagnoli, C.G. Arges, *Patterns (Cell Press)*, **2021**

Luis Briceno-Mena
PhD candidate

Prof. José Romagnoli

Goal: Use ML to identify material properties and cell operating parameters for optimizing power constrained to 68% fuel efficiency and 0.3 $mg_{PGM}\ cm^{-2}$ in the MEA

Concluding remarks

Model thin films of electrocatalysts and polymer electrolytes are useful for establishing structure-property relationships and generating a large library of materials data.

This is important for the rationale design of electrodes that enable high performing fuel cell and electrolysis units *as well as the development of Machine Learning (ML) tools that bridge materials properties to cell level performance.*

Acknowledgements

U.S. DEPARTMENT OF ENERGY | Energy Efficiency & Renewable Energy

ADVANCED MANUFACTURING OFFICE

Award # DE-EE0009101

Postdocs and Graduate students

Mario Ramos-Garcés (Postdoc)
Matthew Jordan
Gokul Venugopalan
Varada Palakkal (PhD 2020)
Le Zhang (MS 2018)
Subarna Kole
Deepra Bhattacharya
Qi Lei (MS 2020)
Luis Briceno-Mena
(advised by Prof. José Romagnoli)

Los Alamos NATIONAL LABORATORY EST. 1943
Yu Seung Kim

TOYOTA
Hongfei Jia

XERGY
Bamdad Bahar

Argonne NATIONAL LABORATORY

Advanced Photon Source

Joe Strzalka (ANL)

Thank you for your attention!

Questions?

H_3PO_4 dopedPBI is commercial and mature

Acid-Doped Polybenzimidazoles: A New Polymer Electrolyte

J. S. Wainright,*[a] J-T. Wang,[a] D. Weng,[a] R. F. Savinell,*[a] and M. Litt[b]

[a] Department of Chemical Engineering and [b] Department of Macromolecular Science and Engineering, E. B. Yeager Center for Electrochemical Sciences, Case Western Reserve University, Cleveland, Ohio 44106-7217, USA

J. Electrochem. Soc. **1995**

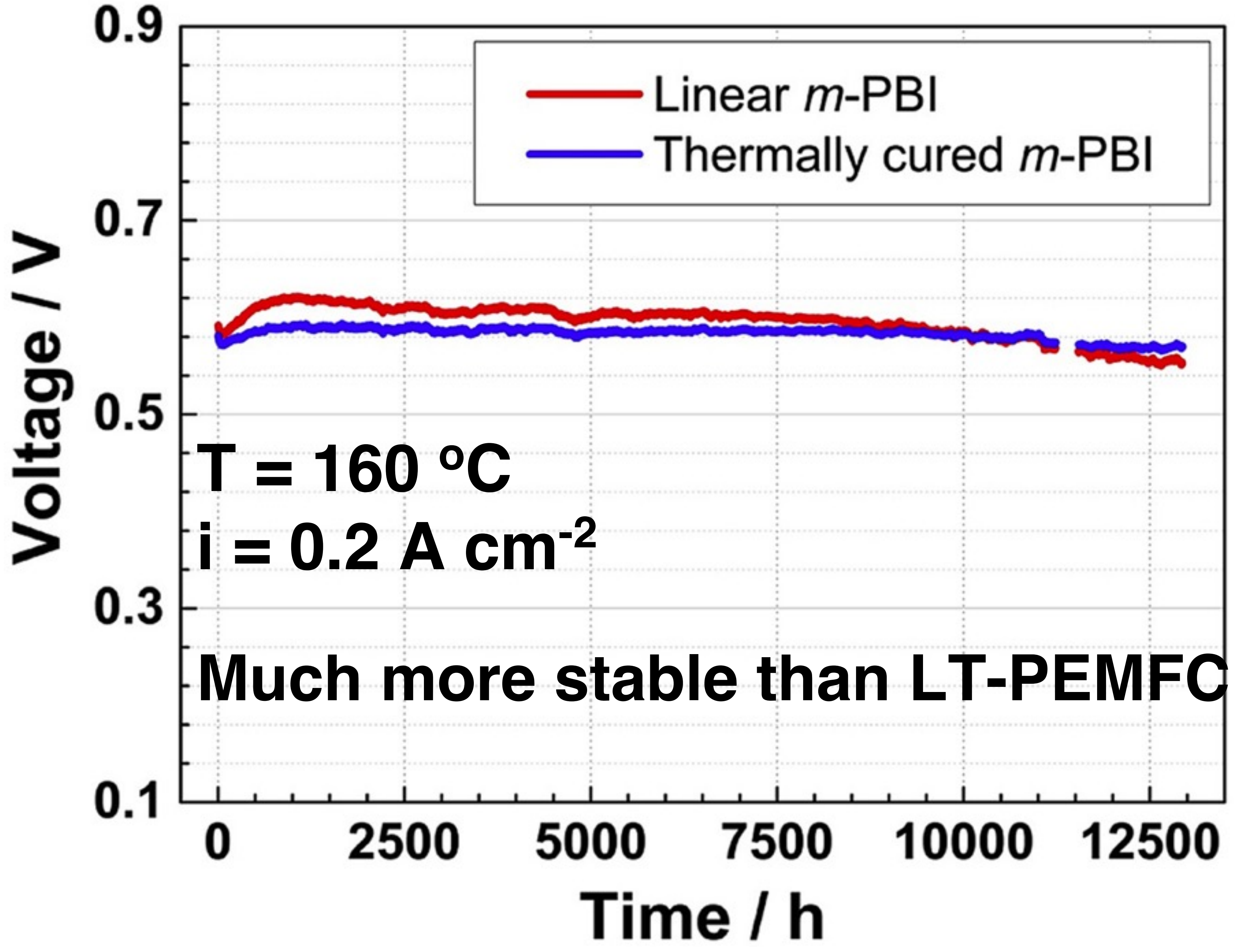

BASF Celtec®

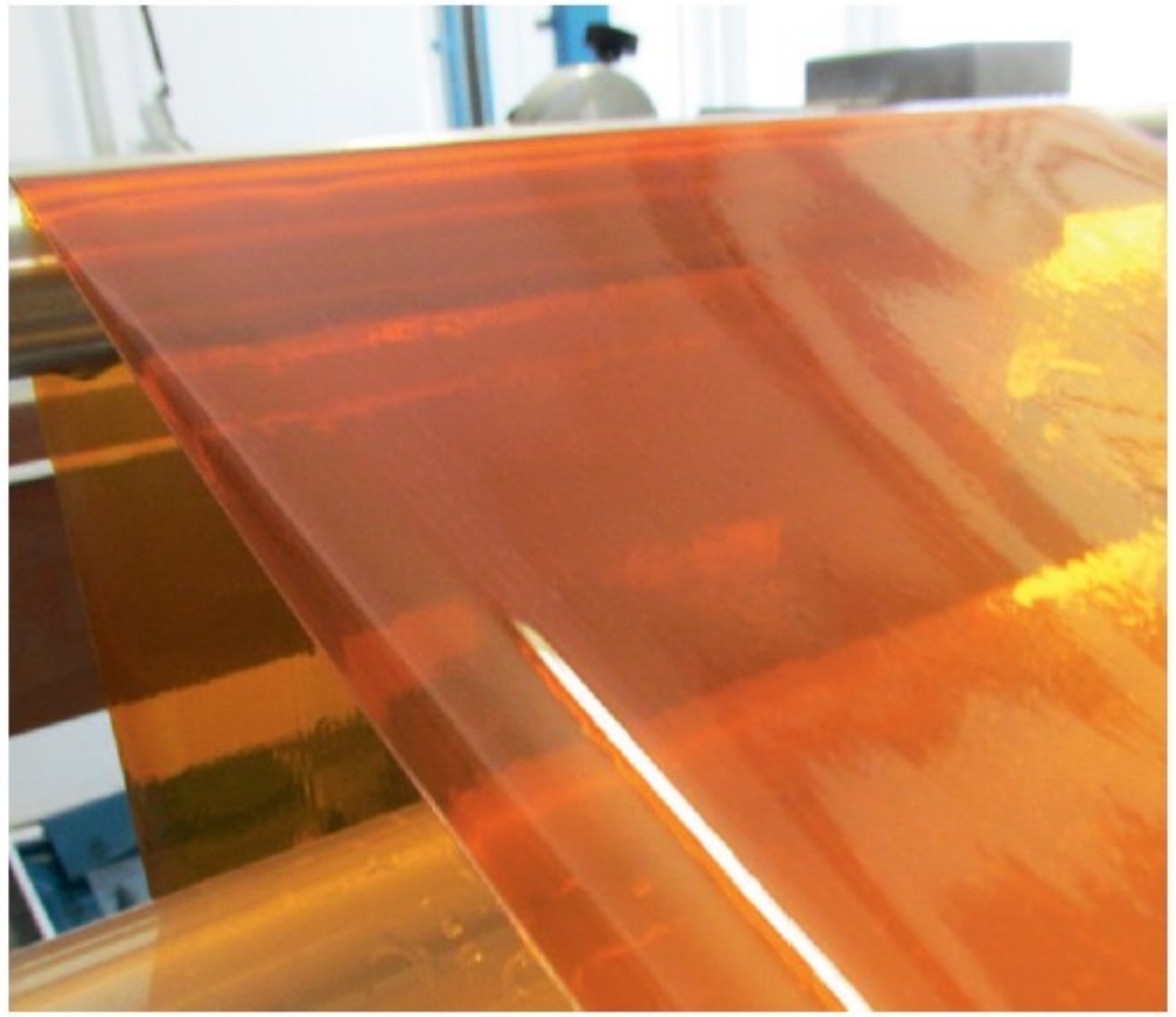

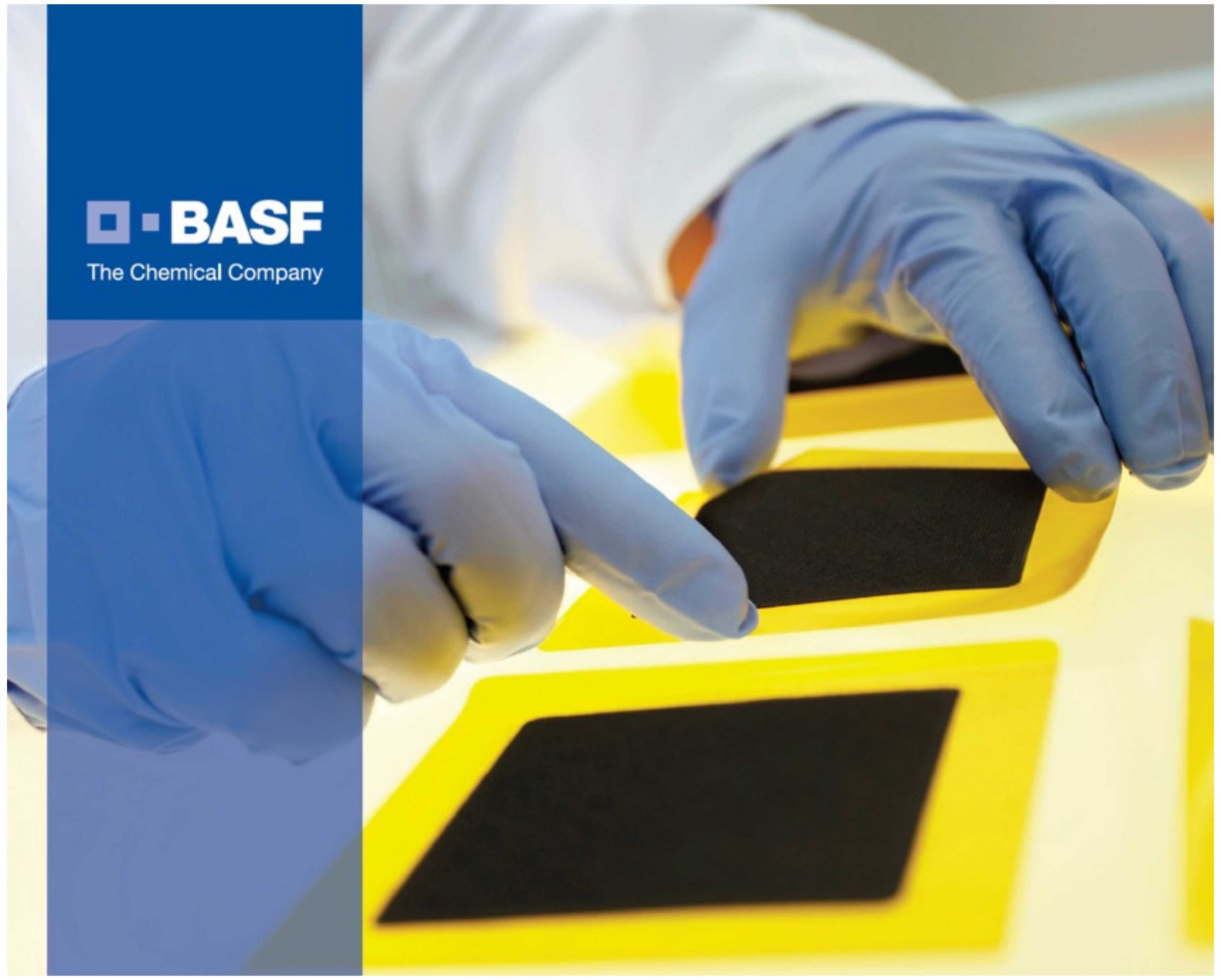

Other limitations of PBI

- **Cells use +1 mg$_{Pt}$ cm^{-2} (large Pt loadings)**
- **Low power (400 mW cm^{-2} w/ H_2 & air)**

These properties limit it to niche applications (e.g., stationary power)

B.C. Benicewicz. *et al. Chem. Mater.*, **2005**

J.O. Jensen *et al. J. Power Sources*, **2017**

Ion-pair HT-PEMs as superior alternatives to PBI

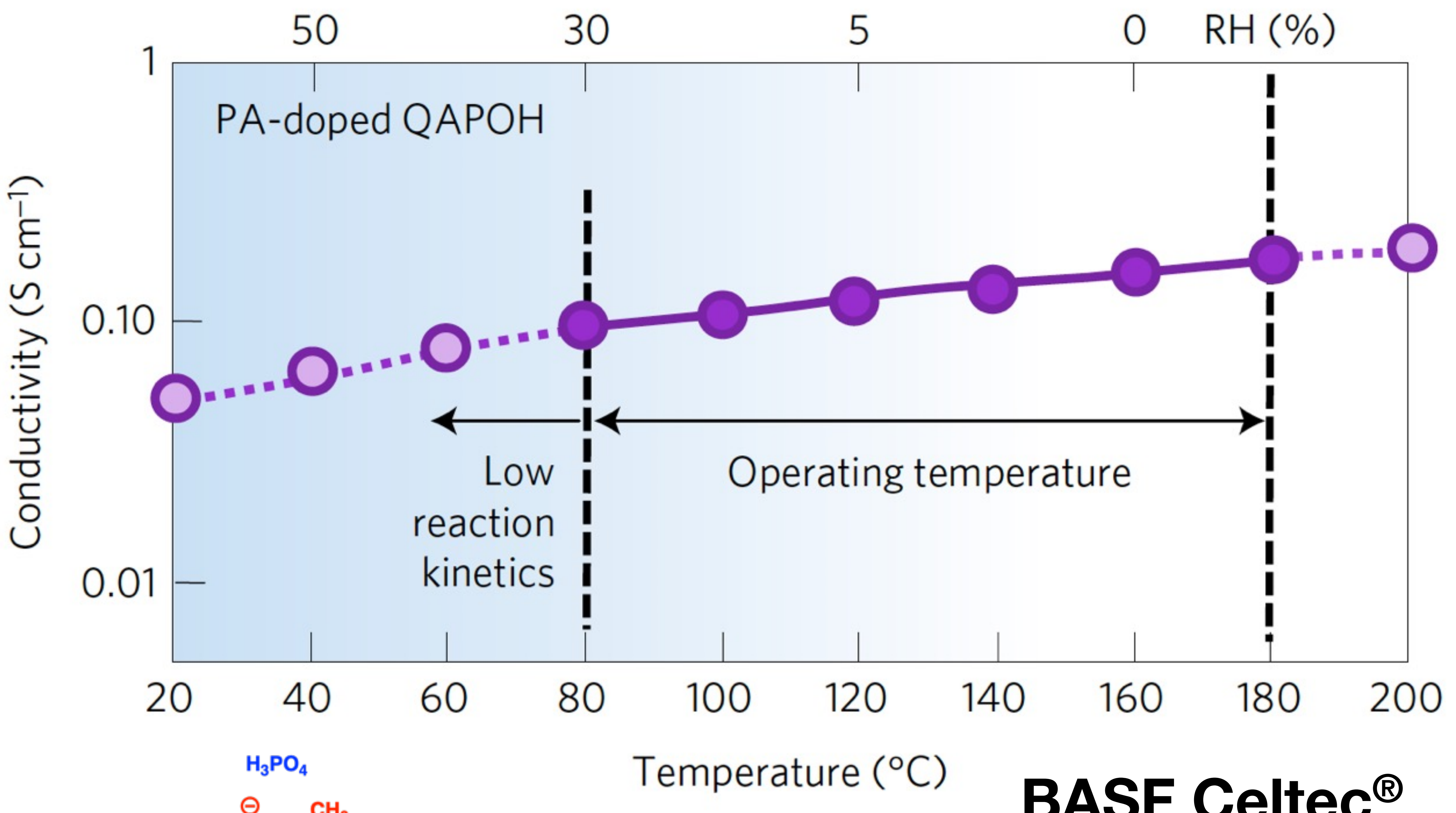

H3PO4 weight loss from the polymer

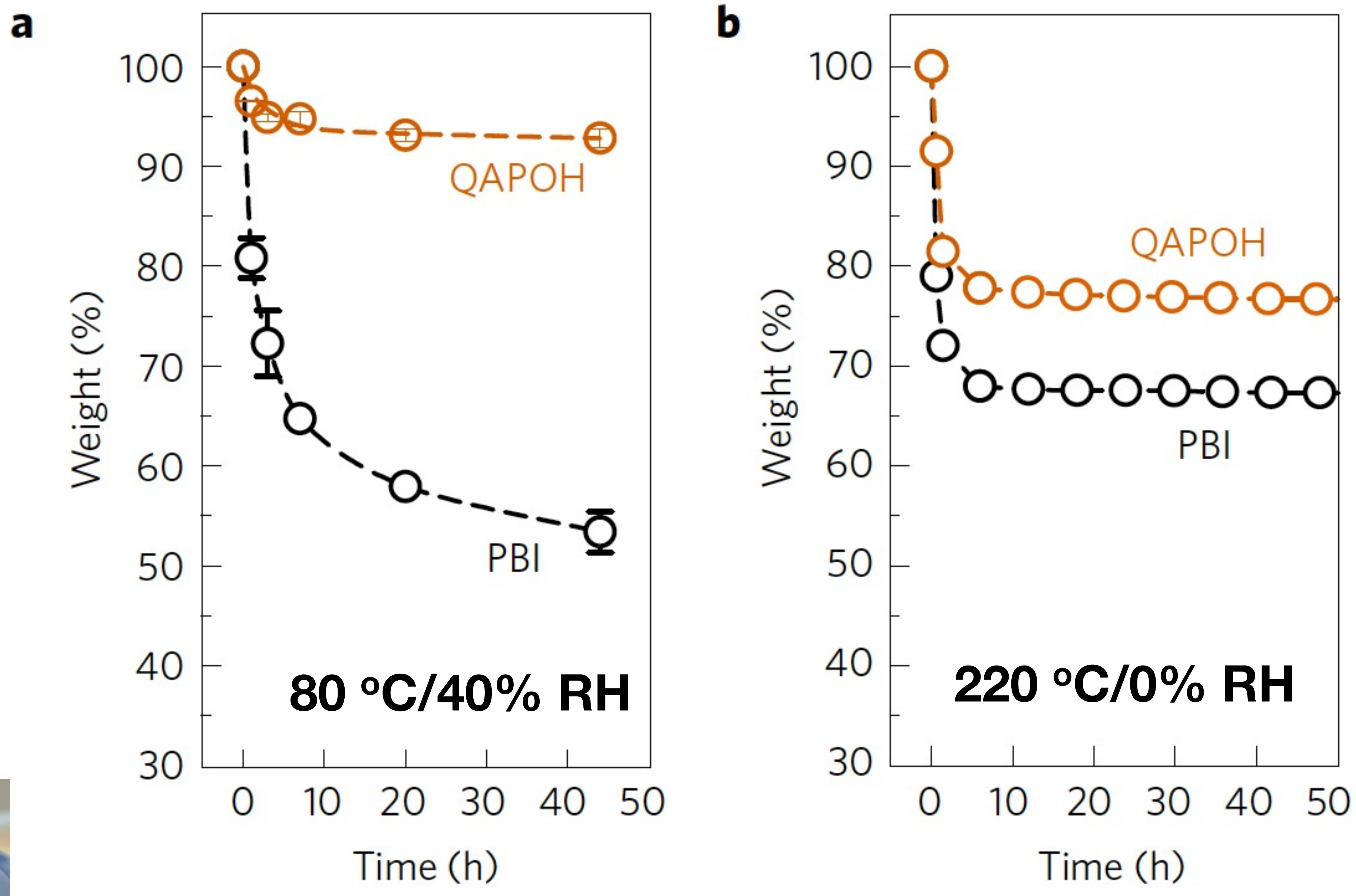

80 °C/40% RH

220 °C/0% RH

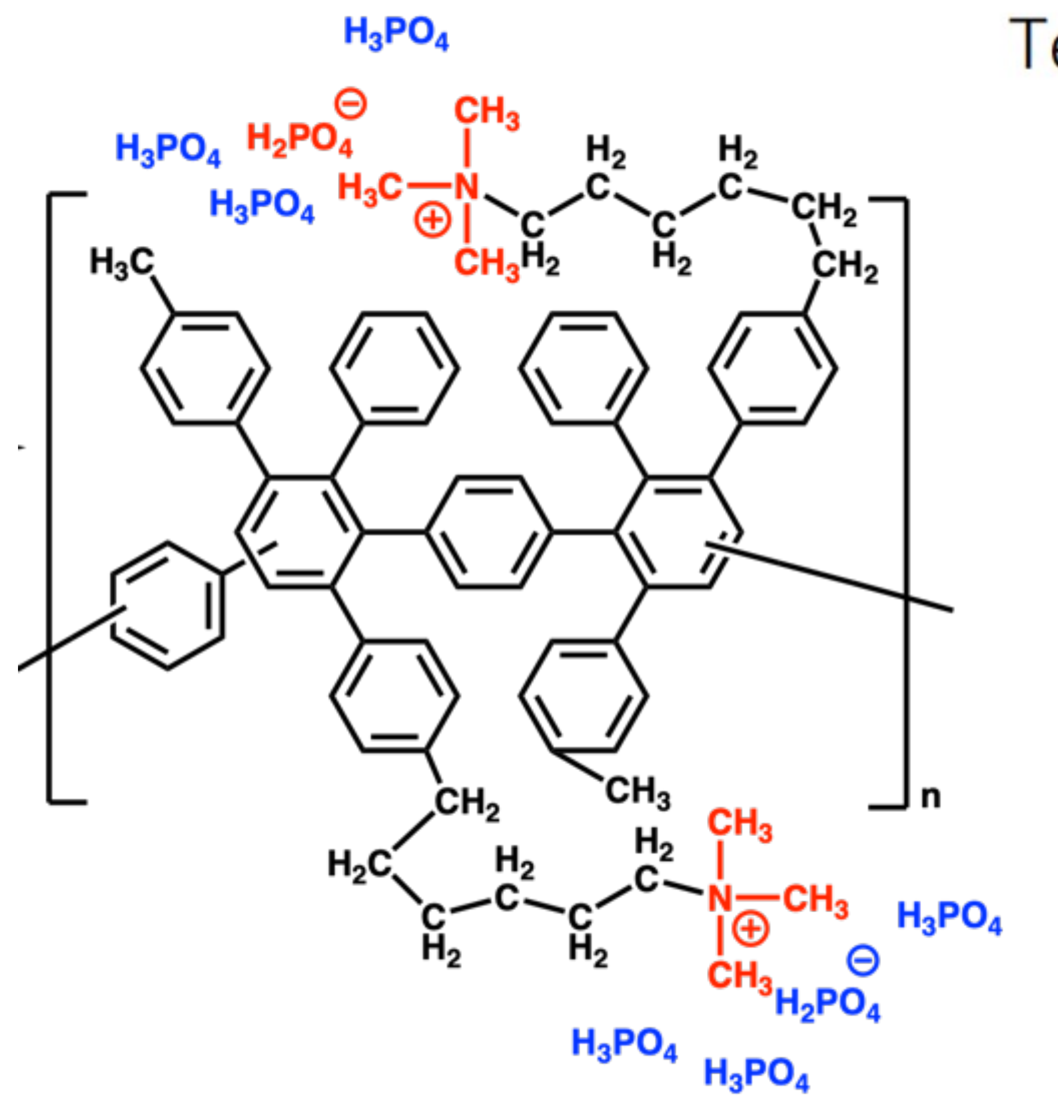

vs

BASF Celtec®
(PBI-H_3PO_4)

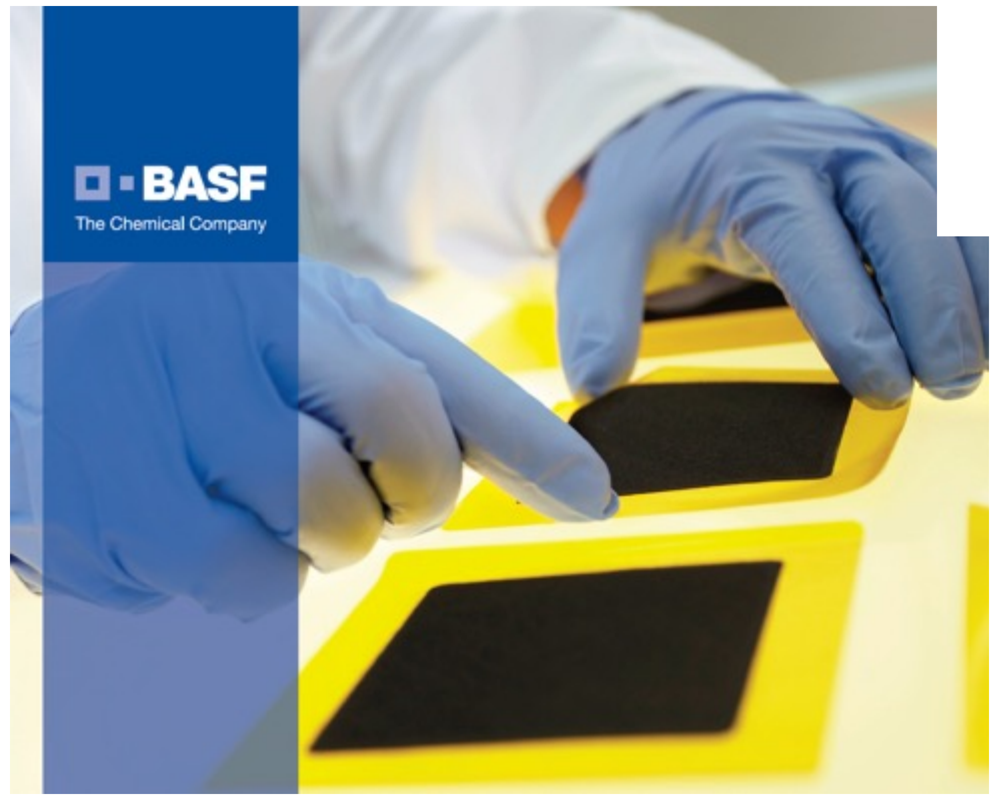

Quaternary ammonium group provides a strong ion pair interaction for stability

K.-S. Lee, Y.S. Kim. *et al. Nature Energy*, **2016**

Ion-pair HT-PEMs as superior alternatives to PBI

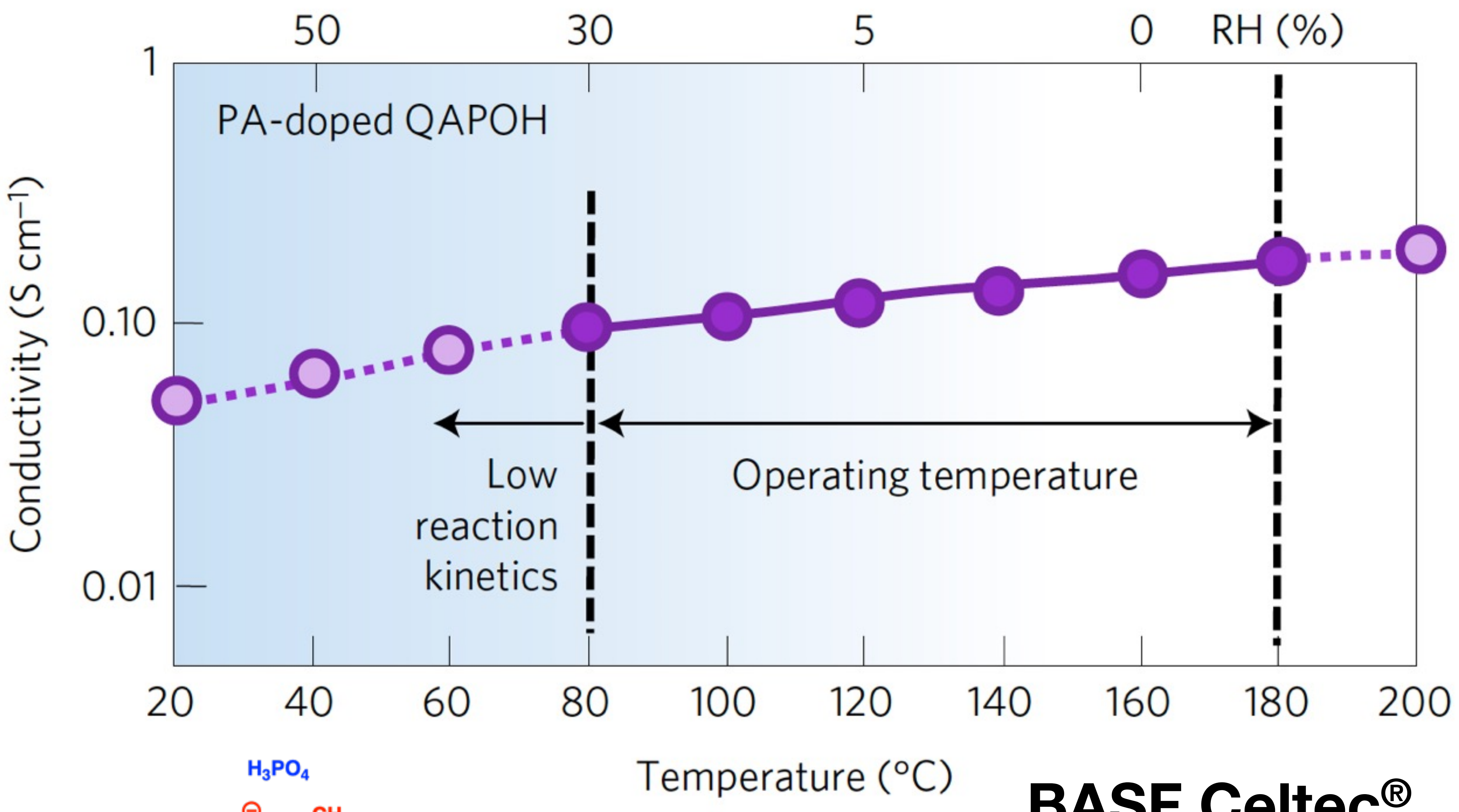

H_3PO_4 weight loss from the polymer

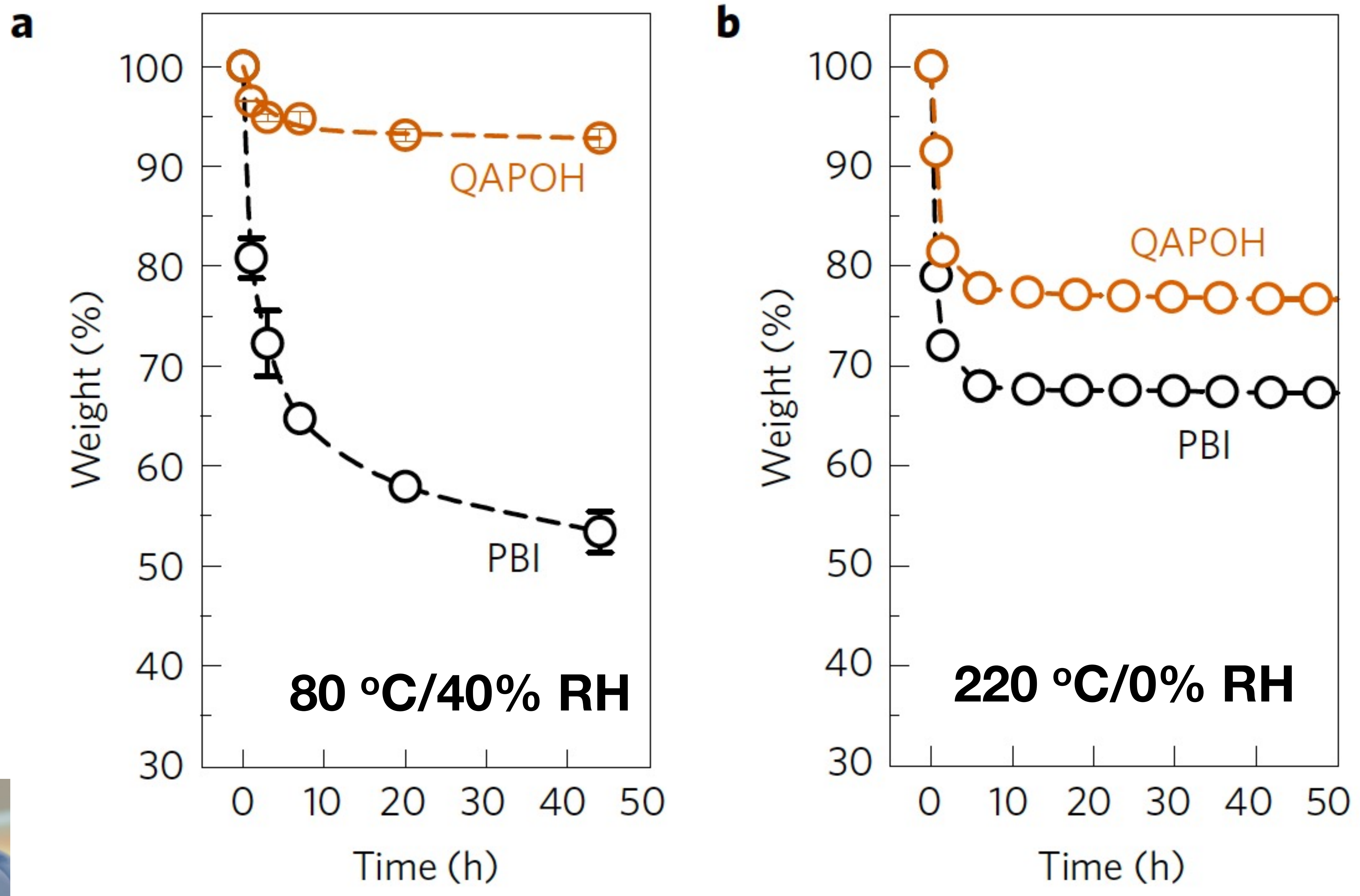

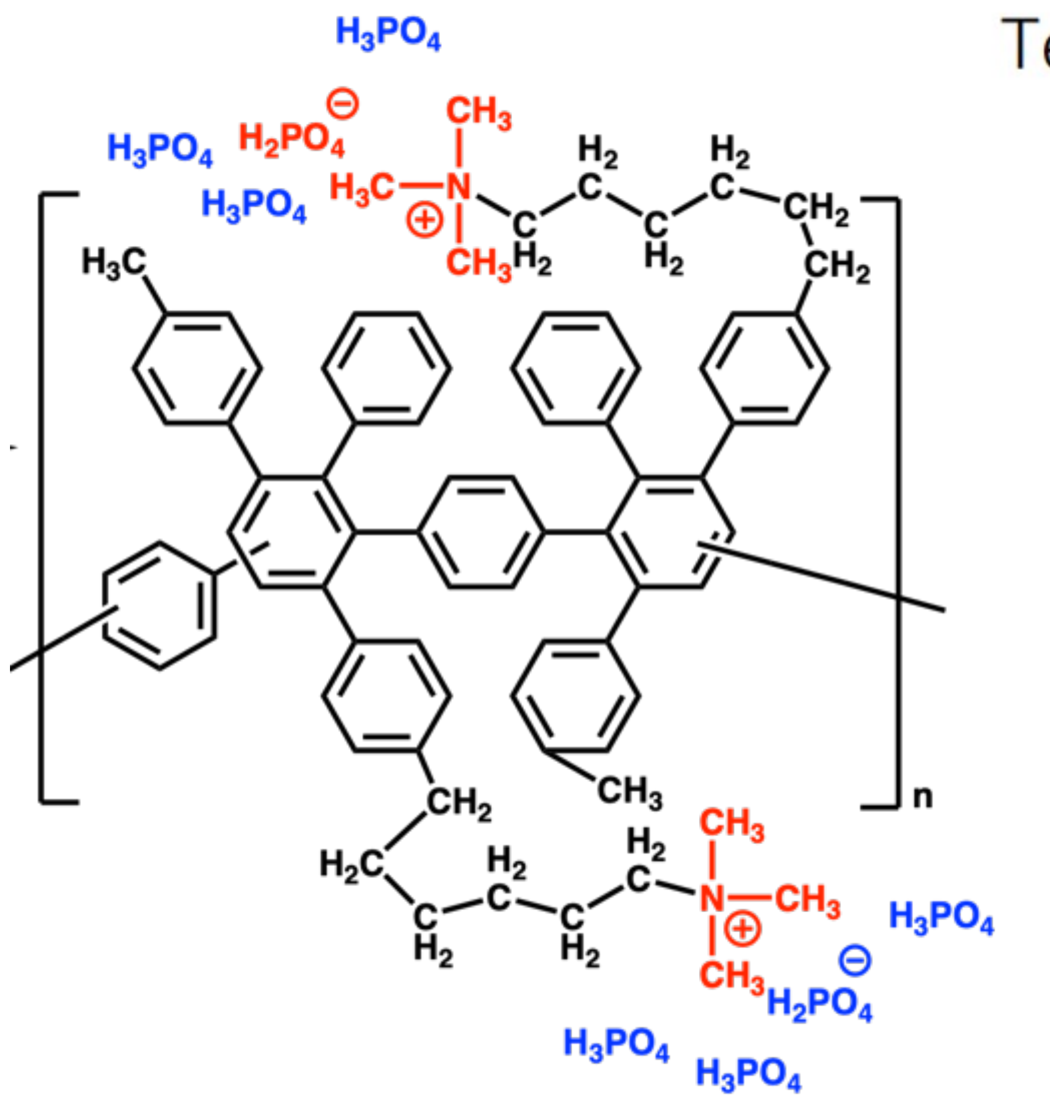

vs

BASF Celtec®
(PBI-H_3PO_4)

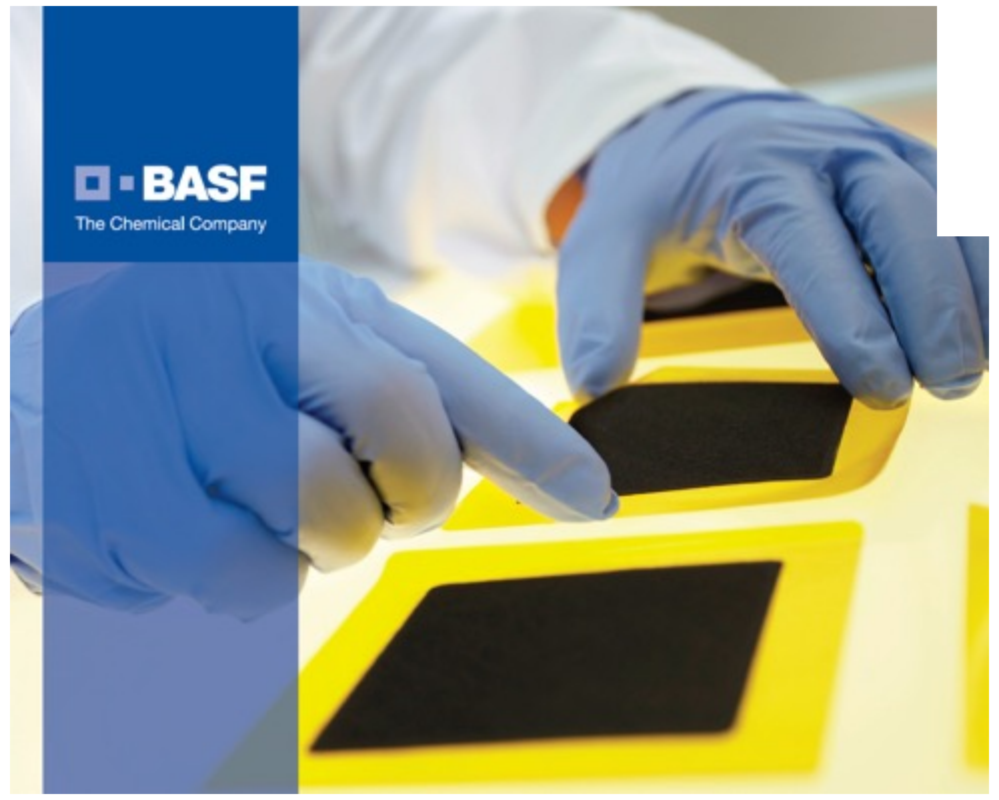

Ion-coordinated HT-PEMs have better stability when compared to Celtec® and comparable proton conductivity

K.-S. Lee, Y.S. Kim. *et al. Nature Energy*, **2016**

Sources of resistances in the fuel cell and cell stability

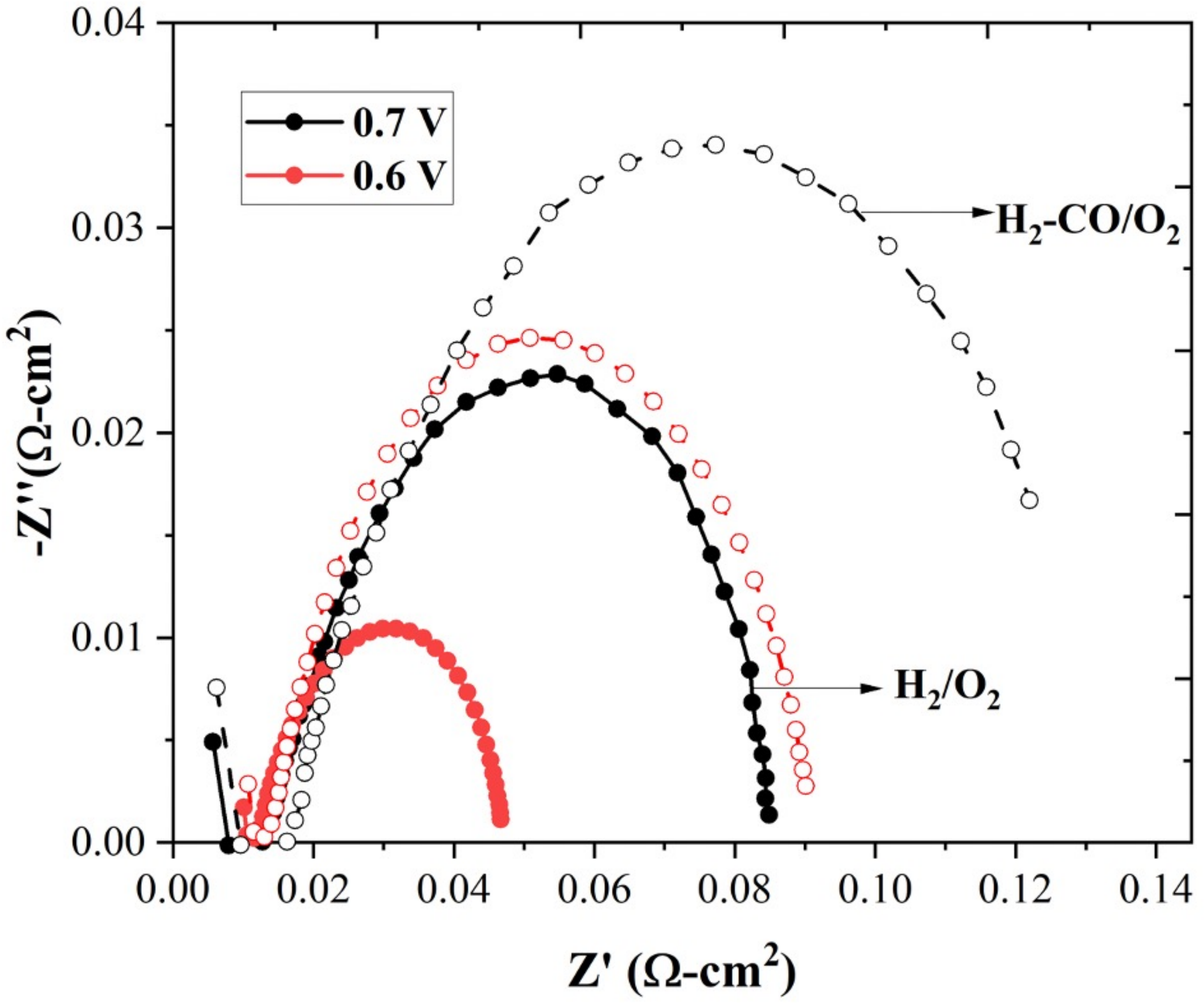

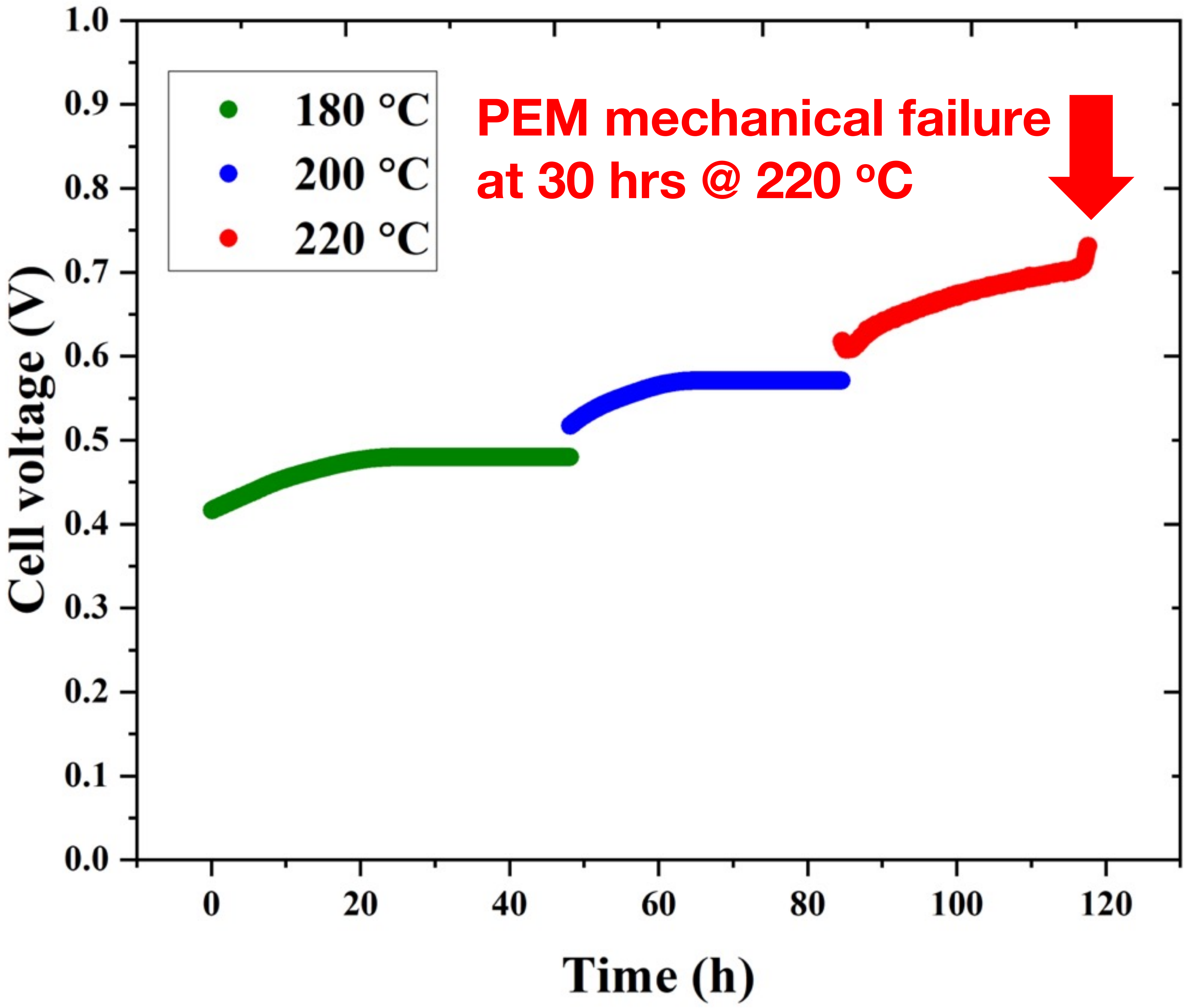

HFR: 15 mΩ-cm²

Kinetic/charge-transfer resistances dominate

We also suspect mass transfer limitations

Stable 90+ hours in 180 to 200 °C

G. Venugopalan, C.G. Arges *et al., ACS Applied Energy Materials*, **2020**

QPPSf with different IEC values

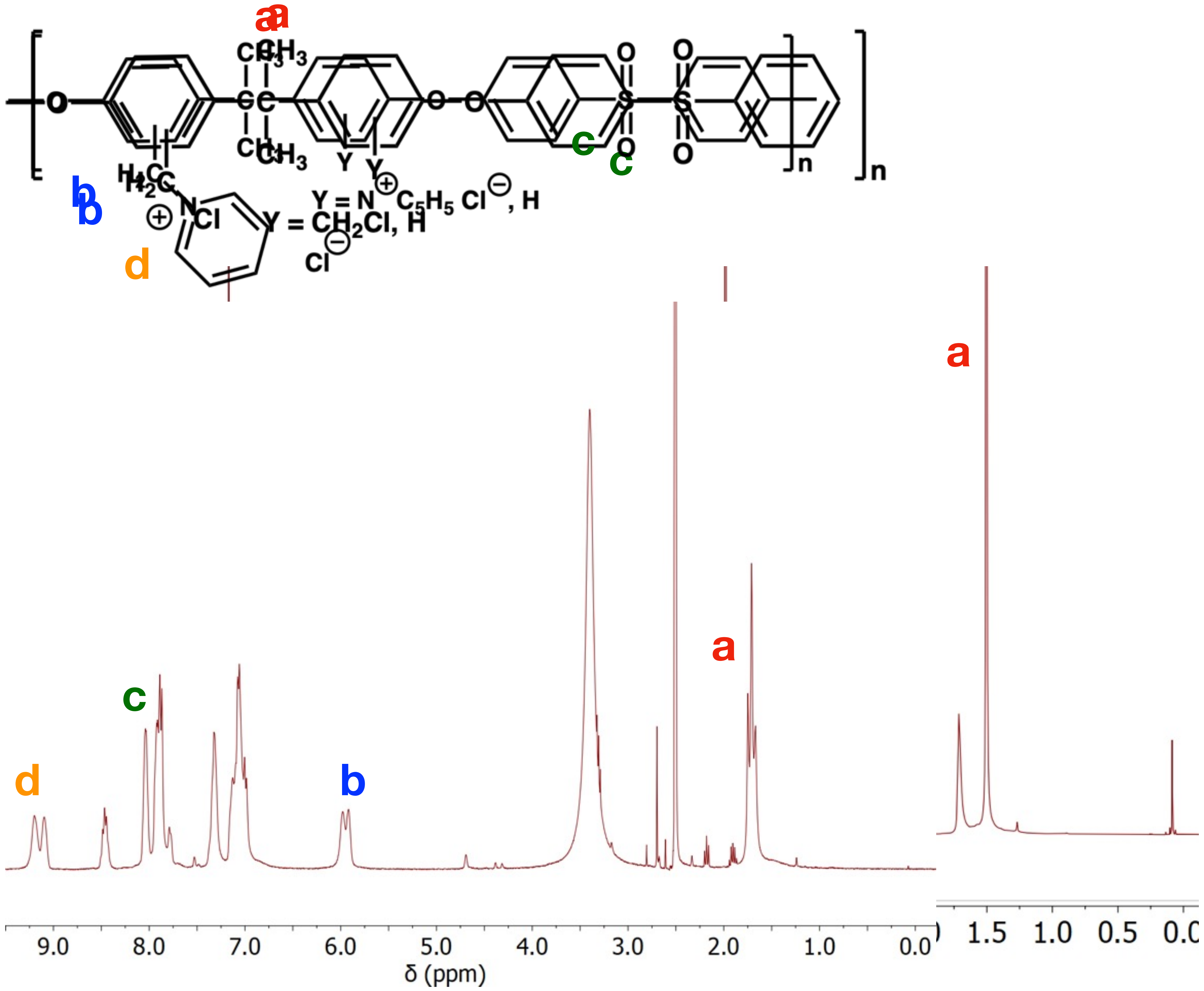

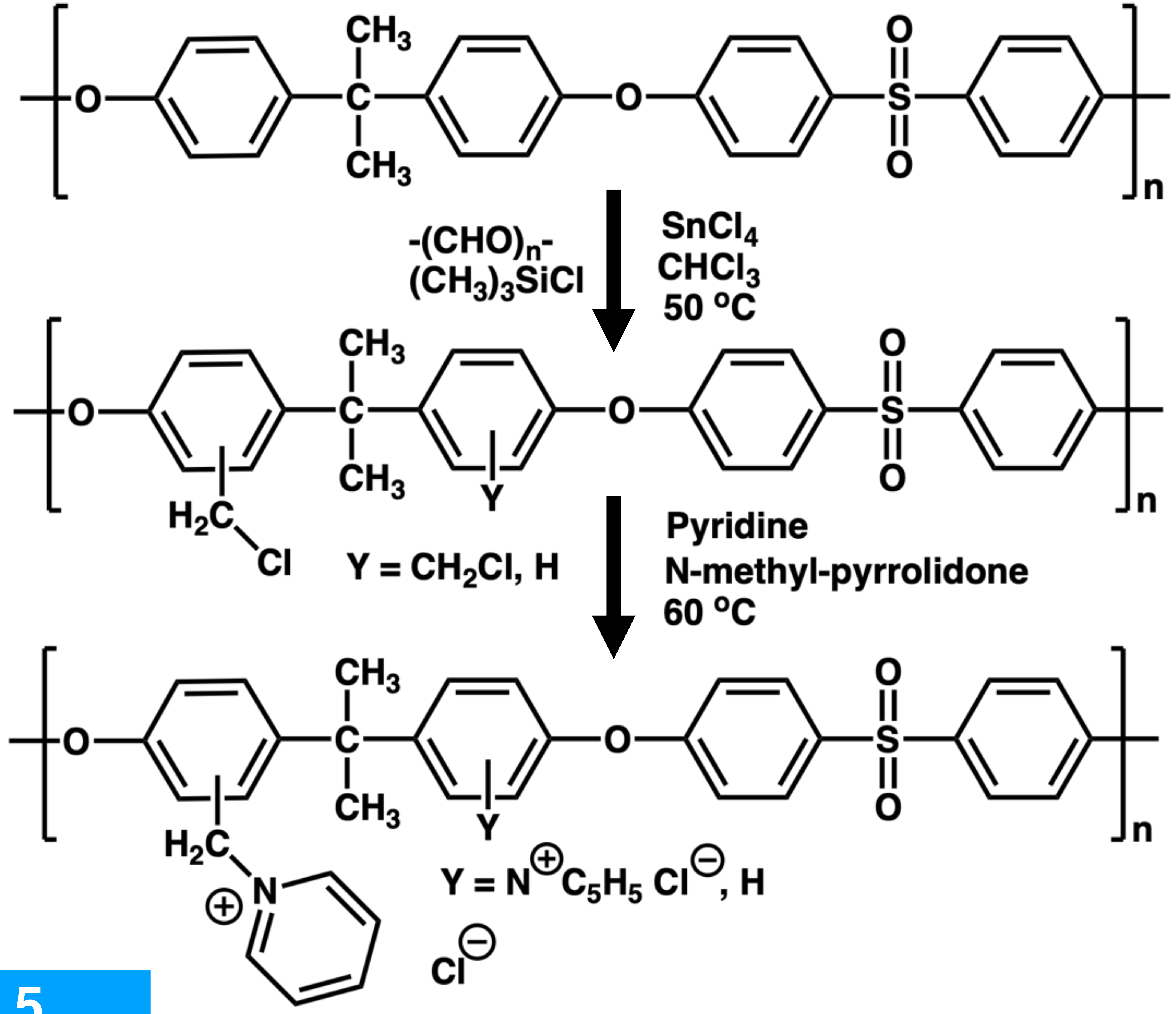

CMPSf (DF)	0.7	0.9	1.1	1.26	1.5
QPPSf IEC (mmol g^{-1})	0.9	1.24	1.45	1.76	1.96

L. Briceno-Mena, G. Venugopalan, J.A. Romagnoli, C.G. Arges, *Patterns (Cell Press)*, **2021**

PGM nanostructures – loading & surface area

Sample ID	Mass loading ($\mu g_{PGM}\ cm^{-2}_{geo}$)	Thickness (nm)	Specific Surface Area ($cm^2_{PGM}\ cm^{-2}_{geo}$)
PS^{40k}-*b*-$P2VP^{44k}$ (Pt)	4.95	11.9	0.94
PS^{40k}-*b*-$P2VP^{44k}$ (Pt, alkylated)	9.68	28.0	1.91
PS^{102k}-*b*-$P2VP^{97k}$ (Pt)	5.85	34.1	1.53
PS^{102k}-*b*-$P2VP^{97k}$ (Pt, alkylated)	11.25	56.6	2.55
$P2VP^{12k}$-*b*-PS^{23k}-*b*-$P2VP^{12k}$ (Pt)	1.58	8.5	0.85
$P2VP^{12k}$-*b*-PS^{23k}-*b*-$P2VP^{12k}$ (Pt, alkylated)	3.83	17.4	2.27
$P2VP^{12k}$-*b*-PS^{23k}-*b*-$P2VP^{12k}$ (IrOx, alkylated)	2.67 (Ir only)	17.7	2.31
PS^{48k}-*b*-$P4VP^{21k}$ (Pt)	3.60	13.3	1.09
PS^{48k}-*b*-$P4VP^{21k}$ (Pt, alkylated)	11.72	22.3	2.34

The alkylated block copolymer templates give larger PGM loadings and surface area values.

D. Bhattacharya, C.G. Arges, *Small*, **2021** *(accepted, doi: 10.1002/smll.202100437)*

Processing SEM images for structural data

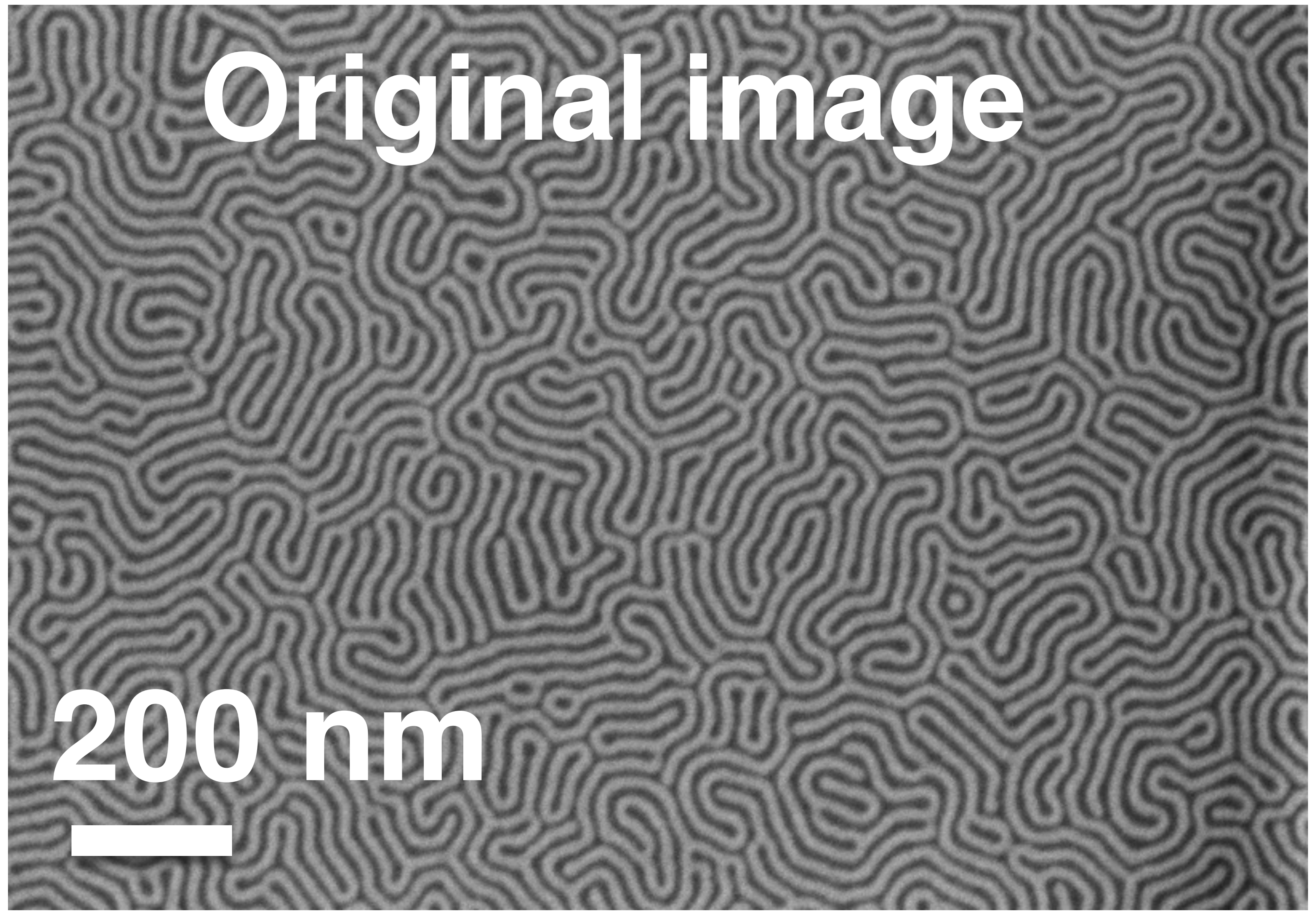

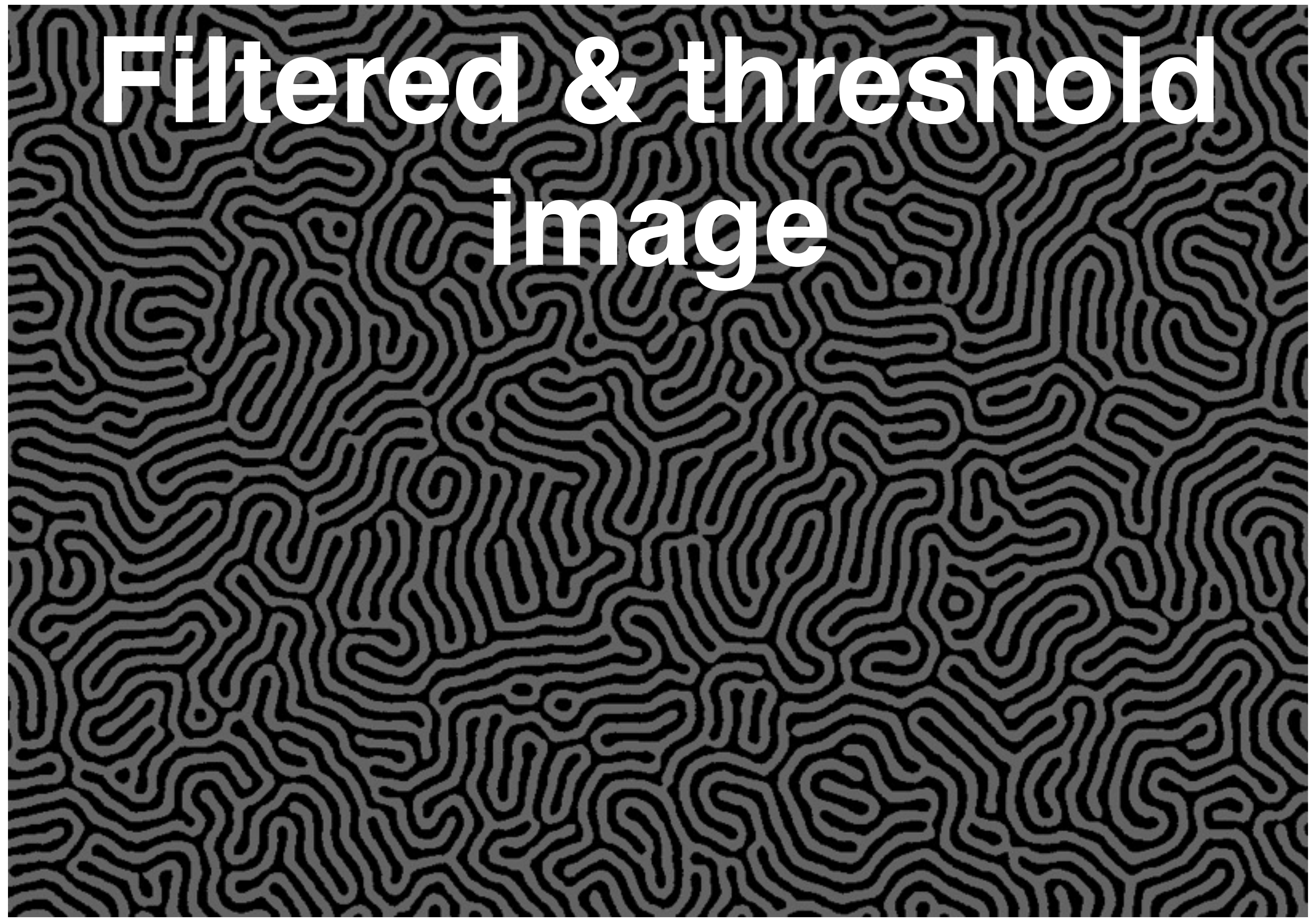

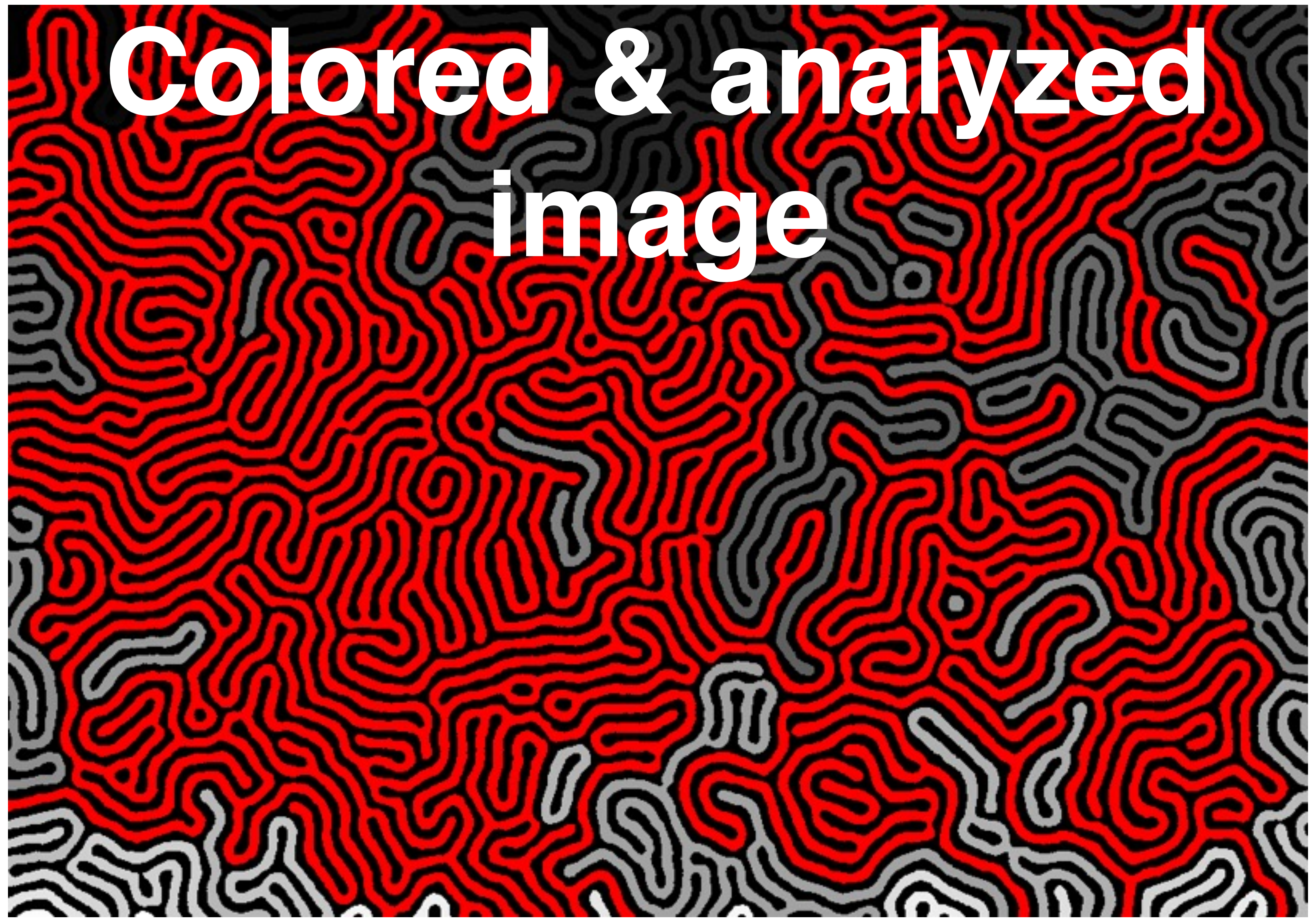

Skeleton images

Branched point defects

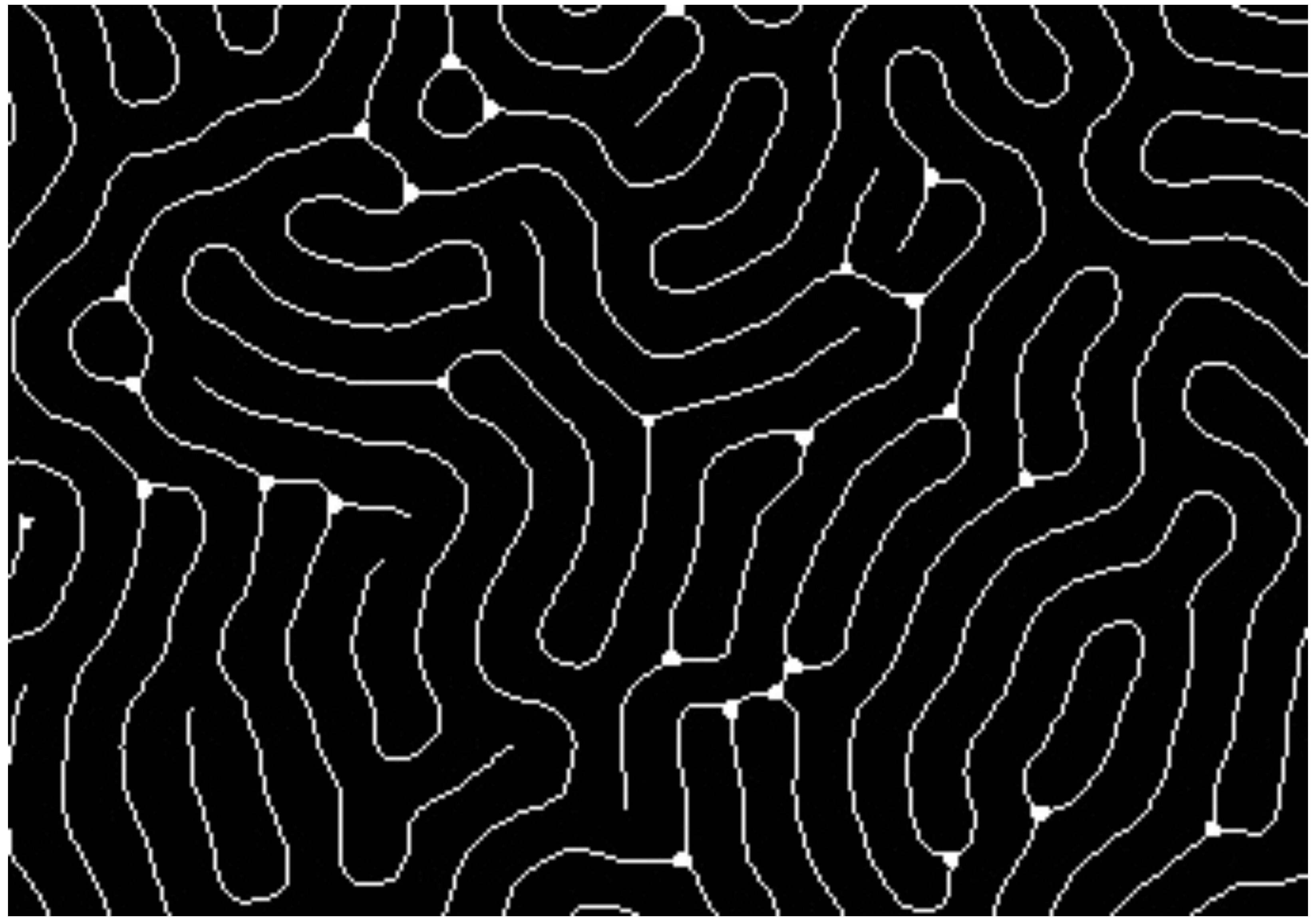

Terminal point defects

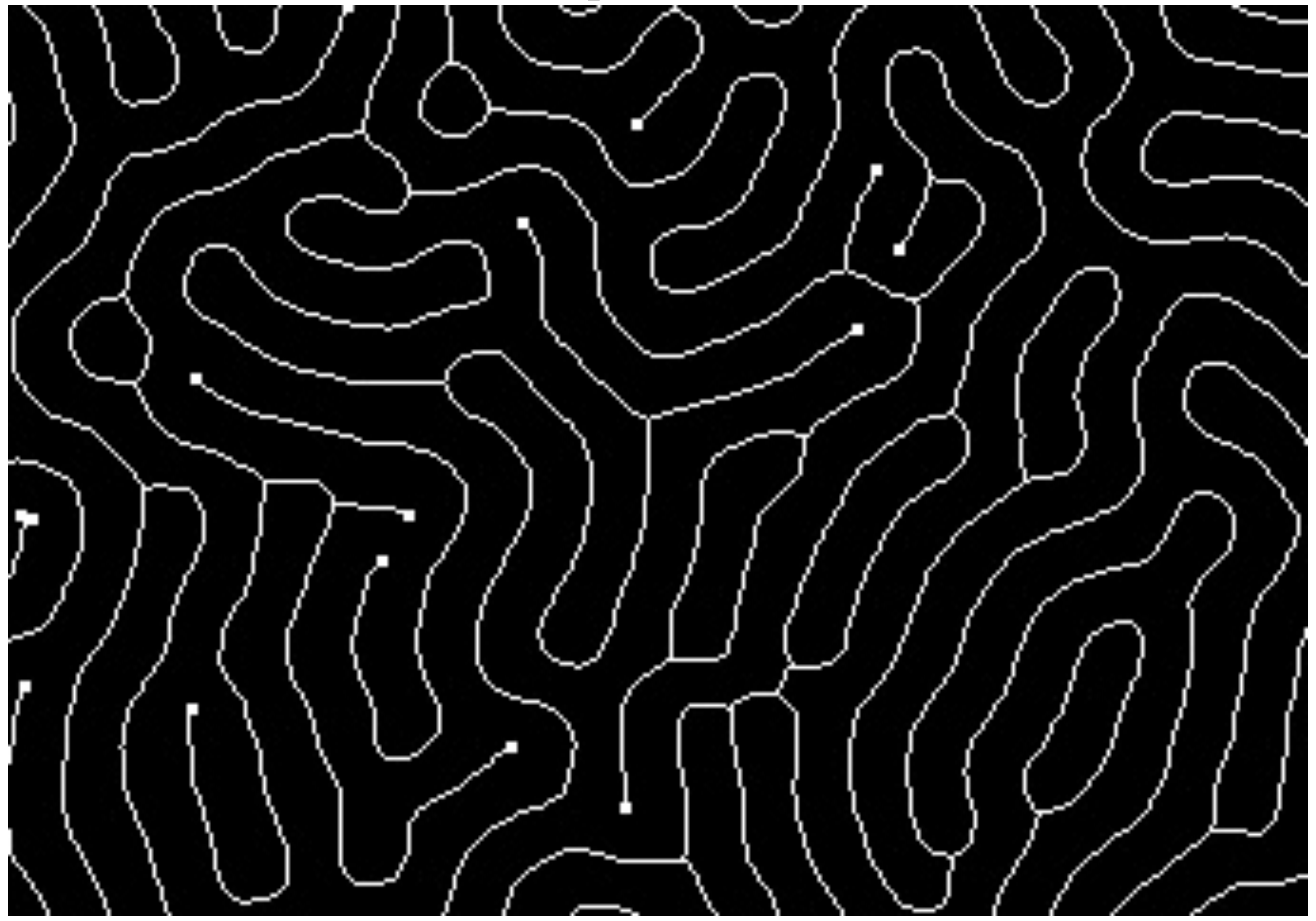

C.G. Arges, P.F. Nealey *et al. J. Mater. Chem. A.*, **2017**

Poor connectivity of the nanowire electrocatalysts prevents shorting the IDE

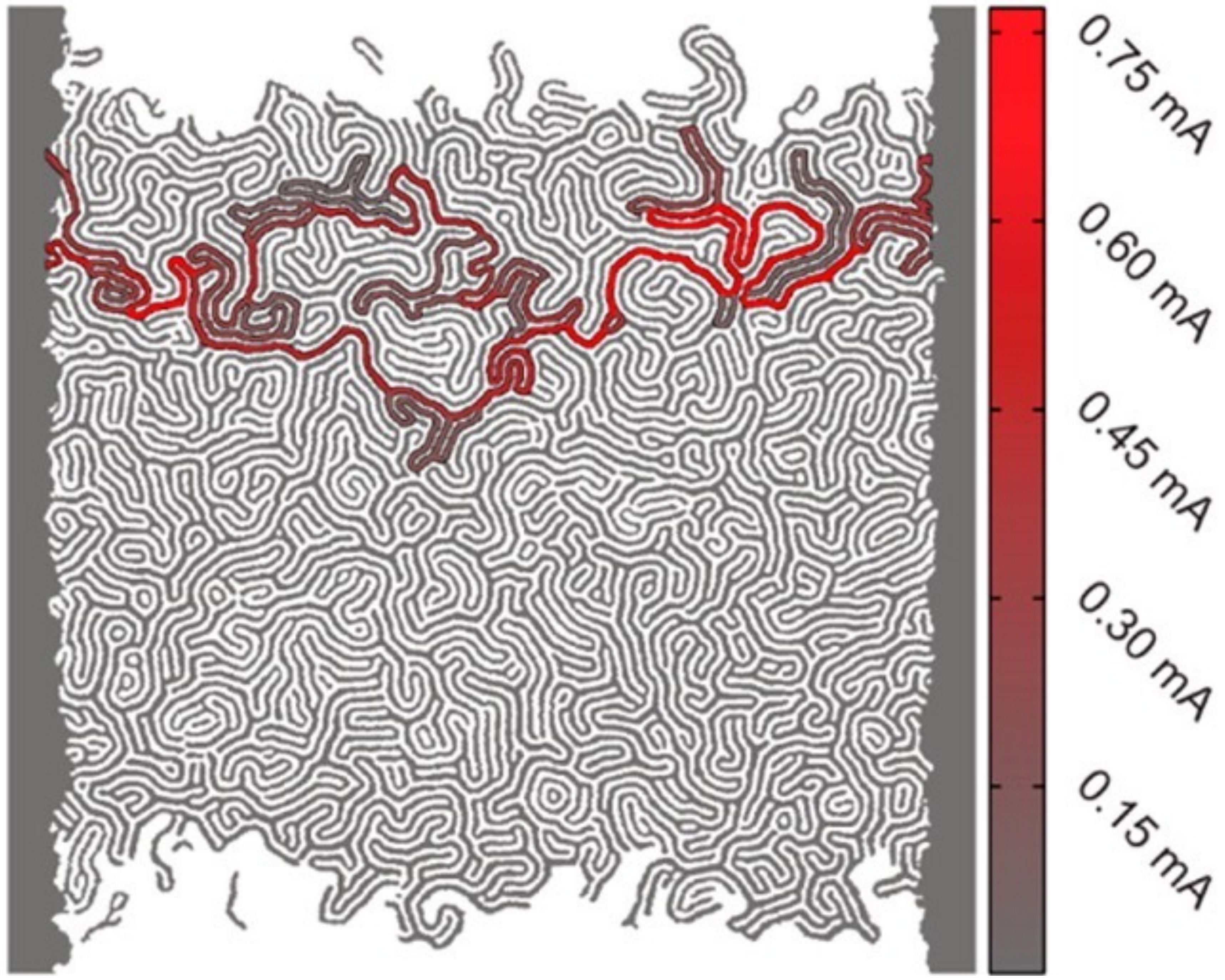

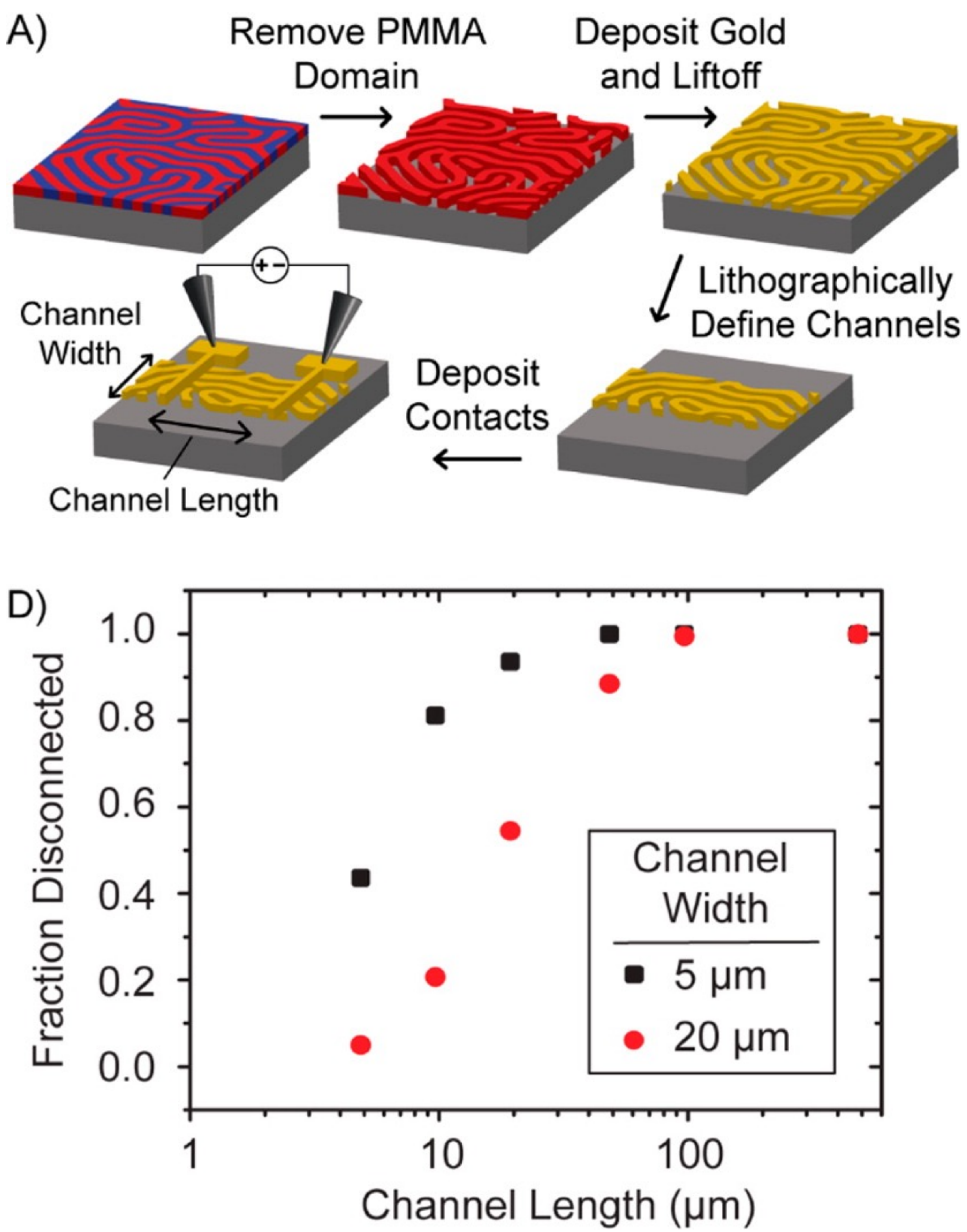

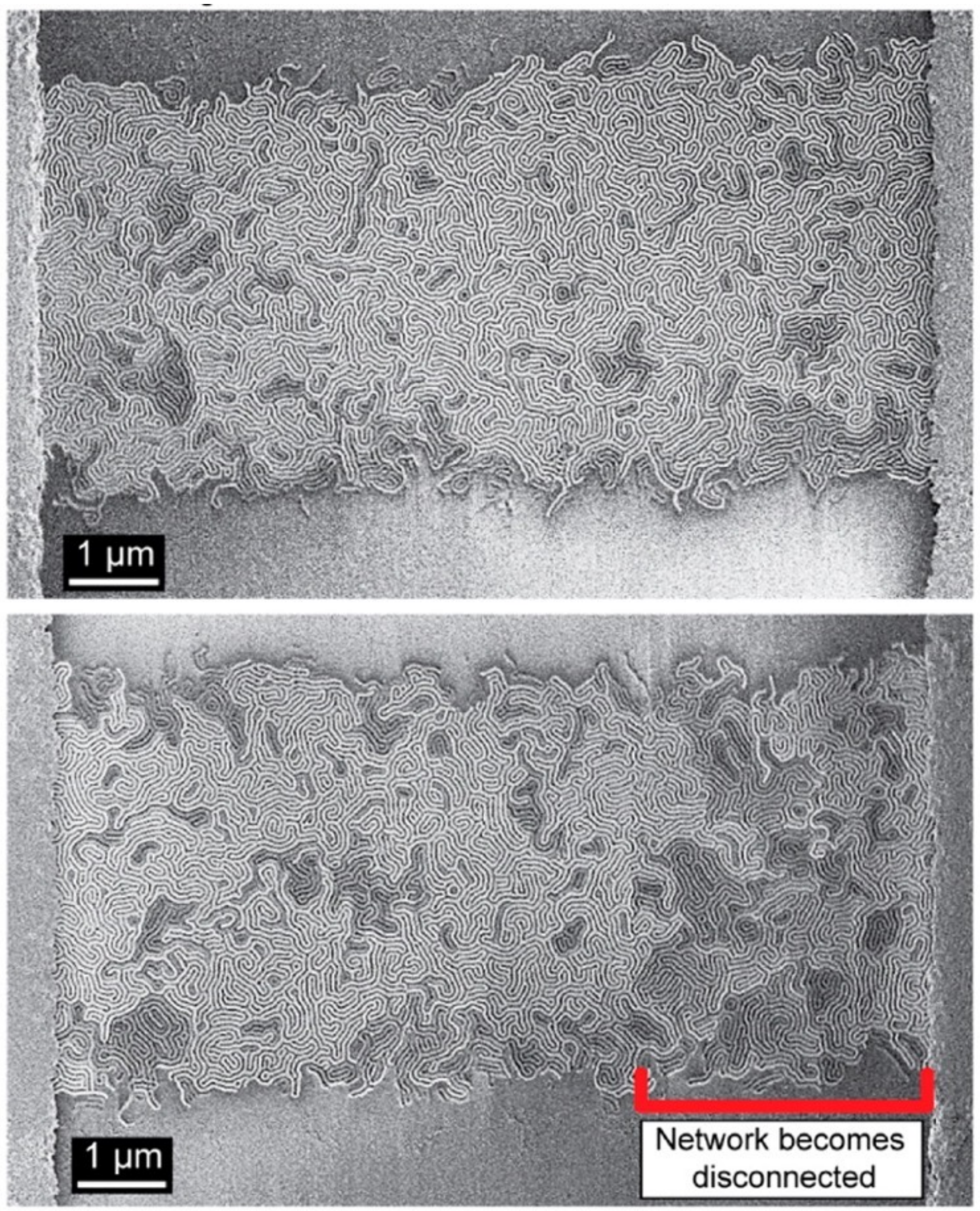

K. M. Diederichsen, R. R. Brow, M. P. Stoykovich, *ACS Nano*, **2015**